The role of mTORC1 in muscle proteostasis

Inauguraldissertation

zur
Erlangung der Würde eines Doktors der Philosophie
vorgelegt der
Philosophisch-Naturwissenschaftlichen Fakultät
der Universität Basel
von

Marco Kaiser

aus Grellingen (BL), Schweiz

Basel, 2019

Genehmigt von der Philosophisch-Naturwissenschaftlichen Fakultät
auf Antrag von

Prof. Dr. Markus A. Rüegg
Prof. Dr. Christoph Handschin

Basel, den 25.06.2019

Prof. Dr. Martin Spiess
Dekan der Philosophisch-Naturwissenschaftlichen Fakultät

Table of Contents

1. Acknowledgements

First, I would like to thank Prof. Markus A. Rüegg for giving me the opportunity to do my PhD in his laboratory. Not only the opportunity to do my PhD but also to give me the chance, after a Master in computational biology and no experience in the laboratory, to completely change into the lab for my PhD and to work on my own, fascinating project! I highly appreciated your guidance, advice and support as a mentor during my whole PhD. The last four years were a big and great challenge, with many throwbacks but also with many fascinating findings, results, analyses and discussions. Thank you Markus for all of your support, education and advice you gave me during this time and thank you for having always an open door for me and for guiding me through my PhD.

Secondly, I would like to thank Prof. Christoph Handschin and Prof. Mihaela Zavolan for being part of my PhD committee. Your critical advice, detailed discussions, suggestions and personal guidance was essential for keeping me on track and to critically questioning my own work and the strategy of the project.

I thank Dr. Lionel Tintignac for all of his support in experimental questions, especially in the beginning of my PhD, but also later on for all the scientific and personal concerns I had. Special thanks goes to Dr. Maitea Guridi: For the very first teaching in laboratory work but especially for telling me the most important wisdom about doing a PhD. Particularly, I also want to thank Aurel Leuchtmann for all of his support and proofreading during the last phase of my PhD.

I would like to thank also all of the lab members. Thank you all for your immense help, suggestions, discussions and funny times we had. Particularly, I would like to mention Dr. Giulia Milan for the collaboration on this project, Dr. Judith Reinhard for her huge experimental support, Dr. Shuo Lin for all of his support on animal experiments, Dr. Daniel Ham for an enormous number of ideas, suggestions and proofreading and Filippo Oliveri for his indispensable technical, experimental and personal support. Additionally, I would like to thank all the members of the “coffee gang”. I enjoyed our discussions – it was an amazing time!

Special thanks go to my family and friends for their enormous support and motivation throughout my whole PhD and life. Even if you did not fully understand all the scientific parts and it was very difficult to relive the challenges I got during my PhD, you always knew when I needed support or distraction. Thank you very much – without you I would not stand at the same position as today!

Lastly, words cannot express how grateful I am to have Loredana Gschwind at my side. You were the best support and energy I could have imagined. Thank you for made me laugh after exhaustive days, for your motivation, your help in scientific questions, your patience and for your love. Thank you for always being here for me! Without you, I would not have succeeded!

2. List of abbreviations

4E-BP1 (eIF4EBP1)	eIF4E binding protein 1
AAA+ ATPase	ATPases associated with diverse cellular activities
ADRM1	Adhesion regulating molecule 1
Akt (PKB)	Thymoma viral proto-oncogene (Protein kinase B)
ALP	Autophagy-lysosomal pathway
AMBRA1	Autophagy and beclin-1 regulator 1
ANOVA	Analysis of variance
ARE	Antioxidant response element
Atf4	*Activating transcription factor 4*
ATG	Autophagy related proteins
ATG12	Autophagy related 12
ATG5	Autophagy related 5
ATP	Adenosine triphosphate
ATPase	Adenosinetriphosphatase
BACH1	BTB and CNC homology 1, basic leucine zipper transcription factor 1
BACH2	BTB and CNC homology 1, basic leucine zipper transcription factor 2
BECN1	Beclin1, autophagy related
BNIP3	BCL2/adenovirus E1B interacting protein 3
BTZ	Bortezomib
C. elegans	*Caenorhabditis elegans*
CASTOR1	Cytosolic arginine sensor for mTORC1 subunit 1
CASTOR2	Cytosolic arginine sensor for mTORC1 subunit 2
CDK	Cyclin-dependent kinase
CL	Cleaved
CNC	Cap-n-collar [*Drosophila melanogaster*]
CNC-bZIP	Cap'n'collar basic-region leucine zipper
CP	26S proteasome core particle
CSA	Cross-sectional area
CTSL	Cathepsin L
D-BSSE	Department of Biosystems Science and Engineering
DDI2	DNA-damage inducible protein 2
DE	Differentially expressed
DES	Desmin
DMEM	Glutamax Dulbecco's modified Eagle's medium
DMSO	Dimethyl sulfoxide
DNA	Deoxyribonucleic acid
DNM1	Dynamin 1
DUB	Deubiquitinase
EDL	*Musculus extensor digitorum longus*
EGFP	Enhanced green fluorescent protein
eIF4E	Eukaryotic translation initiation factor 4E
EpRE	Electrophile response element
ER	Endoplasmic reticulum
ERAD	ER-associated degradation
ERt2	Human estrogen receptor type 2
FBS	Fetal bovine serum

Fbxo21 / Smart	*F-box protein 21 / Specific of muscle atrophy and regulated by transcription*
Fbxo30 / Musa1	*F-box protein 30 / Muscle ubiquitin ligase of SCF complex in atrophy 1*
Fbxo32 / Atrogin-1	*F-box protein 32 / Atrogin-1*
FBXW7	F-box and WD-40 domain protein 7
FKBP1A / FKBP12	FK506-binding protein 1a
FL	Full-length
FLCN	Folliculin
FNIP2	Folliculin interacting protein 2
FoxO	Forkhead box O
FTH1	Ferritin heavy polypeptide 1
FTL1	Ferritin light polypeptide 1
GABARAPL1	Gamma-aminobutyric acid (GABA) receptor-associated protein-like 1
Gadd45a	*Growth arrest and DNA-damage-inducible 45 alpha*
GAP	GTPase-activating proteins
GAST	*Musculus gastrocnemius*
GATOR1	GTPase-activating protein complex 1
GATOR2	GTPase-activating protein complex 2
GCLC	Glutamate-cysteine ligase, catalytic subunit
GCLM	Glutamate-cysteine ligase, modifier subunit
GDP	Guanosine diphosphate
GEF	Guanosine triphosphate exchange factors
GlcNAc	O-linked N-acetylglucosamine
GSS	Glutathione synthetase
GST	Glutathione S-transferase
GTP	Guanosine triphosphate
GTPase	Guanosinetriphosphatase
HAS	Human skeletal α-actin
HCFC1	Host cell factor C1
HIF1A	Hypoxia-inducible factor 1α
HMOX1	Heme oxygenase 1
HRP	Horseradish peroxidase-conjugated
IGF	Insulin-like growth factor
IRS1	Insulin-receptor substrate 1
iTSCmKO	Inducible TSC1 muscle specific knockout
IκB	Inhibitor of kappa light polypeptide gene enhancer in B cells
JUN	Jun proto-oncogene
KEGG	Kyoto Encyclopedia of Genes and Genomes
KO	Knockout
LAMA2-MD	Laminin-α2-related muscular dystrophy
LC3 / Map1lc3a	Microtubule-associated protein 1 light chain 3 alpha
LCR-F1 / Nrf1β	Locus control region-factor 1
m^7GTP-cap	7-methylguanosine 5'-triphosphate cap
Maf	Musculoaponeurotic fibrosarcoma proteins
MCL	Mantle-cell lymphoma
ME1	Malic enzyme 1, NADP(+)-dependent, cytosolic
ME2	Malic enzyme 2, NAD(+)-dependent, mitochondrial
MEF	Mouse embryonic fibroblast

MerCreMer	Cre recombinase containing two mutated estrogen receptor ligand-binding domains
MLST8	mTOR associated protein, LST8 homolog
MT1	Metallothionein 1
MT2	Metallothionein 2
mTOR	Mammalian (or mechanistic) target of rapamycin
mTORC1	Mammalian (or mechanistic) target of rapamycin complex 1
mTORC2	Mammalian (or mechanistic) target of rapamycin complex 2
MyHC / Myh	Myosin heavy chain
NASH	Non-alcoholic steatohepatitis
NFE2	Nuclear factor-erythroid 2
NFE2L1 / Nrf1	Nuclear factor, erythroid derived 2, -like 1
NFE2L2 / Nrf2	Nuclear factor, erythroid derived 2, -like 2
NFE2L2 / Nrf3	Nuclear factor, erythroid derived 2, -like 3
NF-κB	Nuclear factor of kappa light polypeptide gene enhancer in B cells
NGLY1	N-glycanase 1
Nhb1	N-terminal homology box 1
NIBR	Novartis Institutes for BioMedical Research, Cambridge, MA, USA
NMJ	Neuromuscular junction
NQO1	NAD(P)H dehydrogenase, quinone 1
OGT	O-linked GlcNAc transferase
p97 / VCP	ATPase p97 / Valosin containing protein
PA	Proteasome activator
PA200 / PSME4	Proteasome activator 200 / Proteasome activator subunit 4
PACE	Proteasome associated control element
PCA	Principal component analysis
PDK1	3-phosphoinositide dependent protein kinase 1
Pen/strep	Penicillin-streptomycin
PI3K	Phosphoinositide-3-kinase
PLA	*Musculus plantaris*
PNK	Polynucleotide kinase
PPARGC1A / PGC-1α	Peroxisome proliferator–activated receptor γ coactivator 1α
Ppp1r15a	*Protein phosphatase 1, regulatory subunit 15A*
PRAS40 / Akt1s1	Proline-rich Akt substrate of 40 kDa / Akt1 substrate 1 (proline-rich)
PRDX1	Peroxiredoxin 1
PSM	Proteasome (prosome, macropain) 26S subunit
PSME1	Proteasome activator subunit 1 / PA28 alpha
PSME2	Proteasome activator subunit 2 / PA28 beta
PSME3	Proteasome activator subunit 3 / PA28 gamma
QGF	Quantitative Genomics Facility
QUAD	*Musculus quadriceps femoris*
Rag	Ras-related small G proteins
Raptor / RPTOR	Regulatory-associated protein of mTOR, complex 1
RB1CC1 / FIP200	RB1-inducible coiled-coil 1
RHEB	Ras homolog enriched in brain
Rictor	RPTOR independent companion of mTOR, complex 2
RLU	Relative luminescence units
RP	26S proteasome regulatory particle
RPN4	Stress-regulated transcription factor RPN4 [*Saccharomyces cerevisiae]*
RPS6 / S6	Ribosomal protein S6

S6K1 / RPS6KB1	Ribosomal protein S6 kinase, polypeptide 1
SBMA	Spinal and bulbar muscular atrophy
SEM	Standard error of the mean
SEM1	SEM1, 26S proteasome complex subunit
SESN2	Sestrin 2
SFP1	Split finger protein 1
SIN1 / MAPKAP1	Mitogen-activated protein kinase associated protein 1
SKN-1	Protein skinhead-1 [*Caenorhabditis elegans*]
SLC38A9	Solute carrier family 38, member 9
SMA	Spinal muscular atrophy
SMN1	Survival motor neuron 1
SOL	*Musculus soleus*
SQSTM1 / p62	Sequestosome 1
SREBP1 / SREBF1	Sterol regulatory element binding transcription factor 1
SYVN1 / Hrd1	Synovial apoptosis inhibitor 1, synoviolin
TA	*Musculus tibialis anterior*
TBC1D7	TBC1 domain family, member 7
TMT	Tandem Mass Tag
Trim63 / MuRF1	*Tripartite motif-containing 63 / Muscle ring finger 1*
TRP53 / p53	Transformation related protein 53
TSA	Trichostatin A
TSC1	TSC complex subunit 1 / tuberous sclerosis complex 1
TSC2	TSC complex subunit 2 / tuberous sclerosis complex 2
TSCmKO	TSC1 muscle specific knockout
TXN1	Thioredoxin 1
Ub	Ubiquitin
UBC	Ubiquitin C
UBE4B	Ubiquitination factor E4B
UCHL5	Ubiquitin carboxyl-terminal esterase L5
ULK1	Unc-51 like kinase 1
UPS	Ubiquitin-proteasome system
USP14	Ubiquitin specific peptidase 14
v-ATPase	Vacuolar adenosinetriphosphatase
VPS34	Vacuolar protein sorting 34
WCL	Whole-cell lysates
β-TrCP	beta-transducin repeat containing protein

3. Abstract

Skeletal muscle is crucial for human daily life. It is essential for locomotion and breathing and it affects whole-body metabolism. Preservation of muscle mass is thus critical to maintain body function and health. Current views indicate that muscle mass is controlled by the tight balance between protein synthesis and protein degradation, called proteostasis. Perturbation of this balance by extrinsic factors, as for example seen in cachexia (i.e., muscle loss as a secondary consequence of e.g. cancer, AIDS, or cardiac and kidney disease) or in sarcopenia (i.e., loss of muscle mass and function as a consequence of aging), is a main cause of loss of life quality and increased mortality. Thus, a better molecular understanding of muscle proteostasis is of fundamental importance to develop possible treatment strategies to counteract the above diseases.

Two major regulators of muscle proteostasis are the mammalian (or mechanistic) target of rapamycin complex 1 (mTORC1) and the forkhead box O (FoxO) transcription factors. While mTORC1 controls proteostasis by increasing translation and protein synthesis, FoxO regulates catabolic processes by increasing the expression of genes encoding for proteins involved in protein degradation. Thus, increased activation of FoxO causes muscle loss (atrophy), whereas activation of mTORC1 is associated with muscle gain (hypertrophy). However and in striking contrast to the expected outcome of muscle gain, sustained activation of mTORC1 in muscle by knockout of its upstream inhibitor TSC1 (TSCmKO mice) results in atrophy. This phenotype is observed despite the marked increase in protein synthesis. Hence, the mechanisms involved in muscle atrophy in TSCmKO mice remain unresolved.

The purpose of this thesis was to provide new insights on the role of mTORC1 in regulating muscle proteostasis. Particularly, to characterize the mechanism of this mTORC1-driven atrophy observed in TSCmKO mice. Furthermore, the aim was to investigate if sustained activation of mTORC1 increases overall protein degradation *via* the thymoma viral proto-oncogene (Akt)-FoxO-signaling or by distinct other catabolic pathways.

In this thesis, it was established that sustained activation of mTORC1 in muscles of TSCmKO mice leads to a significant increase of the ubiquitin-proteasome system (UPS). This was characterized by increased expression of ubiquitin-E3-ligases, increased ubiquitinylation, increased proteasomal biosynthesis and increased proteasome activity. The increase of the UPS was reversed by short-term treatment with the mTORC1-inhibitor rapamycin. Interestingly, the same increase of the UPS was observed upon acute muscle-specific deletion of *Tsc1* for 3 weeks. Surprisingly, constitutive activation of Akt in muscle resulted in a similar induction of proteasomal biosynthesis and proteasome activity as observed in TSCmKO mice. Hence, this suggests a mechanism, which is independent of the activation of FoxO transcription factors. Finally, it was established that the increased UPS activity was

accompanied by a concomitant increase of the transcription factor “nuclear factor, erythroid-derived 2,-like 1” (NFE2L1, hereafter called Nrf1).

In short, this thesis demonstrated that mTORC1 activation is a major driver of the ubiquitin-proteasome system in skeletal muscle and identified Nrf1, together with FoxO transcription factors, as a key mediator of this pathway. Both, mTORC1 signaling as well as the UPS are considered as potential treatment targets in a large variety of distinct muscle wasting diseases. Therefore, understanding the underlying regulatory mechanisms of how mTORC1 controls muscle mass is of fundamental importance to eventually develop new therapeutic agents that could slow-down the massive muscle wasting observed in cachexia and sarcopenia.

4. Introduction

Muscle tissue is the largest organ in most mammalian organisms and accounts for up to 50% of total body mass in humans. Generally, muscle tissue is divided into two subcategories based on its structure and its contractile properties. **Smooth** muscle tissue is an integral part of hollow organs such as blood vessels, the respiratory tract and the digestive tract. Regulated by the autonomic nervous system, smooth muscles contract and relax to adjust the diameter of the lumen. **Striated** muscle tissue includes cardiac (myocardium) and skeletal muscle tissue. Skeletal muscles are required for voluntary locomotion controlled by the somatic nervous system. Their main function is to generate mechanical force, which enables locomotion, precise movements and respiration and to allow keeping an upright posture. Skeletal muscles are composed of multiple muscle fiber bundles, which in turn are formed by differentiated, post-mitotic myofibers. Each myofiber consists of longitudinally arranged myofibrils, composed of large proteins such as titin, myosin and actin, whereas the latter two are organized into thick and thin myofilaments, respectively. Innervating motor neurons provide neuronal stimuli by generating electric signals in the form of action potentials, which triggers the release of calcium ions by the sarcoplasmatic reticulum (Calderon et al., 2014; Kahn and Sandow, 1950; Sandow, 1952). The free calcium enables the formation of cross-bridges between the heads of myosin molecules with the active sites on actin filaments (Calderon et al., 2014). According to the sliding filament theory, hydrolysis of adenosine triphosphate (ATP), which provides the energy for releasing the myosin heads from actin, the thick (myosin) and the thin (actin) filaments slide along each other causing the muscle to contract (Huxley and Niedergerke, 1954; Huxley and Hanson, 1954).

Skeletal muscle fiber type classification and composition

Skeletal muscles (hereafter, simply referred to as muscle) were initially classified as being fast or slow based on their shortening velocity (Buller et al., 1960). This classification corresponds to morphological but also metabolic differences observed between these two types of muscle. Slow muscles appear red because of their high myoglobin content giving them a higher oxidative capacity compared to the white fast muscles, which preferentially rely on anaerobic glycolysis for ATP production. (Schiaffino, 2010; Scott et al., 2001). Most muscles are a heterogeneous mixture of different muscle fiber types. Zooming from the level of the whole muscle into the level of single fibers, reveals three distinct groups of fiber types, differing in their twitch characteristics, fatigue resistance and histochemical features: fast-twitch, fatigable, glycolytic fibers; fast-twitch, fatigue-resistant, glycolytic-oxidative fibers; and slow-twitch, fatigue-resistant, oxidative fibers (Barnard et al., 1971; Burke et al., 1971). In parallel, the correlation found between the speed of muscle fiber shortening and their myosin

adenosinetriphosphatase (ATPase) activity led to the division into type II (fast) fibers and type I (slow) fibers (Barany, 1967). The myosin ATPase activity correlates with the particular myosin heavy chain (MyHC or Myh) isoform (Scott et al., 2001). The three MyHC isoforms that were originally identified in humans (four in rodents), MyHC-I, MyHC-IIa and MyHC-IId/x (MyHC-IIb / MyHC-IId/x in rodents) can be identified by myosin ATPase staining and led to the general classification of type I, IIa and IId/x (IIb / IId/x in smaller mammals), respectively (Brooke and Kaiser, 1970). Muscle fibers that contain only one MyHC-isoform are referred to as “pure” fibers (Staron and Pette, 1993). The following classification and functional description for these muscle fibers have commonly been accepted (Brooke and Kaiser, 1970; Peter et al., 1972; Schiaffino, 2011):

- Type I fibers: slow-twitch-oxidative
- Type IIa fibers: fast-twitch-oxidative-glycolytic
- Type IIx fibers: fast-intermediate-twitch-glycolytic
- Type IIb fibers: fast-twitch-glycolytic

The fact that each muscle fiber can express more than one MyHC-isoform explains the existence of intermediate – so called “hybrid” muscle fibers – possessing intermediate fiber characteristics (Hamalainen and Pette, 1995; Pierobon-Bormioli et al., 1981; Staron and Pette, 1993).

A previous study examined the fiber type composition and percentage of MyHC-isoforms of most hindlimb muscles in male C57BL6J mice (Augusto, 2004). They showed that the slow-twitch, oxidative *soleus* (SOL) muscle is composed of the more oxidative MyHC-isoforms, i.e. MyHC-I (42%) and -IIa (58%). In contrast, the same study demonstrated that the fast-twitch glycolytic muscles *extensor digitorum longus* (EDL), *tibialis anterior* (TA) and *gastrocnemius* (GAST) are mainly composed of glycolytic fibers, namely type IIb (~60%) and hybrid type IIb/IIx (25%) fibers (Augusto, 2004). Other studies showed that the hindlimb, fast-twitch muscles *plantaris* (PLA) and *quadriceps* (QUAD) are majorly composed of type IIb and IIx fibers (Gentry et al., 2011; Waters et al., 2004). Muscle is a highly plastic tissue and has a remarkable capacity to undergo fiber type changes in response to external stimuli and changing environmental conditions. For example, type II fiber loss has been observed in patients suffering from cancer, diabetes and chronic heart failure. Moreover, age-dependent changes in motor unit composition seem to have similar consequences in elderly people characterized by a fast-to-slow fiber type shift (Ciciliot et al., 2013; Lexell, 1995). In contrast, a reduction in type I fibers and a concomitant increase in type II fibers occurs upon muscle disuse, inactivity and denervation (Wang and Pessin, 2013). In the case of denervation, for example due to spinal cord injury, the loss of neuronal input leads to the activation of the nerve activity-independent, default “fast gene program” resulting in a slow-to-fast fiber type switch (Ciciliot et

al., 2013). Another external stimulus, which has been shown to cause a fiber type switch, is exercise. In humans, heavy resistance exercise leads to an increase in type IIa fibers and a reduction in type IIx fibers (Kraemer et al., 1995; Staron et al., 1994). In rodents, the transcriptional regulator peroxisome proliferator–activated receptor γ coactivator 1α (PPARGC1A, hereafter called PGC-1α) seems to coordinate an exercise-stimulated fast-to-slow fiber type switch (Handschin et al., 2007; Lin et al., 2002). A fiber type switch to more oxidative, slow-type-I fibers correlates with an increase in oxidative capacity and fatigue-resistance (Crow and Kushmerick, 1982; Szentesi et al., 2001) and with improved endurance performance and exercise efficiency (Coyle et al., 1992; Horowitz et al., 1994). Interestingly, a recent study showed that inorganic nitrate increases exercise efficiency and performance by induction of PGC-1α and that this leads to a similar fast-to-slow fiber type switch, as found in transgenic PGC-1α overexpressing mice (Lin et al., 2002; Roberts et al., 2017). In contrast, muscle specific PGC-1α knockout (KO) mice exhibit a switch from oxidative type I and type IIa fibers towards type IIx and IIb fibers, resulting in reduced endurance capacity (and fiber damage) (Handschin et al., 2007). Therefore, the fiber type composition of a muscle largely determines its physiological properties. The high plastic potential of muscle, i.e. its ability to alter its structural and functional properties, enables the adaptation to changes in physiological requirements in distinct environmental conditions.

Muscle proteostasis maintains muscle mass and physiology

The fact that muscle is a highly plastic tissue, also explains why its function is often compromised in pathological conditions as for example seen in cachexia or in sarcopenia. Generally speaking, muscle mass is controlled by the tight balance between protein synthesis and protein degradation, termed proteostasis. Perturbation of this balance can lead to a decline in muscle mass and ultimately to muscle wasting. Muscle wasting has severe consequences on the individual level by reducing quality of life and increasing mortality, but also puts a huge burden on healthcare systems. Cachexia describes a complex metabolic syndrome characterized by the loss of muscle mass that occurs as a sequelae of primary diseases such as cancer, AIDS and cardiac or kidney disease (Evans et al., 2008), whereas sarcopenia describes the age-associated loss of muscle mass and function (Fielding et al., 2011). Preserving muscle mass is critical in these conditions to maintain metabolic and functional capacities, which helps to maintain quality of life and increases chances of survival. Unfortunately, besides exercise, there is at this time no effective and safe treatment option available to counteract muscle wasting in cachexia (Furrer and Handschin, 2019) or sarcopenia (Leuchtmann and Handschin, 2019). Therefore, a better molecular understanding of muscle proteostasis is of fundamental importance to develop novel and effective treatment strategies to counteract the development of sarcopenia and other muscle wasting diseases.

mTORC1 regulates muscle proteostasis by affecting protein synthesis

As described above, muscle proteostasis determines muscle size: if overall rates of protein degradation are lower than the overall rates in protein synthesis muscle will grow (hypertrophy); if overall rates of protein degradation outstrips the overall rates in protein synthesis muscle shrinks (atrophy) (Sandri, 2013).

Therefore, muscle size is tightly controlled and dependent on regulators of protein synthesis and degradation. The mammalian (or mechanistic) target of rapamycin (mTOR) is a serine / threonine protein kinase and a highly conserved regulator of cell growth (Laplante and Sabatini, 2012). Rapamycin, clinically termed sirolimus, was isolated from the bacteria *Streptomyces Hygroscopicus* and was discovered because of its anti-proliferative properties in yeast (Laplante and Sabatini, 2012). Rapamycin forms a complex with the FK506-binding protein 1a (FKBP1A, also FKBP12), which binds to the mediators TOR1 and TOR2 (Cafferkey et al., 1993; Kunz et al., 1993). Later, mTOR was identified as the homologous protein in mammals (Brown et al., 1994; Sabatini et al., 1994; Sabers et al., 1995). mTOR assembles into two structurally and functionally distinct multi-protein complexes, called mTORC1 and mTORC2 (Laplante and Sabatini, 2012; Shimobayashi and Hall, 2014). The essential core components of mTORC1 are regulatory-associated protein of mTOR, complex 1 (Raptor) and mTOR associated protein, LST8 homolog (MLST8), whereas those of mTORC2 are RPTOR independent companion of mTOR, complex 2 (Rictor), mitogen-activated protein kinase associated protein 1 (SIN1, also MAPKAP1) and MLST8 (Shimobayashi and Hall, 2014). Studies in mice have shown that mTOR function in skeletal muscle is largely based on the activity of mTORC1 and not mTORC2 (Bentzinger et al., 2008; Risson et al., 2009). Rapamycin directly interacts and inhibits mTORC1 (Brown et al., 1994; Sabatini et al., 1994).

mTORC1 involves amino acid sensing to localize at the lysosomal surface

mTORC1 is activated by different cellular inputs, such as amino acids, insulin, growth factors and energy status, to drive cell growth through increasing protein translation and lipid synthesis or by activating energy metabolism, ATP production and glycolytic flux (Laplante and Sabatini, 2012). Activation of mTORC1 depends on its translocation to the lysosomal surface. Upon amino acid stimulation, mTORC1 co-localizes and anchors at the lysosomal surface through direct interactions between the Ras-related small G proteins (Rag) and Raptor (Bar-Peled et al., 2013; Bar-Peled et al., 2012; Sancak et al., 2010; Sancak et al., 2008) **(Figure 1)**. The Rag guanosine triphosphatases (GTPases) form heterodimeric complexes comprised of RagA or RagB bound to RagC or RagD (Sancak et al., 2008) and they are held at the lysosomal surface by the Ragulator protein complex (Sancak et al., 2010) **(Figure 1)**. Amino acid sensing by mTORC1 initiates from within the lysosomal lumen and depends on the interplay between multiple distinct factors, including the vacuolar adenosine triphosphatase (v-ATPase) (Zoncu

et al., 2011), the lysosomal amino acid transporter solute carrier family 38, member 9 (SLC38A9) (Rebsamen et al., 2015) and the Ragulator complex but also on the nucleotide state of the Rag GTPases (Bar-Peled et al., 2012; Sancak et al., 2010) **(Figure 1)**. Distinct GTPase-activating proteins (GAPs) or Guanosine triphosphate exchange factors (GEFs) regulate the state of the Rag GTPases. Amongst them, a complex composed of folliculin (FLCN) and folliculin interacting protein 2 (FNIP2) which is a GAP for RagC/RagD (Petit et al., 2013; Tsun et al., 2013). Regulator is a GEF for the RagA/RagB GTPases (Bar-Peled et al., 2012). The GTPase-activating protein complex 1 (GATOR1) has GAP activity on RagA/RagB and is a critical negative regulator of mTORC1, whereas GATOR2 binds to GATOR1 and is a positive regulator of mTORC1 (Bar-Peled et al., 2013) **(Figure 1)**.

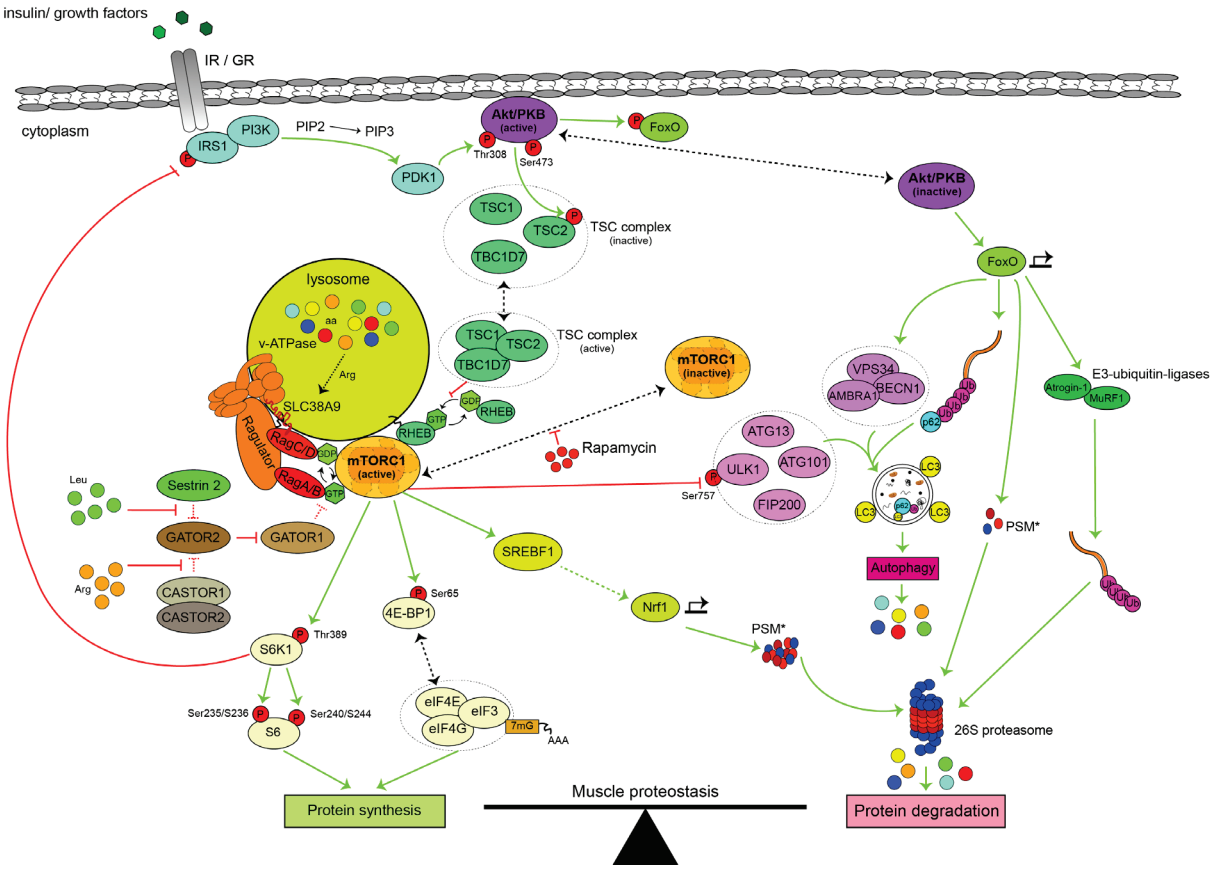

Figure 1: The mTORC1-Akt-FoxO signaling in skeletal muscle regulates muscle proteostasis. By the stimulation with amino acids and growth factors or insulin, mTORC1 is localized at the lysosomal surface in its active form. The left side of the signaling illustrates the role of mTORC1 in regulating anabolic processes. The right side of the signaling depicts the catabolic processes mainly regulated by Akt-FoxO signaling in a continual crosstalk with mTORC1. Important mTORC1-driven mechanisms to regulate catabolic processes are the feedback-loop *via* S6K1 and IRS1 to dampen Akt activity, the blockage of autophagy induction by phosphorylation of ULK1 and the transcriptional induction of Nrf1 to increase proteasomal subunits. Important note: Not all of those interactions have been confirmed in skeletal muscle!

Particularly two amino acids, leucine and arginine, are known to induce mTORC1 localization and to support its activation at the lysosomal surface by the help of specific sensors. Sestrin 2 (SESN2) is a leucine sensor and interacts with GATOR2 to inhibit mTORC1-signaling in the absence of leucine (Chantranupong et al., 2014; Saxton et al., 2016b; Wolfson et al., 2016) **(Figure 1)**. SLC38A9 is a lysosomal arginine sensor, which forms a supercomplex with Ragulator, to transmit arginine sufficiency to mTORC1 (Jung et al., 2015; Rebsamen et al., 2015; Wang et al., 2015) **(Figure 1)**. SLC38A9 functions in parallel with cytosolic arginine sensor for mTORC1 subunit 1 (CASTOR1) to regulate mTORC1 in response to arginine. CASTOR1 heterodimerizes with CASTOR2 to interact with GATOR2 and negatively regulate mTORC1 activtiy **(Figure 1)**. Arginine disrupts this interaction by binding to CASTOR1, which leads to the activation of the mTORC1 pathway (Chantranupong et al., 2016; Saxton et al., 2016a).

mTORC1 activation by growth factors and insulin

Although essential, the dynamic regulation of mTORC1 localization by amino acid availability is not sufficient for the activation of mTORC1, which also requires the presence of the GTPase Ras homolog enriched in brain (RHEB) (Sancak et al., 2010). The guanosine triphosphate (GTP) / guanosine diphosphate (GDP) loading state of RHEB is controlled by the presence of growth factors and GTP-bound RHEB is a direct activator of mTORC1 (Dibble and Manning, 2013; Long et al., 2005) **(Figure 1)**. A protein complex (the TSC complex) comprising TSC1, TSC2 (tuberous sclerosis complex 1 and 2) and TBC1D7 (TBC1 domain family, member 7) functions as GAP for RHEB (Long et al., 2005). Therefore, the TSC complex functions as an upstream inhibitor of mTORC1 and is essential for the growth factor-induced mTORC1 activation (Inoki et al., 2002; Manning et al., 2002) **(Figure 1)**. Binding of growth factors, including insulin and insulin-like growth factors (IGF), to its cell-surface receptors promotes the intracellular recruitment of the insulin-receptor substrate 1 (IRS1), the subsequent activation of the phosphoinositide-3-kinase (PI3K) and the recruitment of the protein kinase B (PKB, hereafter called Akt) to the plasma membrane (Laplante and Sabatini, 2009) **(Figure 1)**. At the plasma membrane, Akt is activated by 3-phosphoinositide dependent protein kinase 1 (PDK1) through phosphorylation at threonine 308 (Alessi et al., 1997; Stokoe et al., 1997; Wick et al., 2000). Akt phosphorylates TSC2, which disrupts its interaction with TSC1 and TBC1D7, which in turn leads to the dissociation of the TSC complex from the lysosomal surface, allowing GTP-loaded RHEB to bind to the lysosomal surface and activate mTORC1 (Inoki et al., 2002; Manning et al., 2002; Menon et al., 2014; Potter et al., 2002) **(Figure 1)**. Akt also activates mTORC1 independently from the TSC complex, by phosphorylating and inactivating proline-rich Akt substrate of 40kDa (PRAS40) at threonine 246, which functions as an inhibitor through its binding to raptor (Sancak et al., 2007; Vander Haar et al., 2007).

mTORC1 regulates translation initiation and protein synthesis

mTORC1 functions as a central regulator of cell growth by controlling key players in protein translation and degradation. Active mTORC1 phosphorylates its targets S6 kinase 1 (S6K1) and 4E-binding protein 1 (4E-BP1) (Ma and Blenis, 2009) **(Figure 1)**. Phosphorylation of 4E-BP1 leads to its dissociation from eukaryotic translation initiation factor 4E (eIF4E), which is essential to start the signaling cascade resulting in the assembly of the 48S pre-initiation complex (Ma and Blenis, 2009) **(Figure 1)**. Phosphorylation of S6K1 promotes protein synthesis by activating ribosomal protein S6 and therefore ribosome biogenesis but also by regulating translation initiation factors (Ma and Blenis, 2009). These activities make mTORC1 a major hub to control mammalian cell size, particularly also in regulating muscle fiber growth.

mTORC1 activation also affects protein catabolism in muscle

Based on the function of mTORC1 in controlling protein synthesis, stimulation of mTORC1 activity was described as mediator of muscle hypertrophy (Bodine et al., 2001; Ruegg and Glass, 2011; Sandri, 2013) and recently proposed as a possible treatment option for muscle wasting conditions (Yoon, 2017).

The results obtained from studies using mice in which TSC1 is specifically deleted in skeletal muscle fibers (called TSCmKO mice), which leads to constantly active mTORC1, however, challenges this concept as most muscles are already atrophic at young age (Bentzinger et al., 2013) and because the mice develop a severe myopathy causing death at the age of approximately one year (Castets et al., 2013). The phenotypic similarity between skeletal muscles of mice that are deficient for *autophagy related 7* (*Atg7)*, a gene essential for macroautophagy (hereafter called autophagy) (Masiero et al., 2009), and of the TSCmKO mice suggested that impairment of autophagy might be responsible for the late-onset myopathy in TSCmKO mice.

The role of mTORC1 in regulating the autophagy-lysosomal pathway

Autophagy is the preferred degradation route for large, cytoplasmic molecules (such as protein aggregates, organelles, lipid droplets or invading bacteria) and is a process that is essential for the clearing of aberrant proteins and cell organelles by delivering the cytosolic substrates to the lysosome for degradation (Dikic, 2017). The autophagy-lysosome pathway (ALP) starts with the engulfment of cellular material, targeted for degradation, by a double-membrane structure called the phagophore, which closes to form the autophagosome (Lamb et al., 2013). Autophagosomes fuse with lysosomes, which provides degradative lysosomal proteases, converting it into an autolysosome (Lamb et al., 2013). The lysosomal proteases degrade the sequestered cytoplasmic material into amino acids and macromolecules that are transported

across the lysosomal membrane to the cytosol for reuse, for example, in the production of new proteins (Lamb et al., 2013). In this context, autophagy provides molecular building blocks during periods of nutrient deprivation but also eliminates unwanted cellular contents. The core machinery that is necessary and sufficient to drive this highly complex process involves more than 30 autophagy-related (ATG) proteins that function sequentially in the formation of the autophagosome (Wang and Klionsky, 2003). The unc-51 like kinase 1 (ULK1) is the most upstream kinase within the autophagy core machinery and its phosphorylation status is the main determinant of autophagy activation. ULK1 is part of a multiprotein complex with ATG13, ATG101 and RB1-inducible coiled-coil 1 (RB1CC1, also known as FIP200) which induces autophagosome formation together with another multiprotein complex composed of vacuolar protein sorting 34 (VPS34), Beclin1, autophagy related (BECN1) and autophagy and beclin-1 regulator 1 (AMBRA1) (Ganley et al., 2009; Hara et al., 2008; He and Levine, 2010; Hosokawa et al., 2009) **(Figure 1)**. The formation of the phagophore requires two ubiquitin-like conjugation systems: the conjugation of ATG12 and ATG5, which are localized to the phagophore and the conjugation to phosphatidylethanolamine of microtubule-associated protein 1 light chain 3 (Map1lc3a, hereafter called LC3) and gamma-aminobutyric acid (GABA) receptor-associated protein-like 1 (GABARAPL1) which are localized to both the phagophore and the autophagosomal membrane (Weidberg et al., 2010). Therefore, LC3 and GABARAPL1 family members have a dual function in contributing to the maturation of the phagophore and interacting with selective autophagy adaptors to facilitate substrate sequestration (Dikic, 2017). Because of all these distinct steps, monitoring of autophagy is very complex and challenging. Importantly, one has to distinguish measurements that monitor the numbers of autophagic elements (such as autophagosomes or autolysosomes), from measurements that measure autophagic flux as the complete process (Klionsky et al., 2012). An important measurement is the accumulation of sequestosome 1 (SQSTM1, hereafter called p62), an ubiquitin receptor for facilitating the degradation of ubiquitinylated proteins in autophagosomes (Rogov et al., 2014), which is used as a readout for autophagy impairment. Another important measurement is the rate of conversion of soluble LC3I to autophagosome-associated LC3II, which is representative of the accumulation of autophagosomes (Klionsky et al., 2012).

mTORC1 phosphorylates and inactivates ULK1 at serine 757, thereby blocking autophagy induction (Kim et al., 2011) **(Figure 1)**. Indeed, autophagy induction was completely blocked in TSCmKO mice due to the phosphorylation of ULK1, and inhibition of mTORC1 activation by rapamycin alleviated this blockage (Castets et al., 2013). The impairment of autophagy induction in TSCmKO mice was further supported and characterized by accumulations of p62, increased levels of LC3I and LC3II and increased expression of genes involved in the ALP, such as *Gabarapl1*, *LC3b*, *cathepsin L* (*Ctsl*) and *BCL2/adenovirus E1B interacting protein 3* (*Bnip3*) (Castets et al., 2013). While inhibition of autophagy can explain the late-onset

myopathy in the TSCmKO mice, the muscle atrophy observed in young TSCmKO mice cannot be explained by this mechanism. Instead, overall protein degradation rates may exceed the rates in protein synthesis, resulting in an imbalanced proteostasis. One possibility for the increased protein degradation could be an overall dampening of Akt signaling as a consequence of sustained mTORC1 activation. This inhibition of Akt could be based on a well-described feedback loop from mTORC1 via S6K1 and IRS1 to Akt (Bentzinger et al., 2008; Harrington et al., 2004) **(Figure 1)**. Inhibition of Akt result in the activation of forkhead box O (FoxO) pathways, which in turn could result in the activation of the ubiquitin-proteasome-system (UPS) **(Figure 1)**.

The crosstalk between mTORC1 and Akt-FoxO-signaling to regulate muscle proteostasis

The discovery that sustained activation of mTORC1 in muscle leads to decreased Akt activity, and that mTORC1 therefore regulates both, muscle anabolism and catabolism in parallel, further highlights the importance of mTORC1 in regulating muscle proteostasis. The protein kinase Akt was established as the major hub at the crossroad in between protein synthesis or protein breakdown. Under nutrient-rich conditions, Akt activates mTORC1 and promotes protein synthesis. In parallel, when the IRS1-PI3K-Akt signaling pathway is active, FoxO transcription factors are inactive and sequestered in the cytosol (Sandri et al., 2004). In contrast, in catabolic states where Akt activity is inhibited, the FoxO transcription factors enter the nucleus and become transcriptionally active (Sandri et al., 2004).

The FoxO transcription factor family is a subclass of forkhead transcription factors characterized by a winged helix deoxyribonucleic acid (DNA)-binding domain known as a forkhead box (Kaestner et al., 2000). The mammalian FoxO family comprises four members: FoxO1, FoxO3, FoxO4 and FoxO6. FoxO transcription factors are involved in several physiological and pathological processes, including aging, cancer and neurological diseases (Greer and Brunet, 2008; Maiese et al., 2008; Webb and Brunet, 2014). Emerging evidence from multiple systems indicate that FoxO transcription factors orchestrate the expression of genes involved in cellular quality control, and in particular the proteostasis network (Kikis et al., 2010). In muscle, activation of FoxO transcription factors induces autophagy and causes atrophy in various catabolic conditions, such as denervation or starvation (Sandri et al., 2004; Zhao et al., 2007). Muscle atrophy involves a transcriptional regulation of a set of genes that are commonly increased or decreased in atrophying muscles during different catabolic conditions and that are named atrogenes (Lecker et al., 2004; Sacheck et al., 2007). These genes are involved in protein degradation (ALP and UPS), antioxidant stress response, DNA repair, mitochondrial function and energy balance pathways (Lecker et al., 2004; Sacheck et al., 2007). Initially, FoxO1, 3 and 4 (hereafter together referred to as FoxO) were identified as the main transcription factors regulating the expression of the atrogenes and ubiquitin-E3-

ligases *F-box protein 32* (*Fbxo32*, hereafter called *Atrogin-1*) and *muscle ring finger 1* (*MuRF1*, also called *Trim63*) (Sacheck et al., 2004; Sandri et al., 2004) **(Figure 1)**. Importantly, FoxO regulates the transcription of various genes involved in autophagy (i.e. *LC3b*, *Gabarapl1*, *Beclin1, Bnip3 and Ctsl*) and thereby induces autophagy (Mammucari et al., 2007; Zhao et al., 2007). Recently, FoxO was shown to be required for the induction of several atrogenes and the newly identified ubiquitin-E3-ligases *F-box protein 30* (*Fbxo30*, also called *Musa1*) and *F-box protein 21* (*Fbxo21*, also called *Smart*) (Milan et al., 2015; Sartori et al., 2013).

In muscles, the two major degradation systems, the ALP and the UPS, are coordinately regulated to remove proteins and organelles upon atrophy (Mammucari et al., 2007; Sandri, 2010; Zhao et al., 2007). Besides regulating the increase of autophagy-related genes and various ubiquitin-E3-ligases, FoxO induces the transcription of some additional atrogenes, which are involved in the UPS. Amongst them are few genes encoding for proteasomal subunits **(Figure 1)**, such as *protease (prosome, macropain) 26S subunit, alpha type 1* (*Psma1)*, *Psmc4*, *Psmd11* and *Psme4*, the *ubiquitin C* gene (*Ubc*), the deubiquitinating enzyme *ubiquitin specific peptidase 14* (*Usp14*) and the E3/E4 enzyme *ubiquitination factor E4B* (*Ube4b*) (Milan et al., 2015). These genes are critical in several steps of the UPS and might have an important role in the control of the proteasome degradation. Therefore, current views indicate that FoxO is the major transcription factor involved in regulating catabolic processes and driving muscle atrophy. Nevertheless, further work is necessary to understand the interplay between the autophagy-lysosomal and the ubiquitin-proteasome degradation system.

Further investigations are also required to understand the crosstalk between mTORC1 and FoxO in regulating muscle proteostasis. This includes not only the regulation of Akt-FoxO-signaling upon sustained activation of mTORC1 mentioned above, but also the regulation of autophagy and of the UPS, both essential processes allowing muscle fibers to adapt to cellular stress and nutritional restrictions. For example, autophagy is associated with both, mTORC1- and FoxO-signaling. While FoxO was shown to be required to induce and sustain autophagic flux, mTORC1 was shown to block autophagy induction completely (Castets et al., 2013; Mammucari et al., 2007; Milan et al., 2015). Under low nutrient condition, mTORC1 is inactive and therefore does not block autophagy induction, while FoxO is essential to induce autophagy to overcome the lack of amino acid and cellular stress (Milan et al., 2015). In contrast, sustained activation of mTORC1 blocks basal and starvation-induced autophagy irrespective of whether FoxO and its autophagy-related target genes are increased or not (Castets et al., 2013). Altogether, these findings suggest that mTORC1 is the dominant regulator of autophagy induction in muscle. Nevertheless, mTORC1 as well as FoxO are essential for maintaining muscle proteostasis and the interplay between both of them ensures a tight coordination of metabolic pathways. Even though, mTORC1 and FoxO both were found to increase the

expression of proteasomal genes, their role in regulating the UPS remains to be resolved. (Milan et al., 2015; Zhang et al., 2014). A further understanding of this mechanism might be important to understand another aspect of the crosstalk between mTORC1 and FoxO in regulating muscle proteostasis.

The ubiquitin-proteasome system

Besides the ALP, the UPS is responsible for maintaining cellular homeostasis. The UPS is the primary degradation system for short-lived, misfolded and damaged proteins (Dikic, 2017). The protein degradation through the UPS starts from attaching a chain of multiple ubiquitin (Ub) molecules to the target proteins of the proteasome **(Figure 2)**. Ubiquitin is a highly conserved small protein with 76-amino acids, which can be covalently coupled to a lysine within a substrate protein (Dikic, 2017). Ubiquitination is both inducible and reversible and requires a cascade of three enzymatic reactions: In the first step, the Ub-activating enzyme (E1) activates Ub and transfers it to the Ub conjugating enzyme (E2), which cooperates with ubiquitin-E3-ligases to attach it to the substrate protein (Dikic, 2017) **(Figure 2)**. Ubiquitin itself contains seven lysine residues that can be targeted in recurrent rounds of this cascade, giving rise to differently linked and branched Ub chains (poly-ubiquitinylation) (Dikic, 2017). The action of ubiquitin-E3-ligases can be reversed by specific deubiquitinases (DUBs) that can cleave Ub from substrates or process different types of Ub chains. (Dikic, 2017) **(Figure 2)**. The key component of the UPS for degradation is the 26S proteasome **(Figure 2)**.

Proteasome structure and function

The 26S proteasome recognizes ubiquitinylated proteins that, upon ATP hydrolysis, translocate into the 20S core particle where they are degraded to short peptides and amino acids (Finley et al., 2016). The 26S proteasome is a multi-catalytic, ATP-dependent protein complex, composed of various subunits that are assembled into two distinct subcomplexes - the 20S proteasome core particle (CP, red in **Figure 2**) and the 19S proteasome regulatory particle (RP, blue in **Figure 2**), which is attached to one or both ends of the 20S proteasome (Finley et al., 2016). In the CP, four stacked heptameric rings of subunits are assembled into an α7β7β7α7 architecture. Thus, the outer rings are formed by the α-subunits and the inner rings are formed by β-subunits (Finley et al., 2016) **(Figure 2)**. Three out of the seven β-subunits are proteolytically active including chymotrypsin-like (cleavage after hydrophobic amino acids, mediated by the β5 subunit), caspase-like (cleavage after acidic residues, mediated by the β1 subunit), and trypsin-like (cleavage after basic residues, mediated by the β2 subunit) activities (Groll et al., 2000) **(Figure 2)**. Because of its closed architecture, the CP requires activators to facilitate gate opening and substrate degradation. The most comprehensively characterized proteasome activator (PA) is the 19S RP, also termed PA700.

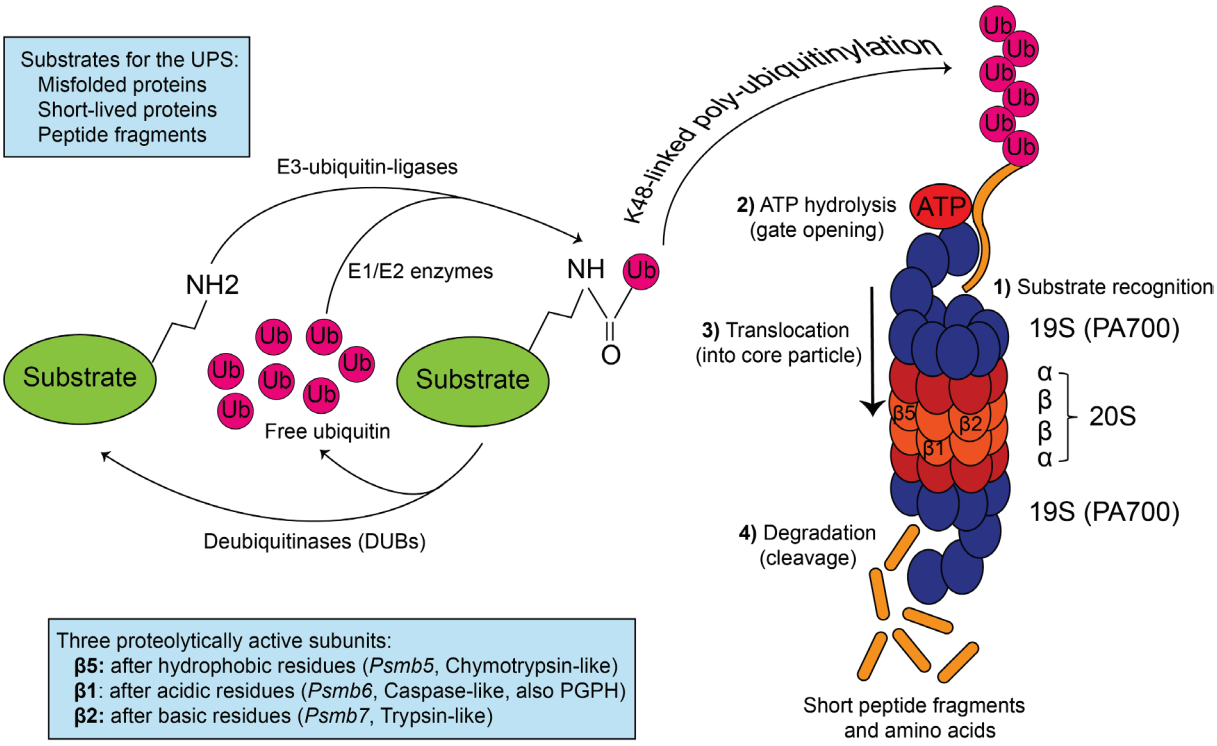

Figure 2: The ubiquitin-proteasome system (UPS) for the degradation of misfolded and short-lived proteins and peptide fragments. The UPS involves attaching of free Ubiquitin (Ub) to substrates using the Ub-activating enzyme (E1), the Ub conjugating enzyme (E2) and the ubiquitin-E3-ligases. The 26S proteasome recognizes K48-linked poly-ubiquitinylated substrates and degrades them to short peptide fragments and amino acids.

The 19S RP regulates proteasome function by identification, binding, deubiquitination, unfolding and translocation of substrates to the proteolytic chamber of the CP (Livneh et al., 2016). The RP is divided into two additional subcomplexes: the “base” and the “lid” (Livneh et al., 2016). The “base” consists of a hexameric ring of six proteasomal ATPases associated with diverse cellular activities (AAA)-family ATPase subunits (PSMC1-PSMC6) (Finley et al., 2016) as well as three ubiquitin receptor subunits, recognizing substrates targeted to the proteasome (PSMD2, PSMD4 and adhesion regulating molecule 1 (ADRM1)) and PSMD1 (Diaz-Villanueva et al., 2015; Fu et al., 1998; Husnjak et al., 2008; Shi et al., 2016). The ATPase ring assists the gate opening of the 20S CP and converts energy from ATP hydrolysis into mechanical force which leads to the unfolding and translocation of proteasome substrates (Maillard et al., 2011; Nyquist and Martin, 2014; Rabl et al., 2008). The “lid” consists of nine different proteasomal subunits (PSMD3, PSMD6, PSMD7, PSMD8, PSMD11, PSMD12, PSMD13, PSMD14 and SEM1, 26S proteasome complex subunit (SEM1)) which form a horseshoe-shaped structure (Livneh et al., 2016). A main function of the lid is deubiquitination of recognized substrates, which is carried out by the DUBs and particularly by PSMD14 and by proteins that transiently associate with the RP, such as the ubiquitin carboxyl-terminal esterase L5 (UCHL5) and USP14 (Leggett et al., 2002; Verma et al., 2002).

Alternative proteasome activators binding to the core particle

The degradation of ubiquitinylated proteins relies on the 26S proteasomes. Nevertheless, some additional proteins can compete with the 19S RP for the occupancy of the ends of the 20S CP, including proteasome activator subunit 1 (PSME1, also PA28α), PSME2 (PA28β), PSME3 (PA28γ) and proteasome activator 200 (PA200, also PSME4) (Finley et al., 2016). PA28α/β/γ are oligomeric ring complexes, belonging to the 11S family of proteasome activators (Stadtmueller and Hill, 2011). PA28α/β assemble into hetero-heptameric, PA28γ into homo-heptameric ring structures with the ability to open the CP by docking to it (Stadtmueller and Hill, 2011). They do not have ATPase activity for substrate translocation into the CP (Finley et al., 2016). However, this does not exclude a role in promoting protein degradation, particularly for substrates that have little or no tertiary structure, such as the cyclin-dependent kinase (CDK) inhibitors p16, p19 and p21, which can diffuse into the CP if the gate is open (Voutsadakis, 2017). Interestingly, PA28α/β/γ do not recognize ubiquitin, which provides an ubiquitin-independent way for protein degradation (Finley et al., 2016). The 20S CP can associate at the same time with either one or two 11S activators, or in combination with 19S RP and a second activator, creating hybrid proteasomes (Tanahashi et al., 2000). PA200 is a 200 kDa monomer that folds into a toroidal shape and promotes only partial opening of the 20S gate (Iwanczyk et al., 2006; Sadre-Bazzaz et al., 2010). PA200 is believed to promote degradation of peptides, but not full-sized proteins and it does not have ATPase activity for translocation (Stadtmueller and Hill, 2011). PA200 is implicated in a variety of processes, including DNA repair (Ustrell et al., 2002), spermatogenesis (Khor et al., 2006), ribosome biogenesis (Lopez et al., 2011), proteasome inhibition and histone degradation (Qian et al., 2013) and mitochondrial fission (Tar et al., 2014). PA200 forms either hybrid proteasomes (19S-20S-PA200), or single / double-capped complexes (PA200-20S and PA200-20S-PA200) (Qian et al., 2013). Reported targets of PA200 are dynamin 1 (DNM1), acetylated histones (Qian et al., 2013) and the transcriptional activator split finger protein 1 (SFP1) (Lopez et al., 2011).

p97 is an essential factor driving the turnover of ubiquitinylated proteins

The chaperone-related, ubiquitin-selective ATPase p97 (also known as VCP) has emerged as an important motor and regulator of many ubiquitin-controlled cellular processes. (Buchberger et al., 2015). p97 is involved in the proteasomal degradation of protein quality control targets, cell cycle regulators, transcription factors and DNA repair proteins, but also in non-proteasomal proteolysis through macroautophagy and the endolysosomal pathway (Meyer et al., 2012). Its involvement in three major cellular proteolysis pathways makes p97 a central element of proteostasis (Buchberger et al., 2015). p97 is a member of the family of AAA ATPases and forms homo-hexameric, ring-structured complexes (Hanson and Whiteheart, 2005) It uses

energy derived from ATP hydrolysis to extract or segregate ubiquitinylated target proteins from stable protein assemblies, membranes and chromatin (Buchberger et al., 2015). p97 was also suggested as proteasome activator but the exact mechanism needs further investigations (Barthelme et al., 2015; Barthelme and Sauer, 2012). Importantly, p97 was found to play a critical role during muscle atrophy in the accelerated degradation of muscle proteins *via* the proteasomal and autophagy pathway (Piccirillo and Goldberg, 2012). In the same study, they showed that the expression of p97 in muscles and myotubes helps to limit muscle growth by promoting protein degradation (Piccirillo and Goldberg, 2012).

Nrf1 induces transcription of proteasomal biogenesis

In yeast, the main transcriptional regulator of proteasome biogenesis is stress-regulated transcription factor RPN4 (RPN4), which binds to the promoters of most PSM genes *via* the conserved proteasome-associated control element (PACE) motif (Mannhaupt et al., 1999). RPN4 is itself rapidly degraded by the proteasome. When RPN4 degradation is compromised, its stabilization and accumulation leads to elevated levels of proteasome synthesis. Therefore, RPN4 is involved in a negative feedback loop, which promotes transcription from most PSM genes (Xie and Varshavsky, 2001). A similar mechanism was described in *Caenorhabditis elegans* (*C. elegans*) for Protein skinhead-1 (SKN-1). When proteasome gene expression and activity are blocked, SKN-1 activates multiple classes of proteasome subunit genes in a compensatory response, thereby maintaining UPS activity (Li et al., 2011). In contrast, when translation elongation is impaired, SKN-1 does not upregulate proteasome genes which results in reduced UPS activity (Li et al., 2011). Altogether, these studies in yeast and *C. elegans* support a model that protein synthesis and degradation may be coupled processes. Mammals lack an RPN4 orthologue but have one of SKN-1. The transcription factor nuclear factor, erythroid derived 2, -like 1 (NFE2L1 and TCF11, hereafter called Nrf1) provides a comparable feedback mechanism, which is also activated by proteasome inhibitors, such as bortezomib (Radhakrishnan et al., 2010; Steffen et al., 2010).

The CNC-bZIP family of transcription factors

Nrf1 is a member of the cap'n'collar basic-region leucine zipper (CNC-bZIP) family of transcription factors that further comprises the activators nuclear factor-erythroid 2 (NFE2) p45, NFE2L2 (hereafter called Nrf2), NFE2L3 and locus control region-factor 1 (LCR-F1 or Nrf1β), and the repressors BACH1 and BACH2 (BTB and CNC homology 1, basic leucine zipper transcription factor 1 and 2) and the founding member *Drosophila melanogaster* CNC protein (Zhang and Xiang, 2016). Several other important transcriptional regulators belong to the CNC-bZIP family, such as jun proto-oncogene (Jun, also AP-1), hypoxia-inducible factor 1α (Hif1α), nuclear factor κB (NF-κB) and transformation-related protein 53 (p53) (Zhang and

Xiang, 2016). The CNC domain that characterizes this family of proteins binds to the antioxidant or electrophile response element (ARE or EpRE), a DNA element with the consensus sequence 5′-TGACNNNGC-3′ (Rushmore et al., 1991). The ARE/EpRE element is found in the enhancers of promoters of many enzymes involved in antioxidant responses, xenobiotic metabolism and inflammatory responses (Hayes et al., 1999; Nguyen et al., 2003; Rushmore et al., 1991). In response to oxidative stress, transcriptional expression of ARE/EpRE-driven genes is regulated primarily by CNC–bZIP family factors, aiming to maintain an appropriate redox homoeostasis. Amongst others, ARE/EpRE-target genes encoding for NAD(P)H dehydrogenase, quinone 1 (NQO1), heme oxygenase 1 (HMOX1), metallothionein 1 and 2 (MT1, MT2), glutamate-cysteine ligase (GCLC, GCLM), glutathione synthetase (GSS), glutathione S-transferases (GSTs), ferritin (FTH1, FTL1), peroxiredoxin 1 (PRDX1), thioredoxin 1 (TXN1) and malic enzymes (ME1 and ME2) (Bugno et al., 2015; Zhang and Xiang, 2016).

Transcriptional activity is different between Nrf1 and Nrf2

Of the CNC transcription factors, Nrf1 and Nrf2 represent the primary factors that heterodimerize with the small musculoaponeurotic fibrosarcoma (Maf) proteins (MafF, MafG, MafK) in the nucleus and bind to the ARE/EpRE (Biswas and Chan, 2010; Itoh et al., 1997; Jaiswal, 2004). Altough, both Nrf1 and Nrf2, similarly regulate an ARE/EpRE-driven transcriptional programm against cellular stress, Nrf1 fullfils some unique functions that are distinct of Nrf2. Nrf1, but not Nrf2, is indispensable for development and healthy growth, demonstrated by a global knockout of *Nrf1* in mice causing embryonic lethality (Chan et al., 1998; Chan et al., 1996; Leung et al., 2003). Conditional KO of *Nrf1* in liver results in oxidative stress, non-alcoholic steatohepatitis (NASH) and hepatic cancer (Ohtsuji et al., 2008; Xu et al., 2005). Importantly, Nrf2 is not able to compsensate for a loss of Nrf1 function in liver, suggesting an independent activation of ARE/EpRE-target genes (Ohtsuji et al., 2008). In contrast, Nrf2 appears to be dispensable for the expression of most ARE/EpRE-driven cytoprotective genes and Nrf2 KO mice develop normally (Chan et al., 1996). Moreover, tissue-specific loss of Nrf1 in mouse pancreas, brain and bone results in pathologies of diabetes (Zheng et al., 2015), neurodegeneration (Kobayashi et al., 2011; Lee et al., 2011) and reduced bone formation (Kim et al., 2010). These remarkable phenotypic changes are accompanied by significant disorders of glucose, lipid and protein metabolism, in addition to severe endogenous oxidative stress (Zhang and Xiang, 2016). Together, these findings demonstrate that Nrf1 fulfils a unique and indispensable biological function in regulating antioxidative response, which is distinct from that of Nrf2.

Nrf1 is a critical regulator of genes encoding for 26S proteasomal subunits

The funciton of Nrf1 and its role as transcription factor received even more attention when it was shown that it is involved in the regulation of proteasomal biogenesis (Radhakrishnan et al., 2010; Steffen et al., 2010). Besides neurodegeneration, mice lacking Nrf1 in brain displayed an impaired proteasome function, which was accompanied by a coordinated down-regulation of various genes encoding for 26S proteasomal subunits (Lee et al., 2011). Although Nrf2 knockout brains showed evidence of oxidative stress, impairment in proteasome activity was not detected and the regulation of proteasomal genes was shown to be Nrf1-specfific (Lee et al., 2011). Tissue-specific *Nrf1* KO in liver revealed a similar reduced expression of PSM genes as found in the brain KO and also diminished proteasome activity (Lee et al., 2013). Nrf2 has also been reported to activate the expression of proteasomal subunits, but only upon exposure to oxidative stress (Kwak et al., 2003). It is important to note that Nrf1 regulates PSM gene expression through the activation of the ARE in the promoter region of the PSM genes (Radhakrishnan et al., 2010; Steffen et al., 2010). In addition to the coordinated induction of all proteasomal subunits, Nrf1 also regulates p97 (Sha and Goldberg, 2014) and p62 (Sha et al., 2018), which are both essential for the UPS.

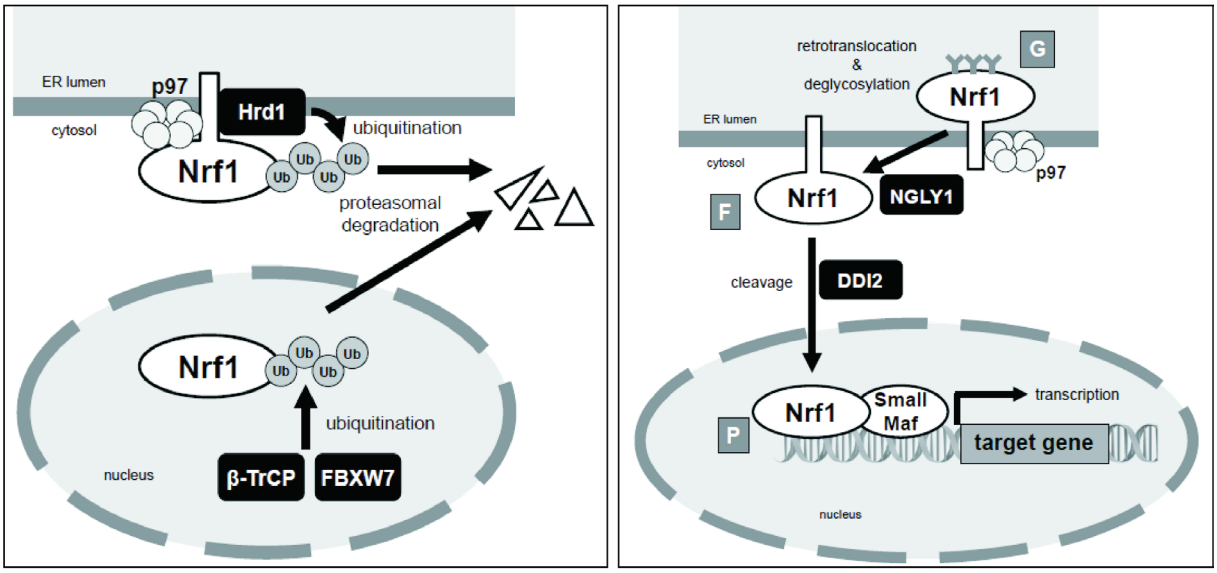

Figure 3: Nrf1 is the mammalian regulator of the "bounce-back" response to increase proteasomal biosynthesis upon proteasomal perturbation. *Left:* Under normal conditions, Nrf1 is a short-lived protein and maintained at low levels. ER-anchored Nrf1 is ubiquitinylated (Hrd1/SYVN1), retrotranslocated (p97) and degraded by the proteasome. In the nucleus, Nrf1 is ubiquitinylated (β-TrCP and FBXW7) and degraded by the proteasome. *Right:* When proteasome function is compromised, Nrf1 is stabilized and transcriptionally active. Nrf1 is glycosylated (G) in the ER and retrotranslocated (p97). In the cytosol, polysaccharides attached to Nrf1 are removed by NGLY1 to generate the full-length Nrf1 (F, also Nrf1 FL), which is cleaved by DDI2 and produces the cleaved, processed Nrf1 (P, also Nrf1 CL). Processed Nrf1 translocates from the ER into the nucleus and promotes the expression of target genes including genes encoding for proteasomal subunit. (Koizumi et al., 2018)

Importantly, Nrf1 was identified as the mammalian regulator of a, in higher eukaryotes well conserved (Lundgren et al., 2005; Meiners et al., 2003; Mitsiades et al., 2002), positive-feedback circuit (also called “bounce-back” response), which increases proteasomal biosynthesis upon proteasomal pertubation (i.e. with proteasomal inhibitors as chemotherapeutic drugs) (Radhakrishnan et al., 2010; Sha and Goldberg, 2014; Steffen et al., 2010). Nrf1 is ubiquitously expresssed as an endoplasmic reticulum (ER) transmembrane protein possessing a long C-terminal portion with N-linked glycosylation in the ER lumen and a short N-terminal portion in the cytosol (**Figure 3**) (Radhakrishnan et al., 2014; Zhang et al., 2007). Thus, newly synthesized Nrf1 is anchored and embedded into the ER membrane with its N-terminal homology box 1 (Nhb1) domain (Zhang et al., 2007). Nrf1 is a short-lived protein, which is generally maintained at low levels by subjecting it to ER-associated degradation (ERAD) (Koizumi et al., 2018). Under normal conditions, Nrf1 is constitutively ubiquitinylated by the ER-resident ubiquitin-E3-ligase Hrd1 (also called synovial apoptosis inhibitor 1, synoviolin (SYVN1)), the luminal portion of Nrf1 is retrotranslocated to the cytoplasm by the p97 ATPase and then degraded by the proteasome (Radhakrishnan et al., 2014; Steffen et al., 2010) (**Figure 3**). In the nucleus, Nrf1 stability is regulated through ubiquitinylation by beta-transducin repeat containing protein (β-TrCP) and F-box and WD-40 domain protein 7 (FBXW7) and then degraded by the proteasome (Biswas et al., 2011; Tsuchiya et al., 2011) (**Figure 3**). Nrf1 is stabilized and accumulates to high levels when proteasome function is compromised resulting in a release of processed Nrf1 (P) from the ER into the nucleus and transcriptional activation of PSM genes (Radhakrishnan et al., 2014). During this process, the glycosylated (G) luminal part of Nrf1 is rapidly exported into the cytosol by p97 (Radhakrishnan et al., 2014) and subsequently deglycosylated by N-glycanase 1 (NGLY1) (Tomlin et al., 2017) to generate full-length Nrf1 (F, also Nrf1 FL) (**Figure 3**). Cleavage of Nrf1 FL at leucine 104 by the aspartic protease DNA-damage inducible protein 2 (DDI2) (Koizumi et al., 2016) produces the processed, cleaved Nrf1 (P, also Nrf1 CL), which translocates to the nucleus (**Figure 3**). In the nucleus, processed Nrf1 (P) heterodimerizes with small Maf proteins and binds to ARE in the promoter region of PSM genes, to upregulate their expression (Koizumi et al., 2016; Radhakrishnan et al., 2014; Radhakrishnan et al., 2010; Steffen et al., 2010) (**Figure 3**). In addition to N-linked glycosylation, O-linked glycosylation was described as an important post-translational modification involved in Nrf1 transcription activity (Han et al., 2017; Sekine et al., 2018). O-linked N-acetylglucosamine (GlcNAc) transferase (OGT) is a positive regulator of Nrf1 transcription activity by increasing the stability of Nrf1 (Sekine et al., 2018). Ogt interacts with Nrf1 *via* host cell factor C1 (HCFC1) and modifies Nrf1 with GlcNAc polysaccharides, which attenuates the ubiquitination of Nrf1 prior to degradation resulting in the stabilization and increased transcriptional activity of Nrf1 (Han et al., 2017; Sekine et al., 2018).

mTORC1-dependent activation of Nrf1 upon proteasome inhibition

Besides regulating various processes involved in protein synthesis, mTORC1 was also implicated in the regulation of lipid synthesis *via* the sterol regulatory element binding transcription factor 1 (SREBF1, also known as SREBP1) (Duvel et al., 2010). More recently, it was shown that mTORC1 induces *Nrf1* transcription through the posttranslational activation of SREBF1, which activates the transcription of proteasomal genes (Zhang et al., 2014) **(Figure 1)**. This mechanism was studied in TSC2-deficient mouse embryonic fibroblasts (MEFs) and in brain and liver tissue. Whether mTORC1 regulates Nrf1 also in muscle tissue and whether this would lead to a similar activation of proteasomal genes has yet to be investigated. Since the “bounce-back” response links protein synthesis to proteasome degradation, this could be a novel mechanism by which mTORC1 additionally regulates catabolic processes to maintain muscle proteostasis.

Proteasome inhibition as a therapeutic mean

Proteasome inhibition has mainly been studied in the context of cancer treatment and neurodegenerative diseases because of its anti-inflammatory activity. Effective proteasome inhibition is achieved by either using proteasome inhibitors, drugs that chemically block the action of proteasomes or by inactivating specific subunits and the assembly of the proteasome. In the latter case, few publications showed that inactivation of subunits or proteasomal assembly in distinct tissues leads to a dysregulation of the proteasome, to the accumulation of damaged and misfolded proteins and even leads to embryonic lethality in mice (Ding et al., 2006; Sasaki et al., 2010; Stohwasser et al., 1996).

Proteasome inhibitors

More promising is the usage of reversible proteasome inhibitors that chemically block the proteolitically active enzymes of the proteasome. One of the most widely used proteasome inhibitors is MG132. MG132 is largely used in *in vitro* experiments and is a very potent and reversible proteasome inhibitor of the chymotrypsin-like activity (Lee and Goldberg, 1998). MG132 belongs to the class of synthetic peptide aldehydes, which also inhibit certain lysosomal cysteine proteases and the calpains (Lee and Goldberg, 1998). The first non-peptidic proteasome inhibitor discovered was lactacystin, which irreversibly inhibited trypsin-like, chymotrypsin-like and caspase-like activity but also inhibits proteases other than the proteasome, namely cathepsin A and tripeptidyl peptidase II. (Craiu et al., 1997; Fenteany et al., 1995). The first specific, natural proteasome inhibitor found was epoxomicin, which irreversibly inhibits all three proteolytically active enzymes of the proteasome and which demonstrates anti-inflammatory activity (Meng et al., 1999). The newest group of proteasome inhibitors, which are further developed until today belong to the group of dipeptidyl boronic

acids. These inhibitors bind reversibly to the chymotryptic enzyme of the proteasome, show much higher potency and do not inhibit other cellular proteases (Adams et al., 1998). PS-341 (hereafter called bortezomib, marketed as Velcade) was one of this dipeptidyl boronic acids and was the first proteasome inhibitor that entered clinical trials for cancer treatment (Adams et al., 1999). Bortezomib was the first proteasome inhibitor, that was approved for the treatment of adult patients with multiple myeloma, a particular white blood cell cancer (Adams and Kauffman, 2004). Two other proteasome inhibitors were approved for the treatment of multiple myeloma: Carfilzomib (marketed as Kyprolis) an analog of epoxomicin (Meng et al., 1999; Wang et al., 2013) and ixazomib (marketed as Ninlaro) a boronic acid derivative which was developed by Takeda.

Proteasome inhibitors in cancer treatment

Cancer cells produce proteins that promote both cell survival and proliferation, and/or inhibit mechanisms of cell death. Amongst other functions, the UPS prevents the accumulation of misfolded, damaged or deleterious proteins. Therefore, preclinical testing of proteasome inhibitors aimed to shift the equilibrium of proteostasis towards cell death (Manasanch and Orlowski, 2017). Initially, proteasome inhibitors were developed to prevent cancer-related cachexia (Manasanch and Orlowski, 2017). Then, preclinical studies demonstrated that proteasome inhibitors induce apoptosis in various cancer cell lines and murine models of cancer and were postulated as chemotherapeutics (Manasanch and Orlowski, 2017; Mitsiades et al., 2002). One of the earliest findings was, that proteasome inhibitors with a boronic acid (i.e. bortezomib) could inhibit NF-κB-signaling by blocking the degradation of the NF-κB inhibitor IκB, thereby preventing nuclear translocation of NF-κB, and repressing its transcriptional activity to induce inflammatory mediators, inhibitors of apoptosis and oncogenic proteins (Lee and Goldberg, 1998; Palombella et al., 1994). As mentioned above, bortezomib, carfilzomib and ixazomib are currently approved for the treatment of multiple myeloma or mantle-cell lymphoma (MCL). Full regulatory approval of bortezomib occurred in 2005, following the publication of results from a large phase III trial in patients with relapsed multiple myeloma comparing dexamethasone and bortezomib treatment (Richardson et al., 2005). Therefore, one of the nowadays most widely used combination treatment options for patients with newly diagnosed multiple myeloma comprises bortezomib, lenalidomide and dexamethasone (Richardson et al., 2010). Unfortunately, up to 80% of patients with newly diagnosed multiple myeloma treated with bortezomib develop any grade of neuropathy, but the exact underlying mechanisms are not fully understood (Richardson et al., 2010). In contrast to the boronates (i.e. bortezomib and ixazomib), carfilzomib is an epoxyketone that irreversibly binds to the chymotrypsin-like enzyme of the proteasome, which prolongs the duration of proteasome inhibition (Alsina et al., 2012). The possibility of a long-duration inhibition provided

the rationale for phase I studies of carfilzomib, which revealed that this agent is both tolerable and active against relapsed and/or refractory multiple myeloma (Alsina et al., 2012). Carfilzomib seems to have distinctly different adverse effects compared to that of bortezomib. Whereas the rates of peripheral neuropathy are lower with carfilzomib, a few patients have developed cardiovascular complications (Korde et al., 2015). The major advantage of ixazomib, which is the newest approved proteasome inhibitor, compared to previous proteasome inhibitors is that it can be distributed orally (Richardson et al., 2014). Ixazomib in combination with lenalidomide and dexamethasone demonstrated less neuropathy and improved progression-free survival (the length of time during and after the treatment of the cancer that a patient lives with the disease but it does not get worse) in patients with relapsed or refractory myeloma (Richardson et al., 2015). Additional studies of ixazomib using several distinct settings are underway.

Nrf1 mediates resistance to proteasome inhibitors in malignant cells

Importantly, promising preclinical data, obtained with bortezomib in models of solid tumors, failed to demonstrate any efficacy in clinical studies in patients (Frankland-Searby and Bhaumik, 2012; Johnson, 2015). Therefore, investigations into the mechanisms of resistance are essential to improve the efficacy and the utility of proteasome inhibitors. Interestingly, amongst many other candidates, Nrf1 was associated as mediator of proteasome inhibitor resistance in malignant cells. The observation that therapeutic proteasome inhibition promptly triggers the upregulation of proteasome genes in malignant cells (Mitsiades et al., 2002), was associated with the Nrf1-induced “bounce-back” response (Radhakrishnan et al., 2010; Steffen et al., 2010). Therefore, Nrf1 received significant medical relevance as regulator of an important compensatory response that promotes tumor cell survival and attenuates therapeutic efficacy (Dikic, 2017; Weyburne et al., 2017). Interestingly, increased protein O-linked glycosylation was described in a wide range of cancers and it got attention as a new target in cancer treatments (Fardini et al., 2013). As mentioned earlier, a recent study has revealed that O-linked glycosylation by OGT makes a critical contribution to the proteasome bounce-back response *via* increasing the stability and transcriptional activity of Nrf1 (Han et al., 2017; Sekine et al., 2018). The discovery of the interaction between Nrf1 and the OGT/HCFC1 complex has added a new regulatory axis to the proteasome bounce-back response and identified OGT as a new therapeutic target for sensitizing cancer cells to proteasome inhibitors (Sekine et al., 2018). Interestingly, recent studies demonstrate that increased levels of OGT and O-linked glycosylation, found in obese mice and cancer cells, are caused by higher mTORC1 activity (Park et al., 2014; Sodi et al., 2015; Very et al., 2018).

Proteasome inhibition and muscle proteostasis

The muscle atrophy that occurs in catabolic states largely results from accelerated breakdown of long-lived myofibrillar proteins, such as actin or myosin, by the UPS (Mitch and Goldberg, 1996). Therefore, proteasome inhibitors were tested to counteract muscle atrophy and several *in vivo* studies report beneficial effects on muscle proteostasis and atrophy by applying proteasome inhibitors on distinct catabolic states, such as sepsis (Fischer et al., 2000; Supinski et al., 2009), hindlimb casting (Krawiec et al., 2005; Vargas and Lang, 2008), hindlimb unloading (Jamart et al., 2011) and denervation (Beehler et al., 2006). A study in a murine model of hindlimb immobilization demonstrated that MG132 not only preserves muscle mass and increases cross-sectional area (CSA), but also decreased the expression of *Atrogin-1* and *MuRF1* and diminished the rehabilitation time of these mice (Caron et al., 2011). Importantly, proteasome inhibitors were also applied in mouse models of muscular dystrophies. MG132-treatment of dy^{3K}/dy^{3K} mice, a mouse model for laminin-α2-related muscular dystrophy (LAMA2-MD), significantly improved the dystrophic phenotype of these mice (Carmignac et al., 2011). Surprisingly, proteasome inhibition did not only improve muscle weight and CSA but also muscle histology, decreased marker of apoptosis and improved locomotion and lifespan (Carmignac et al., 2011). Similar results have been obtained by treating dy^{3K}/dy^{3K} mice with bortezomib, which increases the clinical relevance of such a treatment (Korner et al., 2014). Using bortezomib-treatment in a mouse model for spinal muscular atrophy (SMA) revealed an increase of the survival motor neuron 1 (SMN1) protein (Kwon et al., 2011). Decreased expression of this protein is the cause of SMA. Furthermore, bortezomib improved motor function, neuromuscular junction (NMJ) size and muscle pathology in these mice (Kwon et al., 2011). Increased survival was only observed after combining the treatment with the histone deacetylase inhibitor trichostatin A (TSA), which is an inducer of *Smn* gene transcription (Kwon et al., 2011).

Even though bortezomib can shift the balance of muscle proteostasis and can prevent muscle wasting in animal models (Beehler et al., 2006; Carmignac et al., 2011; Caron et al., 2011; Kwon et al., 2011), its use is not approved in patients for treatment of muscle atrophy. Indeed, clinical trials with bortezomib for the treatment of cancer cachexia have not shown consistent results (Madeddu and Mantovani, 2009; Penna et al., 2016). Proteasome inhibitors have various adverse effects and complete blockage of the UPS is detrimental for muscle fibers, as recently confirmed by a study investigating the effect of a *Psmc4* knockout in murine muscles (Kitajima et al., 2014). These muscles showed dysregulated proteasomal activity, basophilic inclusions and disorganization of the sarcomeres in young adult mice, suggesting that appropriate proteasomal activity is important to maintain muscle homeostasis (Kitajima et al., 2014). Therefore, it would be interesting to test the effect of dampening the UPS by intermittent inactivation or destabilization of Nrf1 activity and its consequences on muscle proteostasis.

The role of the UPS and mTORC1 in regulating proteostasis in sarcopenia

Sarcopenia is probably the most frequent but least understood type of systemic muscle loss. The muscle wasting that is characteristic for sarcopenia differs largely from other wasting conditions, as the muscle loss develops slowly and gradually over time (Cohen et al., 2015). Sarcopenia may affect as much as 15% of the population aged 65 years and above and approximately 50% of individuals aged over 80 years old (Cohen et al., 2015). This loss of muscle substantially reduces quality of life and physical activity and independence of older people and the increased frailty leads to falls, fractures and admission to hospitals and nursing homes (Cosqueric et al., 2006; Fielding et al., 2011). Investigating the underlying mechanisms of sarcopenia in patients but also in animal models is difficult. Several other diseases and co-morbidities often accompany sarcopenia and precede or directly contribute to the muscle wasting. Therefore, muscle wasting in sarcopenia can be a combination of many factors and differs largely between individuals. Therefore, it is important to discriminate between age-related and sarcopenic pathology. This might also explain the controversial findings about the state of muscle proteostasis and of the UPS in aging or sarcopenia. In many aging studies, the function of the UPS and the proteasome function in particular, was reported to decrease with age in various tissues and organs (Chondrogianni and Gonos, 2005; Dahlmann, 2007; Gaczynska et al., 2001; Tonoki et al., 2009), including decreased gene expression of proteasomal subunits in aging mice (Lee et al., 1999; Lee et al., 2000). Notably, UPS dysfunction is present in several age-related neurodegenerative disorders, such as Alzheimer's (Keck et al., 2003), Parkinson's (McNaught et al., 2003) or Huntington's disease (Seo et al., 2004). In contrast, by focusing on sarcopenia, a study from aged, 30-month-old rats reported a marked loss of muscle mass accompanied by increased expression of proteasomal subunits, proteasome activity, ubiquitinylation and DUB-activity (Altun et al., 2010). Nevertheless, expression of genes coding for the proteasomal subunits were not increased in aged rats and the expression of the atrogene program differed from the one of rapid atrophy (Altun et al., 2010). Although these findings indicate an increase of the UPS and increased overall protein degradation, there is currently no successful approach for using proteasome inhibitors to attenuate muscle wasting in sarcopenia.

Besides increased proteolysis and muscle wasting, sarcopenic muscles are characterized by a loss of mitochondria, mitochondrial dysfunction, increased apoptosis, disrupted NMJs, increased fiber denervation and decreased rates of protein synthesis (Chai et al., 2011; Combaret et al., 2009; Deschenes et al., 2010; Ibebunjo et al., 2013). The observation that protein synthesis declines with age raises the question, whether activation of mTORC1 is beneficial for sarcopenic muscles and whether it helps to avoid age-related muscle wasting. The role of mTORC1 activity in sarcopenia is still controversially discussed. Several studies reported decreased activity of the Akt-mTORC1 pathway in older age groups compared to

younger groups (Cuthbertson et al., 2005; Leger et al., 2008; Pallafacchina et al., 2002). In contrast, however, recent studies observed hyperphosphorylation of mTORC1 in aged human muscles, but also in muscles of aged mice and rats (Joseph et al., 2019; Markofski et al., 2015; White et al., 2016). Importantly, TSCmKO mice develop precocious sarcopenia (Bentzinger et al., 2013; Castets et al., 2013; Guridi et al., 2015), characterized by fragmentation of the NMJ (Ham et al., 2019, in preparation), severe muscle wasting and progressive loss of muscle mass (Bentzinger et al., 2013; Castets et al., 2013), loss of muscle force (Bentzinger et al., 2013; Castets et al., 2013) and accumulation of misfolded proteins (Guridi et al., 2015). As mentioned above, treatment with rapamycin normalizes autophagy in TSCmKO mice and ameliorates many of the signs of the myopathy (Castets et al., 2013). This is in accordance with a recent study, that describes the beneficial effects of mTORC1 inhibition on muscle wasting observed in aged rats (Joseph et al., 2019). Hence, the understanding of the role of mTORC1 in regulating muscle proteostasis is also of fundamental importance to find means to mitigate sarcopenia.

5. Rationale and objectives of the thesis

Several lines of evidence points to an important role of mTORC1 in controlling muscle proteostasis. Based on its stimulation in nutrient-rich conditions and on its function in regulating translation and protein synthesis, the role of mTORC1 in mediating muscle anabolism is well established. In contrast, the exact mechanism of how mTORC1 stimulates and activates catabolic processes to induce muscle atrophy is unknown. **The overall objective of my PhD thesis was to characterize the role of mTORC1 in maintaining muscle proteostasis *in vivo*.**

The first specific aim of my PhD study was to investigate the underlying mechanisms of the mTORC1-driven muscle atrophy observed in young TSCmKO mice. For this purpose, comprehensive analysis of whole-genome and proteome data of TSCmKO mice was analyzed to identify catabolic processes, which are activated in response to sustained activation of mTORC1.

The identification, of the ubiquitin-proteasome-system (UPS) as major catabolic process, which is induced by sustained activation of mTORC1, in the first part of this thesis was then expanded into an extensive project to study the mTORC1-dependent induction of the UPS.

Thus, the second specific aim of my PhD study was to determine if sustained activation of mTORC1 increases the UPS *via* the Akt-FoxO-signaling or by distinct other, unknown catabolic pathways. To test this, several distinct interventions and different mouse models, targeting specific parts of the mTORC1-Akt-FoxO-signaling, were carried out and led to the identification of Nrf1 as a mediator of mTORC1-driven muscle atrophy.

Lastly, I investigated whether inactivation of Nrf1 is sufficient to disable the activation of the UPS in TSCmKO mice and if this would be sufficient to attenuate mTORC1-driven muscle atrophy

Hence, during my PhD study, I aimed to understand all of how mTORC1 is involved in regulating catabolic processes and muscle proteostasis and thereby maintains body function and health.

6. Results and Discussion

***Part 1* - Manuscript: "mTORC1-dependent increase of the ubiquitin-proteasome system disturbs muscle proteostasis"**

mTORC1-dependent increase of the ubiquitin-proteasome system disturbs muscle proteostasis

Marco Kaiser[1,#], Giulia Milan[1,#], Shuo Lin[1], Kathrin Chojnowska[1], Daniel J. Ham[1], Filippo Oliveri[1], Lionel Tintignac[1,2], Nitish Mittal[1], Christian Zimmerli[1,$], David J. Glass[3], Mihaela Zavolan[1] and Markus A. Rüegg[1]*

[1] Biozentrum, University of Basel, Basel, Switzerland

[2] Neuromuscular Research Group, Departments of Neurology and Biomedicine, University of Basel, University Hospital Basel, Basel, Switzerland

[3] Novartis Institutes for Biomedical Research, Cambridge, MA, USA

[$] present address: European Molecular Biology Laboratory (EMBL), Heidelberg, Germany

[#] These authors contributed equally to this work

key words: mTORC1, Nfe2l1, Nrf1, FoxO, Proteasome, Muscle, Atrophy, Ubiquitin-proteasome system

***Corresponding author:**

Markus A. Rüegg
Biozentrum
University of Basel
Klingelbergstrasse 70
CH-4056 Basel
Switzerland

Email: markus-a.ruegg@unibas.ch
Phone: +41 61 207 22 23
Fax: +41 61 207 22 08

Abstract

Skeletal muscle is crucial for human daily life, ensuring locomotion, breathing and affecting whole-body metabolism. The continuous adjustment of the balance in muscle proteostasis is essential for maintaining regular muscle growth during life. Perturbation of this balance by extrinsic factors, as for example seen in cachexia or in sarcopenia, is a main cause of loss of life quality and increased mortality. Thus, a better molecular understanding of muscle proteostasis is of fundamental importance to develop possible treatment strategies to counteract the above diseases. The mammalian (or mechanistic) target of rapamycin complex 1 (mTORC1) has emerged as an important regulator of cellular growth. Because of its role in regulating translation and protein synthesis, mTORC1 was proposed as mediator of muscle hypertrophy. However and in striking contrast to the expected outcome of muscle gain, sustained activation of mTORC1 in muscle by knockout of its upstream inhibitor TSC1 (TSCmKO mice) results in atrophy. The underlying mechanism of this mTORC1-driven atrophy remained unresolved. Here we demonstrate that sustained activation of mTORC1 in muscles of TSCmKO mice leads to a significant increase of the ubiquitin-proteasome system (UPS). Surprisingly, constitutive activation of Akt in muscle resulted in a similar induction of the UPS as observed in TSCmKO mice, suggesting an UPS activation mechanism, which is, at least in part, independent of the activation of FoxO transcription factors. Finally, we identify the transcription factor Nrf1 (also referred to as NFE2L1) as an important mediator of mTORC1-driven activation of the UPS. Together, these results provide new information about the role of mTORC1 in regulating muscle proteostasis, which might help to develop new therapeutic agents that could slow-down muscle wasting.

Introduction

Skeletal muscle wasting is a hallmark of neuromuscular diseases and is associated with many pathophysiological conditions, such as cancer, aging, AIDS and chronic diseases of the heart or kidney. The balance of muscle proteostasis ultimately determines muscle size: if overall rates of protein degradation are lower than the overall rates in protein synthesis muscle will grow (hypertrophy); if overall rates of protein degradation outstrips the overall rates in protein synthesis muscle shrinks (atrophy) (Sandri, 2013).

Mammalian (or mechanistic) target of rapamycin (mTOR) is a protein serine/threonine kinase that assembles into two distinct multi-protein complexes, called mTORC1 and mTORC2 (Laplante and Sabatini, 2012; Shimobayashi and Hall, 2014). Studies in mice have shown that mTOR function in skeletal muscle is largely based on the activity of mTORC1 and not of mTORC2 (Bentzinger et al., 2008; Risson et al., 2009). High doses of the name-giving drug rapamycin block mTORC1 instantaneously through direct binding of the FK506-binding protein 1a (FKBP1A, also FKBP12)-rapamycin complex (Laplante and Sabatini, 2012). mTORC1 is activated by different cellular inputs, such as amino acids, insulin, growth factors and energy status, to drive cell growth through increasing protein translation and lipid synthesis or by activating energy metabolism, ATP production and glycolytic flux (Laplante and Sabatini, 2012). Activation of mTORC1 involves Ragulator-Rag complex mediated amino acid sensing, which recruits and anchors mTORC1 to the lysosomal membranes (Sancak et al., 2010). In parallel, mTORC1 becomes fully activated by growth factors *via* the insulin receptor substrate 1 (IRS1) – protein kinase B (PKB, hereafter called Akt) pathway (Inoki et al., 2002; Manning et al., 2002; Menon et al., 2014). A protein complex (the TSC complex) comprising TSC1, TSC2 (tuberous sclerosis complex 1 and 2) and TBC1D7 (TBC1 domain family member 7) functions as an upstream inhibitor of mTORC1 and is essential for the growth factor-induced mTORC1 activation (Inoki et al., 2002; Manning et al., 2002). mTORC1 controls protein synthesis by phosphorylating its targets S6 kinase 1 (S6K1) and 4E-binding protein 1 (4E-BP1) (Ma and Blenis, 2009). Phosphorylation of 4E-BP1 leads to its dissociation from eukaryotic translation initiation factor 4E (eIF4E), which is essential to start the signaling cascade resulting in the assembly of the 48S pre-initiation complex (Ma and Blenis, 2009). Phosphorylation of S6K1 promotes protein synthesis by activating ribosomal protein S6 (RPS6, hereafter called S6) and therefore ribosome biogenesis, and by regulating translation initiation factors (Ma and Blenis, 2009). These activities make mTORC1 to a major hub for regulating mammalian cell size. Based on the function of mTORC1 in controlling protein synthesis, stimulation of mTORC1 activity was described as mediator of muscle hypertrophy (Bodine et al., 2001; Ruegg and Glass, 2011; Sandri, 2013).

The previous results obtained using mice in which *Tsc1* is specifically deleted in skeletal muscle fibers (called TSCmKO mice), however, challenged this concept as most muscles are

atrophic at young age (Bentzinger et al., 2013) and because these mice develop a severe myopathy causing death at the age of approximately one year (Castets et al., 2013). The phenotypic similarity between skeletal muscles of mice that are deficient for a gene essential for autophagy (Masiero et al., 2009) and of the TSCmKO mice suggested that impairment of autophagy, a process that is essential for the clearing of aberrant proteins and cell organelles (Dikic, 2017), might be responsible for the late-onset myopathy in TSCmKO mice. Indeed, autophagy induction was completely blocked in TSCmKO mice and inhibition of mTORC1 activation by rapamycin alleviated this blockage (Castets et al., 2013). While inhibition of autophagy can explain this late-onset myopathy in the TSCmKO mice, the muscle atrophy observed in young TSCmKO mice cannot be explained by this mechanism. Instead, overall protein degradation rates may exceed the rates in protein synthesis, resulting in an imbalanced proteostasis. One possibility for the increased protein degradation could be an overall dampening of Akt-signaling as a consequence of sustained mTORC1 activation. This inhibition of Akt could be based on a well-described feedback loop from mTORC1 *via* S6K1 and IRS1 to Akt (Bentzinger et al., 2008; Harrington et al., 2004). Inhibition of Akt would then result in the activation of forkhead box O (FoxO) pathways, which in turn would result in the activation of the ubiquitin-proteasome system (UPS) and increased protein degradation.

The UPS is the primary degradation system for short-lived, misfolded and damaged proteins (Dikic, 2017). The key component of the UPS for degradation is the 26S proteasome, a multi-catalytic, ATP-dependent protein complex, composed of various subunits that are assembled into two distinct subcomplexes - the 20S core particle and the 19S regulatory particle, which is attached to both ends of the core particle (Finley et al., 2016). The 26S proteasome recognizes ubiquitinylated proteins that, upon ATP hydrolysis, translocate into the 20S core particle where they are degraded to short peptide fragments. Degradation requires three specific, proteolytically active subunits: PSMB5 (β5, chymotrypsin-like activity), PSMB6 (β1, caspase-like activity) and PSMB7 (β2, trypsin-like activity) (Finley et al., 2016). Here we demonstrate that sustained activation of mTORC1 in muscles of young TSCmKO mice leads to a significant increase of the UPS, which is largely reversed by short-term application of rapamycin. Surprisingly, constitutive activation of Akt in muscle resulted in a similar induction of the UPS as observed in TSCmKO mice. Increased expression of genes coding for proteasomal subunits and multiple ubiquitin-E3-ligases are thought to be directly regulated by increased transcriptional activity of FoxO family members. In contrast, our results provide evidence that mTORC1 regulates the UPS, particularly the expression of proteasomal subunits, not solely by FoxO but by the transcription factor nuclear factor, erythroid derived 2, -like 1 (Nrf1, also referred to as NFE2L1). Together, these results demonstrate that mTORC1 activation is a major driver of the UPS in skeletal muscle and identified Nrf1 as an important mediator of this pathway. Both, mTORC1 signaling as well as the UPS are considered as potential treatment

targets in a large variety of distinct muscle wasting diseases. Therefore, understanding the underlying regulatory mechanisms of how mTORC1 controls muscle mass is of fundamental importance to eventually develop new therapeutic strategies to slow-down the massive muscle wasting observed in cachexia and sarcopenia.

Results

Young TSCmKO mice display an atrophy-related gene expression signature

TSCmKO mice are phenotypically indistinguishable from Control littermates at young age (Bentzinger et al., 2013). Nevertheless, despite the marked increase in protein synthesis due to sustained activation of mTORC1, most muscles of TSCmKO mice display reduced muscle weight and smaller type IIb fibers (Bentzinger et al., 2013). Within one year, they develop kyphosis and a severe myopathy, due to a blockage in autophagy induction, which is causing premature death (Castets et al., 2013). Young, 3-month-old TSCmKO mice have increased transcript levels of the two ubiquitin-E3-ligases *F-box protein 32* (*Fbxo32*, hereafter called *Atrogin-1*) and *Tripartite motif-containing 63* / *Muscle ring finger 1* (*Trim63*, hereafter called *MuRF1*), indicating that muscle atrophy in these mice in young age precedes the severe myopathy observed around the age of one year (Bentzinger et al., 2013; Castets et al., 2013). While inhibition of autophagy can explain this late-onset myopathy in the TSCmKO mice, the muscle atrophy observed in young TSCmKO mice cannot be explained by this mechanism. Instead, overall protein degradation rates may exceed the rates in protein synthesis, resulting in an imbalanced proteostasis.

To explore the molecular mechanism of muscle proteostasis and with the aim to identify new catabolic processes involved in muscle atrophy, we generated RNA-sequencing data from 3-month-old TSCmKO mice and Control littermates. Principal component analysis (PCA) revealed a decent clustering of biological replicates (**Figure S1A**) and around 4,600 genes were significantly, differentially expressed (DE) between Control and TSCmKO mice (**Figure S1B**). Next, we compared the gene expression of TSCmKO mice with a previous cDNA microarray analysis describing a set of genes (designated as atrogins, hereafter called atrogenes), which are commonly regulated in different types of muscle atrophy (Lecker et al., 2004). We found 91 of those atrogenes expressed in TSCmKO mice (**Figure 1A**). More than 40% (38 out of 91) among these genes were significantly DE in young TSCmKO mice compared to Control littermates and were similarly increased/decreased as previously found in different types of muscle atrophy (**Figure 1B, Table S1**). The majority of these 38 atrogenes is involved either in protein degradation or in energy production (Lecker et al., 2004) (**Figure S1C**). To compare the gene expression profile of TSCmKO mice with the current knowledge about atrophy-related genes, we screened literature of the last decade for genes involved in at least one type of muscle atrophy. Thereby we created an unsupervised list of 249 so-called “atrophy-related genes” (Table S2). Interestingly, we found 103 out of these 249 atrophy-related genes (41%) similarly increased/decreased in young TSCmKO mice (**Figure 1C, Table S3**). Similar to the previously described atrogenes, we found a majority of the annotated, atrophy-related genes to be involved in protein degradation (25%) (**Figure 1D**). Altogether, these results emphasize the large overlap of gene expression between TSCmKO mice and

any other type of muscle atrophy. This is a direct indication for increased protein degradation pathways in TSCmKO mice.

Ubiquitin proteasome system is enriched in young TSCmKO mice

After demonstrating that young TSCmKO indeed exhibit a large atrophy-related gene expression signature, we aimed to identify involved catabolic processes, which functionally could contribute to the mTORC1-driven muscle atrophy we observed in TSCmKO mice. For that reason, we generated proteomics data from 3-month-old TSCmKO mice and Control littermates. PANTHER pathway enrichment analysis (Mi et al., 2019; Mi et al., 2013) on all DE proteins showed the strongest pathway enrichment for the “Ubiquitin-proteasome pathway” (**Figure 2A**). Moreover, using DAVID enrichment analysis algorithms (Huang da et al., 2009a, b) on the same DE proteins, the “Proteasome” was found amongst the strongest enriched pathways using the Kyoto Encyclopedia of Genes and Genomes (KEGG) database (**Figure 2B**). Similarly, DAVID functional annotation clustering (Huang da et al., 2009a, b) revealed a strong enrichment of a cluster of terms belonging to the “Proteasome” (**Figure S2A**). Thus, proteomics data of TSCmKO mice further supports the notion that sustained activation of mTORC1 leads to an induction of the ubiquitin-proteasome system (UPS) and in particular of the 26S proteasome.

To test whether indeed the UPS is increased in TSCmKO mice, we started to examine the activation of the overall system. As we already have reported previously, we found increased transcript expression levels of the two ubiquitin-E3-ligases *Atrogin-1* and *MuRF1* in TSCmKO mice (**Figure 2E**). Concomitantly, TSCmKO mice showed increased levels of ubiquitinylated proteins compared to Control littermates (**Figure 2D**). Importantly, we found transcript and protein expression of various proteasomal subunits (PSM) from distinct proteasomal compartments of the 26S proteasome significantly increased in young TSCmKO mice (**Figure 2C, 2D**). Finally, using a luminescence-based assay for measuring proteasome activity revealed an increase in TSCmKO mice for all of the three main catalytic enzymes (β5, β1 and β2) (**Figure 2F**). Therefore, the expression of proteasomal subunits correlates with the increased proteasome activity. Importantly, similar activation of the UPS was observed in different fast-twitch muscles of TSCmKO mice, independent of gender, age (**Figure S3A-S3D**) or the progression state of the myopathy (**Figure S3E**). Altogether, these results demonstrate that sustained activation of mTORC1 indeed leads to an overall induction of the UPS, which most likely results in increased protein degradation and in an imbalanced muscle proteostasis.

Short-term inhibition with rapamycin reverses the increased UPS in TSCmKO mice

To test if the induction of the UPS in TSCmKO mice is mTORC1-dependently regulated, we

treated young TSCmKO mice and Control littermates with rapamycin for three consecutive days. Successful inhibition of mTORC1 was confirmed by strong reduction of phosphorylated S6 and 4E-BP1 and restoration of Akt activity in TSCmKO mice treated with rapamycin (**Figure S4A, S4B**). Further confirming successful mTORC1 inhibition, we found both, reversed transcript expression and less expression of p62 upon rapamycin treatment in TSCmKO mice (**Figure S4B, S4D**). This is in line with the findings we have previously reported, that rapamycin is sufficient to normalize autophagy induction in TSCmKO mice (Castets et al., 2013).

Interestingly, we found the expression of *Atrogin-1* and *MuRF1* (**Figure 3A**) and the protein expression of most proteasomal subunits (**Figure 3D**) completely reversed in TSCmKO mice treated with rapamycin. More importantly, also β5 and β1 proteasome activity was completely reversed, whereas β2 activity was not altered at all after rapamycin treatment in TSCmKO mice (**Figure 3C**). The latter is in strong contrast to the protein expression of its corresponding protein PSMB7 (**Figure 3D**). The amount of ubiquitinylated proteins remains elevated after rapamycin treatment in TSCmKO mice (**Figure S4C**). This suggests either increased degradation rates due to compensatory autophagy-lysosomal degradation or an accumulation of ubiquitinylated substrates, which cannot be degraded anymore. The finding that expression of p62 was completely absent after rapamycin treatment (**Figure S4B**) favors the first notion of intact degradation. Surprisingly, we did not found an overall reversing of the transcripts encoding for proteasomal subunits upon rapamycin treatment in TSCmKO mice (**Figure 3B**). Indeed, we found a group of PSM genes that was reversed or at least show a trend for this (*Psmb5*, *Psmd8*, *Psme4*), but we also found a group of PSM genes which was even further increased after rapamycin treatment (*Psma1*, *Psma5*, *Psmc4*, *Psmd4*, *Psmd11*) (**Figure 3B**). Since every PSM gene encodes for one individual proteasomal subunit, which is used to build up different parts of the 26S proteasome, it is well possible that multiple transcriptional regulators dynamically regulate PSM genes in a concerted but sequential manner. Therefore, rapamycin-induced inhibition of mTORC1 might not affect all of this transcription factors simultaneously. Together, these results demonstrate that the increase of the UPS observed in TSCmKO mice is a direct consequence of sustained activation of mTORC1, which is largely reversed by short-term inhibition of mTORC1 using rapamycin. Therefore, inhibition of mTORC1 by rapamycin not only restores autophagy flux and ameliorates myopathy in TSCmKO mice (Castets et al., 2013) but also reverses the induction of the UPS.

Activation of mTORC1 for 21 days is sufficient to increase the UPS in adult muscle

Next, we aimed to test if acute muscle-specific deletion of *Tsc1* in adult muscles for 3 weeks would lead to a similar induction of the UPS as observed in TSCmKO mice. For that reason and to exclude any impact of pre-adult skeletal muscle development, we crossed *Tsc1*$^{fl/fl}$ mice

with HSA-mER-Cre-mER mice (McCarthy et al., 2012), which allowed us to induce Cre-mediated ablation of *Tsc1* in adult muscles upon tamoxifen treatment (iTSCmKO mice). First, we addressed the question if mTORC1 activation for 21 days leads to similar molecular and phenotypic characteristics as observed in young, constitutive TSCmKO mice. 21-day iTSCmKO mice showed reduced expression of TSC1 and strong activation of mTORC1, characterized by increased phosphorylation of its targets S6 and 4E-BP1 (**Figure S5A**). In addition, we also found increased translation initiation, represented by the ratio of 4E-BP1 and eIF4E bound to the eukaryotic 7-methylguanosine 5'-triphosphate (m^7GTP)-cap (**Figure S5E**). 21-day iTSCmKO mice further had decreased phosphorylation levels of Akt and its target PRAS40 (**Figure S5B**), increased expression of p62 (**Figure S5B**) and of many transcripts involved in autophagy-lysosomal degradation (**Figure S5F**). All fast-twitch, hindlimb muscles of 21-day iTSCmKO mice show significantly reduced or trends to decreased relative muscle weight, while none of the other organs show any decrease in relative weight (**Figure S5C**). In summary, these results demonstrate that activation of mTORC1 for 21 days exhibits similar characteristics as we previously described for young TSCmKO mice (Bentzinger et al., 2013; Castets et al., 2013; Guridi et al., 2015).

The expression of *Atrogin-1* and *MuRF1* was increased in 21-day iTSCmKO mice (**Figure 4A**) and we found an increased number of ubiquitinylated proteins (**Figure 4E**). Both, transcript and protein expression of proteasomal subunits were significantly increased in 21-day iTSCmKO mice compared to Control littermates (**Figure 4B, 4D**). Similarly, proteasome activity of all three catalytic enzymes was significantly increased (**Figure 4C**). Altogether, these results clearly demonstrate that acute activation of mTORC1 in adult muscle for 21 days is sufficient to induce the UPS. Using iTSCmKO mice allowed us to compare different durations of mTORC1 activation. Therefore, we wondered whether the mTORC1-dependent increase in proteasome activity is progressive or stays constant over time. For that reason, we measured proteasome activity after 10 and 90 days of mTORC1 activation in adult muscles. Interestingly, we found a constant, similar increase of proteasome activity for 10-, 21- and 90-day iTSCmKO mice when compared to Control littermates (**Figure S5D**). This finding supports the hypothesis that sustained activation of mTORC1 in muscle results in a constant, but rather mild, increase of protein degradation rates. During days and months, this increase might results into a progressed atrophy and together with blockage of autophagy induction in the severe myopathy we previously described for 12-month-old TSCmKO mice (Castets et al., 2013).

Hypertrophic *soleus* muscles are resistant to an mTORC1-dependent increase of the UPS

Although, we demonstrated that sustained activation of mTORC1 induces the UPS to increase overall rates of protein degradation, it remains to be resolved if this increase of the UPS

effectively causes atrophy. As we already showed previously, all hindlimb muscles of young TSCmKO mice but not *soleus* (SOL) muscle undergo atrophy (Bentzinger et al., 2013). Instead, the *soleus* was shown to be atrophy-resistant, characterized by strong hypertrophy and increased muscle fiber size (Bentzinger et al., 2013). Similarly, acute activation of mTORC1 in adult muscles showed strongly increased relative muscle weight of the *soleus* in 21-day iTSCmKO mice when compared with Control littermates (**Figure S5C**).

Therefore, we aimed to test whether this atrophy-resistance is related to changes in the mTORC1-signaling or to alterations in the UPS induction. We found strongly increased phosphorylation of S6 and a clear trend for 4E-BP1 at their mTORC1-specific phosphorylation sites (**Figure S5G**), assuming similar activation of mTORC1 as found in *tibialis anterior* (TA) muscles of 21-day iTSCmKO mice (**Figure S5A**). Likewise, we found reduced phosphorylation levels of Akt and its target PRAS40 and increased expression of p62 in the *soleus* of 21-day iTSCmKO mice compared to Control littermates (**Figure S5H**). Up to that point, we could not find any differences in the mTORC1-Akt signaling of *soleus* muscles and we tested whether the UPS is similarly activated as in fast-twitch muscles. Importantly, we found proteasome activity of all three catalytic enzymes unaltered in the *soleus* muscle of 21-day iTSCmKO mice when compared with Control littermates (**Figure 4F**). Concomitantly, the induction of PSM genes and the expression of proteasomal subunits were blunted or much milder in the *soleus* (**Figure 4H, 4I**) in contrast to fast-twitch muscles (**Figure 4B, 4D**). Surprisingly, we found no transcriptional increase for *Atrogin-1* and *MuRF1* nor for other FoxO targets such as *Atf4*, *Bnip3*, *Gadd45a* or *Ppp1r15a* (**Figure 4G, 4J**). Thus, despite sustained activation of mTORC1 and inactive Akt, FoxO transcription factors and the UPS as well, are not activated in *soleus* muscles of 21-day iTSCmKO mice, which could explain the atrophy-resistance and hypertrophy found in those muscles. Altogether, these results raised evidence for the hypothesis that an mTORC1-dependent induction of the UPS in fast-twitch muscles causes muscle atrophy.

Constitutive activation of Akt induces proteasome activity similarly as in TSCmKO mice

To further study the involvement of Akt-FoxO-signaling in regulating the UPS in mTORC1-driven muscle atrophy, we aimed to investigate the mechanism of UPS activation in the absence of FoxO transcription factor activity. For that reason, we used mice with an inducible, muscle-specific, constitutively active form of Akt (hereafter called caAkt mice). We induced constitutive activation of Akt during 14 days and compared caAkt mice with TSCmKO mice and Control littermates. Because TSC2 is inactivated by Akt-dependent phosphorylation, which destabilizes TSC2 and disrupts the TSC complex (Inoki et al., 2002), constitutive mTORC1 activation should be similar as in TSCmKO mice. This is supported by previous

studies, which demonstrated that constitutive activation of Akt in murine skeletal muscle leads to constitutive activation of mTORC1, characterized by increased phosphorylation of S6K1, S6 and 4E-BP1 (Lai et al., 2004; Marabita et al., 2016). In contrast to TSCmKO mice, FoxO transcription factors are not active in caAkt mice. Indeed, we found transcript levels of *Atrogin-1* and *MuRF1* not increased in muscles of caAkt mice, while TSCmKO mice displayed increased expression (**Figure 5A**). Similarly, the transcript expression of various FoxO targets was significantly increased in TSCmKO mice, whereas none of them was increased in caAkt mice (**Figure 5B**). To our surprise, we found proteasome activity for all three catalytic enzymes significantly increased in caAkt mice compared with Control littermates and similar to the activity measured in TSCmKO mice (**Figure 5C**). In addition, most PSM genes showed a similar trend for increased expression as observed in TSCmKO mice (**Figure 5D**). One exception is *Psma1*, a known FoxO-target (Milan et al., 2015), which is strongly increased in TSCmKO mice and not induced in caAkt mice (**Figure 5D**). Thus, FoxO transcription factors are not regulating the majority of PSM genes in caAkt mice. Altogether, these results demonstrate that sustained activation of mTORC1 induces PSM genes and therefore proteasomal biosynthesis and proteasome activity, independently of the activation status of FoxO transcription factors. Hence, this suggests that another transcription factor increases the expression of PSM genes upon sustained activation of mTORC1.

Nrf1 is a key mediator of mTORC1-induced UPS

For that reason, we aimed to identify a transcription factor, which is both, activated by mTORC1 and able to induce transcription of all PSM genes. The transcription factor Nrf1 was shown to increase all PSM genes as a “bounce-back” response to compromised proteasome function (Radhakrishnan et al., 2010; Sha and Goldberg, 2014; Steffen et al., 2010). Further demonstrating its important role in regulating proteasomal biosynthesis, tissue-specific knockout of Nrf1 in brain, liver and brown adipocytes leads to a dysregulation of proteasomal genes and function (Bartelt et al., 2018; Lee et al., 2013; Lee et al., 2011; Widenmaier et al., 2017). Importantly, it was previously shown in mouse embryonic fibroblasts (MEFs) and in liver and brain tissue that sustained activation of mTORC1 increases the transcript levels of PSM genes *via* Nrf1 (Zhang et al., 2014). Therefore, Nrf1 fulfilled all the criteria as potential transcription factor for the mTORC1-dependent increase of the UPS. Therefore, we aimed to explore the role of Nrf1 in skeletal muscle and particularly if and how Nrf1 regulates muscle proteostasis.

Indeed, we found transcript levels of Nrf1 significantly increased in young TSCmKO mice (**Figure 6A, S6B**), whereas short-term treatment with rapamycin reversed this increase (**Figure 6A**). NAD(P)H dehydrogenase, quinone 1 (NQO1), which is one of the best described

targets of Nrf1 involved in antioxidative response (Leung et al., 2003; Venugopal and Jaiswal, 1998), was transcriptionally but also in protein expression significantly increased in young TSCmKO mice (**Figure 6A, 6B, S6A, S6B**). Surprisingly, we found transcript but not protein expression of NQO1 reversed by 3-day rapamycin treatment (**Figure 6B**). Another well-described target and regulator of Nrf1, valosin containing protein (VCP, or p97) (Radhakrishnan et al., 2014; Sha and Goldberg, 2014), was transcriptionally increased in young TSCmKO mice with a trend of reversing by treating TSCmKO mice with rapamycin for 3 days (**Figure 6A, S6B**). Importantly, we found genes encoding for two known positive regulators of Nrf1 significantly increased in young TSCmKO mice and reversed with rapamycin (**Figure 6A, S6B**). First, the gene encoding for protease *DNA-damage inducible protein 2* (*Ddi2*), which was shown to cleave Nrf1 allowing its translocation to the nucleus (Koizumi et al., 2016). Second, the gene encoding for *O-linked N-acetylglucosamine transferase* (*Ogt*), which was shown to catalyze O-GlcNacylation to stabilize Nrf1 and activate its transcriptional activity (Han et al., 2017; Sekine et al., 2018). Moreover, we found OGT expression significantly increased in young TSCmKO mice, whereas DDI2 at least showed a trend to be increased (**Figure S6A**). Many targets of Nrf1 were shown to be regulated under certain cellular stresses, particularly by another family member, namely nuclear factor erythroid-derived 2-related factor 2 (NFE2L2, hereafter called Nrf2). To exclude any cross-regulation or compensatory mechanism, we tested the protein expression of Nrf2 and did not observe any increase (**Figure S6C**). Sustained activation of mTORC1 for 21 days was sufficient to increase the transcriptional expression of *Nrf1*, its targets and regulators in *gastrocnemius* (GAST) muscle (**Figure 6C, 6D**). In contrast, the transcriptional increase of *Nrf1* and *Nqo1* was completely blunted in the *soleus* muscle of 21-day iTSCmKO mice (**Figure 6C**). Similarly, we found significantly increased expression of NQO1 in TA muscle of 21-day iTSCmKO mice, but no induction in the *soleus* (**Figure 6E**). Finally, our experiments demonstrate that *Nrf1*, but not *Nqo1*, is transcriptionally increased upon constitutive activation of Akt (**Figure 6F**). Thus, our data clearly identifies Nrf1 as an mTORC1-dependent mediator of the UPS, which most likely regulates the expression of PSM genes and the UPS.

Inactivation of Nrf1 in TSCmKO mice decreases the expression of PSM genes

To test this Nrf1-dependent regulation of PSM genes in muscle, we aimed to inactivate Nrf1 in young TSCmKO mice. For that reason we designed a plasmid that drives expression of a shRNA directed to all existing transcript variants of Nrf1 (Nrf1 knock-down, Nrf1-kd). First, we tested Nrf1 inactivation in MEFs and treated them with the proteasome inhibitor bortezomib (BTZ), which should lead to a strong accumulation of cleaved Nrf1 (Nrf1 CL) (Radhakrishnan et al., 2014; Widenmaier et al., 2017). Indeed, we found Nrf1 FL and Nrf1 CL strongly accumulated in MEFs treated with BTZ compared with vehicle-treated MEFs (**Figure 7A**). This

accumulation was reduced in MEFs transfected with Nrf1-kd shRNA and even non-treated MEFs demonstrate a clear reduction of Nrf1 FL and Nrf1 CL comparing MEFs transfected with scramble shRNA and Nrf1-kd shRNA (**Figure 7A**).

Next, we electroporated TA muscles of TSCmKO mice and Control littermates with plasmids driving scramble shRNA and Nrf1-kd shRNA, to inactivate Nrf1 specifically in muscle fibers for two weeks. Unfortunately, we realized that the most frequently used Nrf1-antibody for Western blot analysis (Cell Signaling Technology, #8052) but also other antibodies, displayed strong unspecific binding in skeletal muscle tissue on different molecular weights. This makes it almost impossible to detect and quantify differences in Nrf1 protein expression between different genotypes. In MEFs, we could not observe this effect, and it seems not to be the case for any other tissue, where this antibody was used before. Nevertheless, we confirmed successful inactivation of Nrf1 by strongly reduced expression of Nrf1 FL (~120kDa), Nrf1 CL (~85kDa) and locus control region-factor 1 (LCR-F1 or Nrf1β, ~55kDa) in muscles with Nrf1-kd compared to muscles with scramble shRNA in Control and TSCmKO mice (**Figure 7B**). Further demonstrating successful inactivation of Nrf1, we found its transcript expression significantly decreased in TSCmKO mice and Control littermates (**Figure 7D**). Unfortunately, through electroporation, we slightly dampened the genotype-specific differences between muscles from Control and TSCmKO mice. This might be due to new and regenerative fibers, which do not express human skeletal α-actin (HSA) yet and therefore do not have the ablation of TSC1. This was further supported by the fact that the expression of TSC1 was reduced in electroporated muscles of TSCmKO mice, but not as explicit as we normally observe in TSCmKO mice (**Figure S7B**) (Bentzinger et al., 2013; Castets et al., 2013). Significantly decreased relative muscle weight, found in the contralateral, sham-treated TA muscles of TSCmKO mice when compared with Control littermates (**Figure S7A**), further supports the notion that electroporation dampened genotype-specific differences.

Interestingly, TA muscles of both, TSCmKO and Control mice transfected with Nrf1-kd shRNA, showed significantly decreased protein and transcript expression of most proteasomal subunits (**Figure 7B, S7E**). Only *Psme4*/PA200, which is a known FoxO-target (Milan et al., 2015), displayed no decreased expression (**Figure 7B, S7E**). The protein expression of p97 and DDI2 was significantly decreased with Nrf1 inactivation, whereas another potential target of Nrf1, glutamate-cysteine ligase, catalytic subunit (GCLC) was not altered and Nrf2 rather increased than decreased (**Figure S7C**). In contrast, transcript expression of *Nrf2* was significantly decreased (**Figure S7F**), suggesting an Nrf1-dependent regulation which does not get functional relevance. Surprisingly, we found strong induction of NQO1, on protein and transcript levels, only in TSCmKO mice with Nrf1 inactivation (**Figure S7C, S7F**). Therefore, we assume that NQO1 is not solely regulated by Nrf1. In addition we found evidence, that inactivation of Nrf1 affects autophagy. Similarly to NQO1, p62 was transcriptionally and in

protein expression strongly increased in TSCmKO but not Control mice with Nrf1 inactivation (**Figure S7C, S7F**). In contrast, we observed less expression of BECN1 and LC3b upon Nrf1-kd in Control and TSCmKO mice (**Figure S7C**). This implies that either the transcripts encoding for BECN1 / LC3b are direct targets of Nrf1 or that there is less induction of autophagosome formation. Interestingly, we found the amount of ubiquitinylated proteins significantly decreased in TSCmKO mice with Nrf1 inactivation (**Figure S7D**) and the expression of *Atrogin-1* and *MuRF1* significantly further increased (**Figure 7D**). Both might be an indication for a compensatory mechanism induced by FoxO transcription factors. The finding that other FoxO targets, such as *Psme4*, *Ppp1r15a* and *p62* are also significantly increased in the absence of Nrf1 in TSCmKO mice (**Figure S7E, S7F**), further supports the idea of a FoxO-driven compensatory mechanism. Altogether, these results demonstrate that Nrf1-inactivation is sufficient to decrease the expression of most proteasomal subunits. Moreover, inactivation of Nrf1 does not only affect proteasomal subunits, but also other parts of the UPS and autophagy-lysosomal degradation, which needs further investigations. Hence, our data demonstrate that mTORC1 regulates the expression of proteasomal subunits and the UPS by a transcriptional increase of Nrf1.

To link this mTORC1-dependent, Nrf1-induced increase of the UPS with muscle atrophy, we measured the body and muscle weight of contralateral, sham-treated and electroporated TA muscles in Control and TSCmKO mice. The body weight of these mice was not changed (**Figure 7C**). When we compared the ratio of muscle weight between electroporated and contralateral sham-treated muscles, we observed an almost significant, 10% increase in TA muscles of TSCmKO mice with inactivated Nrf1 compared to TSCmKO mice electroporated with scramble shRNA (**Figure 7C**). This data further supports the hypothesis that inactivation of Nrf1 could attenuate the muscle atrophy in TSCmKO mice. To demonstrate this, prolonged inactivation of Nrf1 and detailed analysis of the muscle histology must be performed.

Discussion

Skeletal muscle size and therefore as well muscle wasting is ultimately determined by the muscle proteostasis. Activation of mTORC1 in skeletal muscle is generally associated with growth and with promoting anabolism. Because of its role in regulating translation and protein synthesis, mTORC1 was proposed as mediator of muscle hypertrophy (Bodine et al., 2001; Ruegg and Glass, 2011; Sandri, 2013; Schiaffino et al., 2013). Nevertheless, we previously showed in mice depleted for TSC1 in skeletal muscle (TSCmKO mice) that sustained activation of mTORC1 leads to atrophy, to a severe late-onset myopathy and to muscle weakness (Bentzinger et al., 2013; Castets et al., 2013). Particularly, the myopathic features of TSCmKO mice, such as vacuoles, damaged organelles and p62 aggregates, were explained by the blockage of autophagy induction (Castets et al., 2013). In contrast, the muscle atrophy, which is already observed in young TSCmKO mice, cannot be explained by this mechanism. In this study, we analyzed the atrophy of TSCmKO mice and identified a new mechanism of how mTORC1 regulates catabolic processes. This knowledge may help to attenuate mTORC1-driven muscle atrophy.

One characteristic of muscle atrophy is the common expression of a set of genes called atrogenes (Lecker et al., 2004; Sacheck et al., 2007). Nevertheless, a recent study highlighted that even the expression of atrogenes vary between different types of muscle atrophy and that the signaling network controlling muscle atrophy is specific for each catabolic condition (Brocca et al., 2017). Additionally to the atrogenes, there is a huge variety of genes, which are related to only one or few specific types of muscle atrophy. Therefore, to understand the underlying gene expression program is essential for designing unique strategies to attenuate each specific type of muscle atrophy. Here, we present a new, unsupervised list of 249 atrophy-related genes. These genes were at least once directly associated with muscle atrophy before. The large expression of atrogenes (40%) but also of atrophy-related genes (41%) we found in young TSCmKO mice is an indication of a prominent atrophy-related gene expression signature that is induced by sustained activation of mTORC1. Importantly, the majority of these genes are involved in protein degradation processes. Together, with the pathway enrichment of the ubiquitin-proteasome system and of the 26S proteasome we found in our proteomics data, this suggests that muscle atrophy in TSCmKO mice involves the activation of mTORC1-dependent catabolic processes.

Indeed, we demonstrate in this study that sustained activation of mTORC1 in TSCmKO mice not only increases protein synthesis and blocks autophagy induction, but also induces the ubiquitin-proteasome system. This induction includes ubiquitin-E3-ligases, ubiquitinylation, transcriptional activation of proteasomal biosynthesis and increased proteasome activity. In addition to the current knowledge that the mTORC1-specific inhibitor rapamycin induces autophagy (Kim et al., 2011) and alleviates the blockage of autophagy induction in TSCmKO

mice (Castets et al., 2013), we found in this study evidence that short-term inhibition with rapamycin reverses the mTORC1-dependent increase of the UPS in young TSCmKO mice. The short-term characteristics of the rapamycin treatment definitely rules out that this induction of the UPS is caused by any pathological factors or occurs in response to extrinsic factors. Instead, we give evidence that the increase of the UPS, particularly the activation of PSM genes, is due to the activation of a signaling cascade resulting in the activation of Nrf1, as a direct consequence of sustained active mTORC1. By inducing a similar activation of the UPS, through activation of mTORC1 for only 21 days in adult muscles of iTSCmKO mice, we can exclude any impact caused by sustained active mTORC1 during pre-adult muscle development. Moreover, results from iTSCmKO mice again demonstrate that the increase of the UPS is based on mTORC1-Nrf1 signaling. Interestingly, proteasome activity is not further increased with prolonged activation of mTORC1 and is as well not further increased in 10-month-old TSCmKO mice with severe myopathy. This finding favors the hypothesis that a relatively mild increase of the UPS slightly shift the balance of muscle proteostasis to the catabolic side. On this way, protein degradation in muscle still provides sufficient amino acids to avoid immediate detrimental effects to whole-body metabolism. On the other hand, a mild increase in protein degradation over days and months could still result in the accumulation of a more and more severe muscle atrophy. Therefore, dampening of this mTORC1-driven increase of the UPS, together with increased protein synthesis could potentially help to build up muscle mass.

Skeletal muscles and muscle fiber types vary in their response to the same stimulus. For example, denervation in the rat diaphragm or any other fast-twitch muscle causes atrophy of the glycolytic, fast-twitch fibers type IIx and IIb, no changes in oxidative, fast-twitch fibers type IIa and hypertrophy of oxidative, slow-twitch type I fibers (Aravamudan et al., 2006; Schiaffino et al., 2013). In contrast, type I fibers of the slow-twitch muscle *soleus* show marked atrophy after denervation (Schiaffino et al., 2013). Thus, the same fiber type undergoes opposite changes in different muscles. Interestingly, the *soleus* muscle is also less sensitive to starvation and shows in general higher rates of protein synthesis and protein degradation compared to fast-twitch muscles (Li and Goldberg, 1976). Furthermore, hypertrophy of the *soleus* muscle induced by growth hormones, showed increased protein synthesis rates without any changes in protein degradation (Goldberg, 1969). Surprisingly, we previously found that the *soleus* muscle was the only muscle with increased relative muscle weight and fiber size upon sustained activation of mTORC1, although it displayed similar blockage of autophagy induction as observed for fast-twitch muscles (Bentzinger et al., 2013; Castets et al., 2013). Here, we demonstrated that activation of mTORC1 for only 21 days in iTSCmKO mice is sufficient to induce hypertrophy in the *soleus* muscle. Moreover, we showed that the *soleus* muscle is resistant to the mTORC1-Nrf1-dependent induction of the UPS. We have already

previously shown that the two ubiquitin-E3-ligases *Atrogin-1* and *MuRF1* were not increased in the *soleus* muscle of TSCmKO mice (Bentzinger et al., 2013). Here, we show in *soleus* muscle of 21-day iTSCmKO mice, despite decreased Akt activity caused by sustained activation of mTORC1, no alterations in the expression of *Atrogin-1* and *MuRF1* as well as of other FoxO targets, such as *Atf4*, *Bnip3*, *Gadd45a* and *Ppp1r15a*. Therefore, this could mean that in *soleus* muscles of TSCmKO mice rates of protein synthesis are increased *via* mTORC1 but no changes in protein degradation rates because FoxO as well as Nrf1 are not increased. Similarly to how it was described earlier on (Goldberg, 1969), increased protein synthesis without any changes in protein degradation could result in the strong hypertrophy we observed in the *soleus* of TSCmKO and iTSCmKO mice. Why FoxO but also Nrf1 in the *soleus* of TSCmKO mice are not induced by mTORC1, needs further investigations. Interestingly, these results demonstrate that even if autophagy induction is blocked, and there is no increased UPS-activity either through Nrf1 or through FoxO, the *soleus* muscle is still able to undergo hypertrophy.

Constitutive activation of Akt was shown to constitutively activate mTORC1 resulting in increased protein synthesis and ribosome biogenesis (Lai et al., 2004; Marabita et al., 2016). In addition, it was shown that constitutive activation of Akt leads to increased expression and to accumulations of p62 (Marabita et al., 2016). This indicates that constitutive activation of Akt and ablation of TSC1 leads to a similar activation of mTORC1 and to a similar blockage of autophagy induction. The big difference between constitutive activation of Akt and TSCmKO mice lies in the activation of FoxO transcription factors. In this study, we could show that caAkt mice have a similar increase of *Nrf1* and proteasome activity as observed in TSCmKO mice. These results, together with the rapamycin treatment in TSCmKO mice and the short-term activation of mTORC1, explicitly means that the mTORC1-dependent induction of proteasomal biosynthesis and proteasome activity is mediated by Nrf1 and excludes involvement of FoxO-signaling in this particular process. Nevertheless, the activity of FoxO is essential to induce a variety of ubiquitin-E3-ligases (Milan et al., 2015; Sacheck et al., 2004; Sandri et al., 2004; Sartori et al., 2013), which are needed for the ubiquitinylation of targets of the 26S proteasome. Therefore, if an mTORC1-Nrf1-driven increase of proteasomal biosynthesis and proteasome activity, without the induction of FoxO-dependent ubiquitin-E3-ligases, is sufficient to efficiently increase protein degradation rates, needs further investigations. Reduced protein degradation rates in mice with constitutive activation of Akt compared to TSCmKO mice, where FoxO and Nrf1 are active, might also explain the strong and fast hypertrophic response, which was shown for mice with constitutive activation of Akt (Lai et al., 2004; Marabita et al., 2016).

In this study, we identify the transcription factor Nrf1 as key mediator of mTORC1-driven muscle atrophy, by transcriptionally regulating proteasomal biosynthesis. Nrf1 was previously associated with an mTORC1-dependent increase of genes encoding for proteasomal subunits

in TSC2$^{-/-}$ MEFs and in brain and liver lysates (Zhang et al., 2014). Here, we further support this finding and show comprehensive *in-vivo* data of skeletal muscle that an mTORC1-dependent increase of Nrf1 leads to an increase of proteasomal biosynthesis and activity, and together with FoxO to an increase of the ubiquitin-proteasome system. Nrf1 was previously shown to be regulated by mTORC1 *via* SREBF1 (Zhang et al., 2014). If SREBF1 regulates Nrf1 in an mTORC1-dependent way in skeletal muscle, needs further investigations. Interestingly, not only Nrf1 but also some of its post-translational, positive regulators, namely p97, OGT and DDI2, are transcriptionally increased in an mTORC1-dependent manner. Increased expression of p97 was previously associated with muscle atrophy and accelerated degradation of myofibrillar proteins, whereas its inhibition caused rapid growth of myofibers (Piccirillo and Goldberg, 2012). More recently, p97 was identified as direct target of Nrf1 (Sha and Goldberg, 2014) and upon proteasome inhibition to be essential for the retrotranslocation of Nrf1 to the cytosolic side of the ER membrane (Radhakrishnan et al., 2014), where Nrf1 escapes proteasomal degradation and is cleaved and activated by DDI2 (Koizumi et al., 2016). OGT was recently described to stabilize and activate Nrf1 upon O-GlcNacylation, which is a major feature of cancer cell metabolism (Sekine et al., 2018). Hence, our findings strongly suggests that sustained activation of mTORC1 leads to a transcriptional increase of Nrf1 but in parallel also to an increase of a variety of positive, post-translational regulators of Nrf1.

Generally, an increase of Nrf1 is directly associated with the evolutionary conserved “bounce-back” response upon proteasome inhibition to maintain cellular proteostasis (Radhakrishnan et al., 2010; Sha and Goldberg, 2014; Steffen et al., 2010). Proteasome inhibitors are used in clinical treatment of multiple myeloma (Adams and Kauffman, 2004; Richardson et al., 2005; Richardson et al., 2010). However, bortezomib alone or in combination with other drugs did not show its real efficacy in the clinical trials to treat solid tumors (Frankland-Searby and Bhaumik, 2012; Johnson, 2015). The observation that therapeutic proteasome inhibition promptly triggers the upregulation of PSM genes in malignant cells (Mitsiades et al., 2002), was associated with the Nrf1-induced “bounce-back” response. Hence, Nrf1 received significant medical relevance as regulator of an important compensatory response that promotes tumor cell survival and attenuates therapeutic efficacy (Yuan et al., 2018). In skeletal muscle, the role of Nrf1 is poorly described so far. One study reported that activation of Nrf1 and Nrf2 improved the muscle histology in a mouse model for spinal and bulbar muscular atrophy (SBMA) (Bott et al., 2016). Nevertheless, this study focussed on the effect that Nrf1 induced by regulating antioxidant enzymes and not on muscle proteostasis *per se*.

Sustained activation of mTORC1 leads to increased expression of *Nrf1* and increased expression of PSM genes. By inactivation of Nrf1 in Control and TSCmKO mice, we showed that Nrf1 regulates most PSM genes in muscle. Here, we present a mechanism in skeletal muscle, which functionally resembles the well-established “bounce-back” response but without

prior perturbation of proteasomes. Therefore, we raise evidence for the hypothesis that sustained active mTORC1 transcriptionally increases *Nrf1* to increase the UPS and protein degradation rates, which results in muscle atrophy. Nrf1-inactivation in TSCmKO mice for only 2 weeks with a minimal n number (n=3) shows a promising trend for increased muscle weight compared to Control mice. To elucidate the role of Nrf1 in regulating muscle proteostasis would require prolonged inactivation. At this stage, it would be interesting to compare the inactivation of Nrf1 in the presence / absence of proteasome inhibitors in TSCmKO mice. Whether this mechanism is effectively induced to regulate muscle proteostasis remains unresolved. It might well be that the initial role of this mechanism was to compensate for the block of autophagy induction, or to provide sufficient amino acids to fulfill increased protein synthesis rates or to deal with misfolded proteins and ER stress. Therefore, the activation of this mechanism needs further investigations.

Altogether, the findings of this study help to understand and explore a new mechanism regulated by mTORC1 and Nrf1 that controls muscle proteostasis and muscle mass. In addition, this knowledge may lead to the identification of a new possible target to slow-down the massive muscle wasting observed in cachexia or sarcopenia.

Materials and methods

Mice

TSCmKO mice were obtained by crossing *Tsc1*-floxed mice (Kwiatkowski et al., 2002) from Jackson Laboratory with transgenic mice expressing Cre recombinase under the control of the human skeletal actin (HSA) promoter (Schwander et al., 2003). iTSCmKO mice were obtained by crossing *Tsc1*-floxed mice (Kwiatkowski et al., 2002) from Jackson Laboratory with transgenic, inducible mice expressing a chimeric Cre recombinase containing two mutated estrogen receptor ligand-binding domains (MerCreMer) under the control of the HSA promoter (McCarthy et al., 2012). caAkt mice were obtained from Dr. David Glass at Novartis Institutes for BioMedical Research (NIBR, Cambridge, MA, USA). These mice express a constitutively active form of Akt1/PKBα fused to enhanced green fluorescent protein (EGFP) and human estrogen receptor type 2 (ERt2) under the control of the HSA promoter. All mice were maintained in a licensed animal facility with a fixed 12 h dark-light cycle and were allowed for food and water *ad libitum*. All animal studies were performed under the guidelines and the law of the Swiss authorities and were regularly controlled and approved by the veterinary office.

Animal experiments

In some experiments mice were intraperitoneally injected with rapamycin (8 mg/kg; LC Laboratories) as previously described (Bentzinger et al., 2013) for three consecutive days. These mice were weighed before each injection. To induce ablation of *Tsc1* in HSA-expressing muscle fibers, tamoxifen (2.5 mg/day; Sigma) diluted in corn oil (Sigma) was injected intraperitoneally for five consecutive days. To induce constitutive activation of Akt in HSA-expressing muscles fibers, tamoxifen (40 mg/kg; Sigma) diluted in corn oil (Sigma) was injected intraperitoneally for five consecutive days, followed by three injections every 48 hours for one week more. In experiments using tamoxifen, only male mice were used.

Cell culture

SV40 immortalized mouse embryonic fibroblasts (MEFs) were maintained in Glutamax Dulbecco's modified Eagle's medium (DMEM Glutamax and pyruvate, Gibco) supplemented with 10% fetal bovine serum (FBS) and 1% penicillin-streptomycin (pen/strep) on cell culture dishes in 37°C incubator with 5% CO_2. For Nrf1-kd, MEFs were transfected with plasmids encoding for Nrf1-kd shRNA (see below) using Lipofectamin 2000 (Invitrogen). Lysis of the cells was started 48 hours after transfection. Cells were scraped and lysed in cold RIPA buffer (50 mM TrisHCl pH 8.0, 150 mM NaCl, 1% NP-40, 0.5% sodium deoxycholate, 0.1% SDS, ddH_2O) supplemented with phosphatase and protease inhibitor cocktail tablets (Roche), DNA was sheared with a syringe (26G needle). Afterwards, the lysate was centrifuged at 16,000 g

for 20 min at 4°C. Supernatant (cleared lysates) were used to determine total protein amount using the Pierce BCA Protein Assay Kit (Thermo Fisher Scientific) according to manufacturer's protocol. Immunoblotting was performed as described below. For Nrf1 accumulation experiment, MEFs were treated with bortezomib (BTZ; 10 nM, Selleck Chemicals) or dimethyl sulfoxide (DMSO) as vehicle four hours prior to lysis.

In vivo muscle transfection and electroporation

The methods to construct plasmid vectors encoding shRNA have been described elsewhere (Kong et al., 2004). The murine 19 nucleotide target sequences correspond to: GGC CCG ATT GCT TCG AGA A (Nrf1). pRFP-C-RS scrambled shRNA plasmid vector was obtained from OriGene (TR30015). For analgesia, mice were injected subcutaneously with Buprenorphine (0.1 mg/kg) before and every 4 to 6 hours after electroporation. During night, Buprenorphine was given orally over the drinking water. *Tibialis anterior* (TA) muscle of anesthetized mice was exposed and injected with 50 µl (8 IU) of hyaluronidase (Sigma). Mice were returned to the cage for two hours. Then, TA muscle of anesthetized mice was injected with 50 µl of 2 µg/µl of the respective shRNA plasmid DNA. The electroporation was performed using an NEPA21 electroporation system (NepaGene). Three pulses lasting 30 ms with a pulse interval of 50 ms and the voltage set to 150 V/cm were applied. Mice were analyzed two to four weeks after electroporation.

Transcript expression analysis (RNA extraction and RT-PCR)

Dissected muscle was rapidly frozen in liquid nitrogen. Total RNA was extracted using the RNeasy Mini Kit (Qiagen) according to manufacturer's protocol. Equal amounts of RNA was transcribed into cDNA using the iScript cDNA Synthesis Kit (BioRad). Selected genes were amplified and detected using the Power SYBR Green PCR Master Mix (Applied Biosystems), quantitative expression was determined by StepOnePlus Real-Time PCR System (Applied Biosystems). Relative gene expression was determined with the StepOne software (v2.3) and normalized to the corresponding housekeeping gene as indicated and relative to expression in Control mice. All primers used for RT-qPCR are listed in **Table S4**.

Western blot analysis

Dissected muscle was rapidly frozen in liquid nitrogen. Frozen muscles were pulverized on a metal plate chilled in liquid nitrogen and directly snap-frozen as pellet in liquid nitrogen. Samples were lysed in cold RIPA buffer (50 mM TrisHCl pH 8.0, 150 mM NaCl, 1% NP-40, 0.5% sodium deoxycholate, 0.1% SDS, ddH_2O) supplemented with phosphatase and protease inhibitor cocktail tablets (Roche), incubated on a rotating wheel for 2 h at 4°C and sonicated

twice for 10 s. Afterwards, the lysate was centrifuged at 16,000 g for 20 min at 4°C. Supernatant (cleared lysates) were used to determine total protein amount using the Pierce BCA Protein Assay Kit (Thermo Fisher Scientific) according to manufacturer's protocol. Proteins were separated on 4-12% Bis-Tris Protein Gels (NuPage Novex, Thermo Fisher Scientific) and transferred to nitrocellulose membrane (GE Healthcare Life Sciences, Amersham). The membrane was blocked with 5% BSA, 0.1% Tween-20, PBS for 1 h at room temperature. The primary antibody diluted in the blocking solution was incubated overnight at 4°C with continuous shaking. The membranes were washed three times for 15 min with PBS-T (0.1% Tween-20, PBS) and incubated with secondary horseradish peroxidase-conjugated (HRP) antibody for 1 h at room temperature. After washing with PBS-T, proteins were visualized by chemiluminescence (KPL LumiGLO®, Seracare). Signal was captured on a Fusion Fx machine (VilberLourmat) and analyzed with FUSION Capt FX software. All antibodies used for immunoblotting are listed in **Table S5**.

Ubiquitinylation analysis

Dissected muscle was rapidly frozen in liquid nitrogen. Frozen muscles were pulverized on a metal plate chilled in liquid nitrogen and directly snap-frozen as pellet in liquid nitrogen. Samples were lysed in cold Ub-lysis-buffer (1 mM EDTA, 25 µM MG 132, 50 mM N-ethylmaleimide, 50 mM TrisHCl pH 8.0, 150 mM NaCl, 1% NP-40, 0.5% sodium deoxycholate, 0.1% SDS, ddH_2O) supplemented with phosphatase and protease inhibitor cocktail tablets (Roche), incubated on a rotating wheel for 2 h at 4°C and sonicated twice for 10 s. Afterwards, the lysate was centrifuged at 16,000 g for 20 min at 4°C. Supernatant (cleared lysates) were used to determine total protein amount using the Pierce BCA Protein Assay Kit (Thermo Fisher Scientific) according to manufacturer's protocol. Immunoblotting was performed as described above.

Proteasome activity assay

Proteasome activity assay was adapted from a protocol described previously (Strucksberg et al., 2010). Briefly, dissected *extensor digitorum longus* (EDL) or *plantaris* (PLA) muscles were rinsed in ice-cold PBS, immediately cut into 5-6 pieces and directly lysed in ice-cold PBS-E (5 mM EDTA pH 8.0, PBS pH 7.2) and sonicated two times for 10 s. Afterwards, the lysate was centrifuged at 13,000 g for 5 min at 4°C. Supernatant (cleared lysates) were used to determine total protein amount using the Pierce BCA Protein Assay Kit (Thermo Fisher Scientific) according to manufacturer's protocol. Three individual luciferase-based Proteasome-Glo™ Assay Systems (Promega) were used to measure the activity of each peptidase of the proteasome. Assay was performed on white, 96-well microplates (greiner BIO-ONE) and

luminescence was measured with Infinite M1000 (Tecan). Human, purified 20S proteasome (Enzo Life Sciences, BML-PW8720) was used as positive control. Proteasome inhibitor MG 132 (50 µM, TOCRIS Biotechne) was used for measuring non-proteasomal activity in this assay, which was used for background subtraction.

m^{7}GTP pulldown

Dissected muscle was rapidly frozen in liquid nitrogen. Frozen muscles were pulverized on a metal plate chilled in liquid nitrogen, before lysis in cold pull-down buffer (20 mM Hepes pH 7.4, 50 mM KCl, 0.2 mM EDTA, 25 mM β-glycerophosphate, 0.5 mM sodium orthovanadate, 1 mM dithiothreitol, 0.5% Triton X-100, and 50 mM sodium fluoride) supplemented with phosphatase and protease inhibitor cocktail tablets (Roche). Cells were disrupted by additional homogenization in a Potter homogenizer, incubated on ice for 10 min before centrifugation for 10 min at 10,000 rpm at 4°C. Supernatant were used to determine total protein amount using the Pierce BCA Protein Assay Kit (Thermo Fisher Scientific) according to manufacturer's protocol. 400 µg of total lysate was used for m^{7}GTP pull-down assay. After preclearing of the samples with agarose beads (Jena Bioscience) for 30 min at 4°C, 20 µl of a 50% slurry of γ-Aminohexyl-m^{7}GTP-Agarose (Jena Bioscience) was incubated with the precleared supernatant overnight at 4°C on a rotating wheel. After three washes, the samples were denatured for 10 min at 95°C before separation on 4-12% Bis-Tris Protein Gels (NuPage Novex, Thermo Fisher Scientific) and transferred to nitrocellulose membrane (GE Healthcare Life Sciences, Amersham). eIF4E and 4E-BP1 abundances on the m^{7}GTP mimicking cap were visualized by chemiluminescence (KPL LumiGLO®, Seracare). Signal was captured on a Fusion Fx machine (VilberLourmat) and analyzed with FUSION Capt FX software.

RNA extraction for RNA-seq

EDL muscles isolated from Control and TSCmKO mice, were used to generate the corresponding cDNA-libraries. Poly-A mRNA were directly isolated from frozen EDL samples by using the Dynabeads™ mRNA DIRECT™ Purification Kit (Invitrogen) with the Mini configuration followed by alkaline hydrolysis. To provide 5' to 3' directionality to fragmented samples, mRNA was treated with phosphatase and then with polynucleotide kinase (PNK). Further, 3' and 5' adaptors (Illumina) were ligated and the resulting product was reverse transcribed to generate cDNA by PCR. During PCR amplification, each prepared sample was uniquely indexed (barcoding) using index primer (Illumina) for multiplexing (differently indexed samples in one lane). PCR products have been purified twice with AMPure beads (Agencourt). The quality of the cDNA-library was verified and quantified by using a Bioanalyzer (Agilent Technologies). Illumina "HiSeq 2000" was used for sequencing at the Quantitative Genomics

Facility (QGF) at the Department of Biosystems Science and Engineering (D-BSSE) of the ETH Zürich in Basel.

Protein isolation for Tandem Mass Tag (TMT)-LC-MS/MS

Dissected muscle was rapidly frozen in liquid nitrogen. Frozen muscles were pulverized on a metal plate chilled in liquid nitrogen and directly snap-frozen as pellet in liquid nitrogen. Samples were lysed in cold lysis buffer (1% sodium deoxycholate, 100 mM ammoniumbicarbonate) and ultra sonicated twice for 10 s with VialTweeter (Hielscher). Afterwards, the lysate was centrifuged at 16,000 g for 10 min at 4°C. Supernatant (cleared lysates) were used to determine total protein amount using the Pierce BCA Protein Assay Kit (Thermo Fisher Scientific) according to manufacturer's protocol. Next, protein was reduced and alkylated. Afterwards, proteins were digested using Trypsin digestion at 37°C overnight. Samples were purified (solid phase extraction). labeled with TMT10plex Label Reagents (Thermo scientific) and then mixed before sample fractionation and clean-up. Labeled samples are analyzed by high resolution Orbitrap LC-MS/MS.

Bioinformatics

Paired-end sequencing reads were annotated and then aligned to the mouse reference genome (UCSC/mm10 and Refseq/GenBank annotation) using CLIPZ (Khorshid et al., 2011). From aligned reads, mRNA expression levels were estimated calculating the relative abundance of mRNA, based on the number of reads associated with a transcript and the transcript length (Jaskiewicz et al., 2012). Transcript counts of the two different genotypes have been analyzed and tested for differential expression by using R and Bioconductor software tools as previously described (Anders et al., 2013). Genes were considered as significantly differentially expressed with a confidence level of 0.05. Volcano plots and principal component analysis (PCA) plots were created using R. Mass-spectrometric data was further statistically validated by the in-house developed software tool SafeQuant (Glatter et al., 2012). Proteins were considered as significantly differentially expressed with a confidence level of 0.05. Characterization and enrichment analysis of the differentially expressed proteins was done using PANTHER pathway enrichment analysis (Mi et al., 2019; Mi et al., 2013) and DAVID analysis and functional annotation clustering (Huang da et al., 2009a, b).

Statistical analysis

All experiments were performed on a minimum of n (number of individual experiments) ≥3 independent biological samples. In all graphs, data are presented as the mean value and the respective standard error of the mean (SEM, error bars). Student's t test was used when two

groups were compared to evaluate statistical significance. One-way or two-way analysis of variance (ANOVA) test with Tukey's correction for multiple comparisons were used to compare more than two groups. A confidence level of 0.05 was accepted for statistical significance.

Acknowledgments

We thank the Biozentrum In-house Imaging Core Facility, Proteomics Core Facility and the Quantitative Genomics Facility (QGF) at the Department of Biosystems Science and Engineering (D-BSSE, ETH Zürich, Basel) for their technical support. SV40 MEFs were obtained from Dr. Dritan Liko as a gift.

Competing interests

No competing interests declared.

Funding

This work was supported by the Cantons of Basel-Stadt and Basel-Landschaft and grants from the Swiss National Science Foundation (to MAR).

Author contributions

MK and GM designed and performed experiments, analyzed data and wrote the manuscript with input from all authors and contributed both equally. SL performed muscle force measurements and electroporation. KC performed behavioral experiments with iTSCmKO mice. DJH discussed the data and performed injections. FO performed intraperitoneally injections, behavioral experiments and amplification of plasmid DNA. LT and NM created cDNA libraries for RNA-sequencing. CZ created proteomics data. DJG created TgN(HSA-caAKT-EGFP-ERt2) mice. MZ supported and supervised the generation of sequencing data and the analysis of RNA-seq data. MAR conceived the project, secured funding and wrote the manuscript.

References

Adams, J., and Kauffman, M. (2004). Development of the proteasome inhibitor Velcade (Bortezomib). Cancer Invest *22*, 304-311.

Anders, S., McCarthy, D.J., Chen, Y., Okoniewski, M., Smyth, G.K., Huber, W., and Robinson, M.D. (2013). Count-based differential expression analysis of RNA sequencing data using R and Bioconductor. Nat Protoc *8*, 1765-1786.

Aravamudan, B., Mantilla, C.B., Zhan, W.Z., and Sieck, G.C. (2006). Denervation effects on myonuclear domain size of rat diaphragm fibers. J Appl Physiol (1985) *100*, 1617-1622.

Bartelt, A., Widenmaier, S.B., Schlein, C., Johann, K., Goncalves, R.L.S., Eguchi, K., Fischer, A.W., Parlakgul, G., Snyder, N.A., Nguyen, T.B.*, et al.* (2018). Brown adipose tissue thermogenic adaptation requires Nrf1-mediated proteasomal activity. Nat Med.

Bentzinger, C.F., Lin, S., Romanino, K., Castets, P., Guridi, M., Summermatter, S., Handschin, C., Tintignac, L.A., Hall, M.N., and Ruegg, M.A. (2013). Differential response of skeletal muscles to mTORC1 signaling during atrophy and hypertrophy. Skeletal Muscle *3*, 6.

Bentzinger, C.F., Romanino, K., Cloetta, D., Lin, S., Mascarenhas, J.B., Oliveri, F., Xia, J., Casanova, E., Costa, C.F., Brink, M.*, et al.* (2008). Skeletal muscle-specific ablation of raptor, but not of rictor, causes metabolic changes and results in muscle dystrophy. Cell Metab *8*, 411-424.

Bodine, S.C., Stitt, T.N., Gonzalez, M., Kline, W.O., Stover, G.L., Bauerlein, R., Zlotchenko, E., Scrimgeour, A., Lawrence, J.C., Glass, D.J.*, et al.* (2001). Akt/mTOR pathway is a crucial regulator of skeletal muscle hypertrophy and can prevent muscle atrophy in vivo. Nat Cell Biol *3*, 1014-1019.

Bott, L.C., Badders, N.M., Chen, K.L., Harmison, G.G., Bautista, E., Shih, C.C., Katsuno, M., Sobue, G., Taylor, J.P., Dantuma, N.P.*, et al.* (2016). A small-molecule Nrf1 and Nrf2 activator mitigates polyglutamine toxicity in spinal and bulbar muscular atrophy. Hum Mol Genet *25*, 1979-1989.

Brocca, L., Toniolo, L., Reggiani, C., Bottinelli, R., Sandri, M., and Pellegrino, M.A. (2017). FoxO-dependent atrogenes vary among catabolic conditions and play a key role in muscle atrophy induced by hindlimb suspension. J Physiol *595*, 1143-1158.

Castets, P., Lin, S., Rion, N., Di Fulvio, S., Romanino, K., Guridi, M., Frank, S., Tintignac, L.A., Sinnreich, M., and Ruegg, M.A. (2013). Sustained activation of mTORC1 in skeletal muscle inhibits constitutive and starvation-induced autophagy and causes a severe, late-onset myopathy. Cell Metab *17*, 731-744.

Dikic, I. (2017). Proteasomal and Autophagic Degradation Systems. Annu Rev Biochem *86*, 193-224.

Finley, D., Chen, X., and Walters, K.J. (2016). Gates, Channels, and Switches: Elements of the Proteasome Machine. Trends Biochem Sci *41*, 77-93.

Frankland-Searby, S., and Bhaumik, S.R. (2012). The 26S proteasome complex: an attractive target for cancer therapy. Biochim Biophys Acta *1825*, 64-76.

Glatter, T., Ludwig, C., Ahrne, E., Aebersold, R., Heck, A.J., and Schmidt, A. (2012). Large-scale quantitative assessment of different in-solution protein digestion protocols reveals superior cleavage efficiency of tandem Lys-C/trypsin proteolysis over trypsin digestion. J Proteome Res *11*, 5145-5156.

Goldberg, A.L. (1969). Protein turnover in skeletal muscle. I. Protein catabolism during work-induced hypertrophy and growth induced with growth hormone. J Biol Chem *244*, 3217-3222.

Guridi, M., Tintignac, L.A., Lin, S., Kupr, B., Castets, P., and Ruegg, M.A. (2015). Activation of mTORC1 in skeletal muscle regulates whole-body metabolism through FGF21. Sci Signal *8*, ra113.

Han, J.W., Valdez, J.L., Ho, D.V., Lee, C.S., Kim, H.M., Wang, X., Huang, L., and Chan, J.Y. (2017). Nuclear factor-erythroid-2 related transcription factor-1 (Nrf1) is regulated by O-GlcNAc transferase. Free Radic Biol Med *110*, 196-205.

Harrington, L.S., Findlay, G.M., Gray, A., Tolkacheva, T., Wigfield, S., Rebholz, H., Barnett, J., Leslie, N.R., Cheng, S., Shepherd, P.R.*, et al.* (2004). The TSC1-2 tumor suppressor controls insulin-PI3K signaling via regulation of IRS proteins. J Cell Biol *166*, 213-223.

Huang da, W., Sherman, B.T., and Lempicki, R.A. (2009a). Bioinformatics enrichment tools: paths toward the comprehensive functional analysis of large gene lists. Nucleic Acids Res *37*, 1-13.

Huang da, W., Sherman, B.T., and Lempicki, R.A. (2009b). Systematic and integrative analysis of large gene lists using DAVID bioinformatics resources. Nat Protoc *4*, 44-57.

Inoki, K., Li, Y., Zhu, T., Wu, J., and Guan, K.L. (2002). TSC2 is phosphorylated and inhibited by Akt and suppresses mTOR signalling. Nat Cell Biol *4*, 648-657.

Jaskiewicz, L., Bilen, B., Hausser, J., and Zavolan, M. (2012). Argonaute CLIP--a method to identify in vivo targets of miRNAs. Methods *58*, 106-112.

Johnson, D.E. (2015). The ubiquitin-proteasome system: opportunities for therapeutic intervention in solid tumors. Endocr Relat Cancer *22*, T1-17.

Khorshid, M., Rodak, C., and Zavolan, M. (2011). CLIPZ: a database and analysis environment for experimentally determined binding sites of RNA-binding proteins. Nucleic Acids Res *39*, D245-252.

Kim, J., Kundu, M., Viollet, B., and Guan, K.L. (2011). AMPK and mTOR regulate autophagy through direct phosphorylation of Ulk1. Nat Cell Biol *13*, 132-141.

Koizumi, S., Irie, T., Hirayama, S., Sakurai, Y., Yashiroda, H., Naguro, I., Ichijo, H., Hamazaki, J., and Murata, S. (2016). The aspartyl protease DDI2 activates Nrf1 to compensate for proteasome dysfunction. Elife *5*.

Kong, X.C., Barzaghi, P., and Ruegg, M.A. (2004). Inhibition of synapse assembly in mammalian muscle in vivo by RNA interference. EMBO Rep *5*, 183-188.

Kwiatkowski, D.J., Zhang, H., Bandura, J.L., Heiberger, K.M., Glogauer, M., el-Hashemite, N., and Onda, H. (2002). A mouse model of TSC1 reveals sex-dependent lethality from liver hemangiomas, and up-regulation of p70S6 kinase activity in Tsc1 null cells. Hum Mol Genet *11*, 525-534.

Lai, K.M., Gonzalez, M., Poueymirou, W.T., Kline, W.O., Na, E., Zlotchenko, E., Stitt, T.N., Economides, A.N., Yancopoulos, G.D., and Glass, D.J. (2004). Conditional activation of akt in adult skeletal muscle induces rapid hypertrophy. Mol Cell Biol *24*, 9295-9304.

Laplante, M., and Sabatini, D.M. (2012). mTOR signaling in growth control and disease. Cell *149*, 274-293.

Lecker, S.H., Jagoe, R.T., Gilbert, A., Gomes, M., Baracos, V., Bailey, J., Price, S.R., Mitch, W.E., and Goldberg, A.L. (2004). Multiple types of skeletal muscle atrophy involve a common program of changes in gene expression. Faseb J *18*, 39-51.

Lee, C.S., Ho, D.V., and Chan, J.Y. (2013). Nuclear factor-erythroid 2-related factor 1 regulates expression of proteasome genes in hepatocytes and protects against endoplasmic reticulum stress and steatosis in mice. Febs J *280*, 3609-3620.

Lee, C.S., Lee, C., Hu, T., Nguyen, J.M., Zhang, J., Martin, M.V., Vawter, M.P., Huang, E.J., and Chan, J.Y. (2011). Loss of nuclear factor E2-related factor 1 in the brain leads to dysregulation of proteasome gene expression and neurodegeneration. Proc Natl Acad Sci U S A *108*, 8408-8413.

Leung, L., Kwong, M., Hou, S., Lee, C., and Chan, J.Y. (2003). Deficiency of the Nrf1 and Nrf2 transcription factors results in early embryonic lethality and severe oxidative stress. J Biol Chem *278*, 48021-48029.

Li, J.B., and Goldberg, A.L. (1976). Effects of food deprivation on protein synthesis and degradation in rat skeletal muscles. Am J Physiol *231*, 441-448.

Ma, X.M., and Blenis, J. (2009). Molecular mechanisms of mTOR-mediated translational control. Nat Rev Mol Cell Biol *10*, 307-318.

Manning, B.D., Tee, A.R., Logsdon, M.N., Blenis, J., and Cantley, L.C. (2002). Identification of the tuberous sclerosis complex-2 tumor suppressor gene product tuberin as a target of the phosphoinositide 3-kinase/akt pathway. Mol Cell *10*, 151-162.

Marabita, M., Baraldo, M., Solagna, F., Ceelen, J.J.M., Sartori, R., Nolte, H., Nemazanyy, I., Pyronnet, S., Kruger, M., Pende, M.*, et al.* (2016). S6K1 Is Required for Increasing Skeletal Muscle Force during Hypertrophy. Cell Rep *17*, 501-513.

Masiero, E., Agatea, L., Mammucari, C., Blaauw, B., Loro, E., Komatsu, M., Metzger, D., Reggiani, C., Schiaffino, S., and Sandri, M. (2009). Autophagy is required to maintain muscle mass. Cell Metab *10*, 507-515.

McCarthy, J.J., Srikuea, R., Kirby, T.J., Peterson, C.A., and Esser, K.A. (2012). Inducible Cre transgenic mouse strain for skeletal muscle-specific gene targeting. Skelet Muscle *2*, 8.

Menon, S., Dibble, C.C., Talbott, G., Hoxhaj, G., Valvezan, A.J., Takahashi, H., Cantley, L.C., and Manning, B.D. (2014). Spatial control of the TSC complex integrates insulin and nutrient regulation of mTORC1 at the lysosome. Cell *156*, 771-785.

Mi, H., Muruganujan, A., Ebert, D., Huang, X., and Thomas, P.D. (2019). PANTHER version 14: more genomes, a new PANTHER GO-slim and improvements in enrichment analysis tools. Nucleic Acids Res *47*, D419-D426.

Mi, H., Muruganujan, A., and Thomas, P.D. (2013). PANTHER in 2013: modeling the evolution of gene function, and other gene attributes, in the context of phylogenetic trees. Nucleic Acids Res *41*, D377-386.

Milan, G., Romanello, V., Pescatore, F., Armani, A., Paik, J.H., Frasson, L., Seydel, A., Zhao, J., Abraham, R., Goldberg, A.L.*, et al.* (2015). Regulation of autophagy and the ubiquitin-proteasome system by the FoxO transcriptional network during muscle atrophy. Nat Commun *6*, 6670.

Mitsiades, N., Mitsiades, C.S., Poulaki, V., Chauhan, D., Fanourakis, G., Gu, X., Bailey, C., Joseph, M., Libermann, T.A., Treon, S.P.*, et al.* (2002). Molecular sequelae of proteasome inhibition in human multiple myeloma cells. Proc Natl Acad Sci U S A *99*, 14374-14379.

Piccirillo, R., and Goldberg, A.L. (2012). The p97/VCP ATPase is critical in muscle atrophy and the accelerated degradation of muscle proteins. Embo J *31*, 3334-3350.

Radhakrishnan, S.K., den Besten, W., and Deshaies, R.J. (2014). p97-dependent retrotranslocation and proteolytic processing govern formation of active Nrf1 upon proteasome inhibition. Elife *3*, e01856.

Radhakrishnan, S.K., Lee, C.S., Young, P., Beskow, A., Chan, J.Y., and Deshaies, R.J. (2010). Transcription factor Nrf1 mediates the proteasome recovery pathway after proteasome inhibition in mammalian cells. Mol Cell *38*, 17-28.

Richardson, P.G., Sonneveld, P., Schuster, M.W., Irwin, D., Stadtmauer, E.A., Facon, T., Harousseau, J.L., Ben-Yehuda, D., Lonial, S., Goldschmidt, H.*, et al.* (2005). Bortezomib or high-dose dexamethasone for relapsed multiple myeloma. N Engl J Med *352*, 2487-2498.

Richardson, P.G., Weller, E., Lonial, S., Jakubowiak, A.J., Jagannath, S., Raje, N.S., Avigan, D.E., Xie, W., Ghobrial, I.M., Schlossman, R.L.*, et al.* (2010). Lenalidomide, bortezomib, and dexamethasone combination therapy in patients with newly diagnosed multiple myeloma. Blood *116*, 679-686.

Risson, V., Mazelin, L., Roceri, M., Sanchez, H., Moncollin, V., Corneloup, C., Richard-Bulteau, H., Vignaud, A., Baas, D., Defour, A.*, et al.* (2009). Muscle inactivation of mTOR causes metabolic and dystrophin defects leading to severe myopathy. J Cell Biol *187*, 859-874.

Ruegg, M.A., and Glass, D.J. (2011). Molecular mechanisms and treatment options for muscle wasting diseases. Annu Rev Pharmacol Toxicol *51*, 373-395.

Sacheck, J.M., Hyatt, J.P., Raffaello, A., Jagoe, R.T., Roy, R.R., Edgerton, V.R., Lecker, S.H., and Goldberg, A.L. (2007). Rapid disuse and denervation atrophy involve transcriptional changes similar to those of muscle wasting during systemic diseases. Faseb J *21*, 140-155.

Sacheck, J.M., Ohtsuka, A., McLary, S.C., and Goldberg, A.L. (2004). IGF-I stimulates muscle growth by suppressing protein breakdown and expression of atrophy-related ubiquitin ligases, atrogin-1 and MuRF1. Am J Physiol Endocrinol Metab *287*, E591-601.

Sancak, Y., Bar-Peled, L., Zoncu, R., Markhard, A.L., Nada, S., and Sabatini, D.M. (2010). Ragulator-Rag complex targets mTORC1 to the lysosomal surface and is necessary for its activation by amino acids. Cell *141*, 290-303.

Sandri, M. (2013). Protein breakdown in muscle wasting: role of autophagy-lysosome and ubiquitin-proteasome. Int J Biochem Cell Biol *45*, 2121-2129.

Sandri, M., Sandri, C., Gilbert, A., Skurk, C., Calabria, E., Picard, A., Walsh, K., Schiaffino, S., Lecker, S.H., and Goldberg, A.L. (2004). Foxo transcription factors induce the atrophy-related ubiquitin ligase atrogin-1 and cause skeletal muscle atrophy. Cell *117*, 399-412.

Sartori, R., Schirwis, E., Blaauw, B., Bortolanza, S., Zhao, J., Enzo, E., Stantzou, A., Mouisel, E., Toniolo, L., Ferry, A.*, et al.* (2013). BMP signaling controls muscle mass. Nat Genet *45*, 1309-1318.

Schiaffino, S., Dyar, K.A., Ciciliot, S., Blaauw, B., and Sandri, M. (2013). Mechanisms regulating skeletal muscle growth and atrophy. Febs J *280*, 4294-4314.

Schwander, M., Leu, M., Stumm, M., Dorchies, O.M., Ruegg, U.T., Schittny, J., and Muller, U. (2003). Beta1 integrins regulate myoblast fusion and sarcomere assembly. Dev Cell *4*, 673-685.

Sekine, H., Okazaki, K., Kato, K., Alam, M.M., Shima, H., Katsuoka, F., Tsujita, T., Suzuki, N., Kobayashi, A., Igarashi, K.*, et al.* (2018). O-GlcNAcylation Signal Mediates Proteasome Inhibitor Resistance in Cancer Cells by Stabilizing NRF1. Mol Cell Biol.

Sha, Z., and Goldberg, A.L. (2014). Proteasome-mediated processing of Nrf1 is essential for coordinate induction of all proteasome subunits and p97. Curr Biol *24*, 1573-1583.

Shimobayashi, M., and Hall, M.N. (2014). Making new contacts: the mTOR network in metabolism and signalling crosstalk. Nat Rev Mol Cell Biol *15*, 155-162.

Steffen, J., Seeger, M., Koch, A., and Kruger, E. (2010). Proteasomal degradation is transcriptionally controlled by TCF11 via an ERAD-dependent feedback loop. Mol Cell *40*, 147-158.

Strucksberg, K.H., Tangavelou, K., Schroder, R., and Clemen, C.S. (2010). Proteasomal activity in skeletal muscle: a matter of assay design, muscle type, and age. Anal Biochem *399*, 225-229.

Venugopal, R., and Jaiswal, A.K. (1998). Nrf2 and Nrf1 in association with Jun proteins regulate antioxidant response element-mediated expression and coordinated induction of genes encoding detoxifying enzymes. Oncogene *17*, 3145-3156.

Widenmaier, S.B., Snyder, N.A., Nguyen, T.B., Arduini, A., Lee, G.Y., Arruda, A.P., Saksi, J., Bartelt, A., and Hotamisligil, G.S. (2017). NRF1 Is an ER Membrane Sensor that Is Central to Cholesterol Homeostasis. Cell *171*, 1094-1109 e1015.

Yuan, J., Zhang, S., and Zhang, Y. (2018). Nrf1 is paved as a new strategic avenue to prevent and treat cancer, neurodegenerative and other diseases. Toxicol Appl Pharmacol *360*, 273-283.

Zhang, Y., Nicholatos, J., Dreier, J.R., Ricoult, S.J., Widenmaier, S.B., Hotamisligil, G.S., Kwiatkowski, D.J., and Manning, B.D. (2014). Coordinated regulation of protein synthesis and degradation by mTORC1. Nature *513*, 440-443.

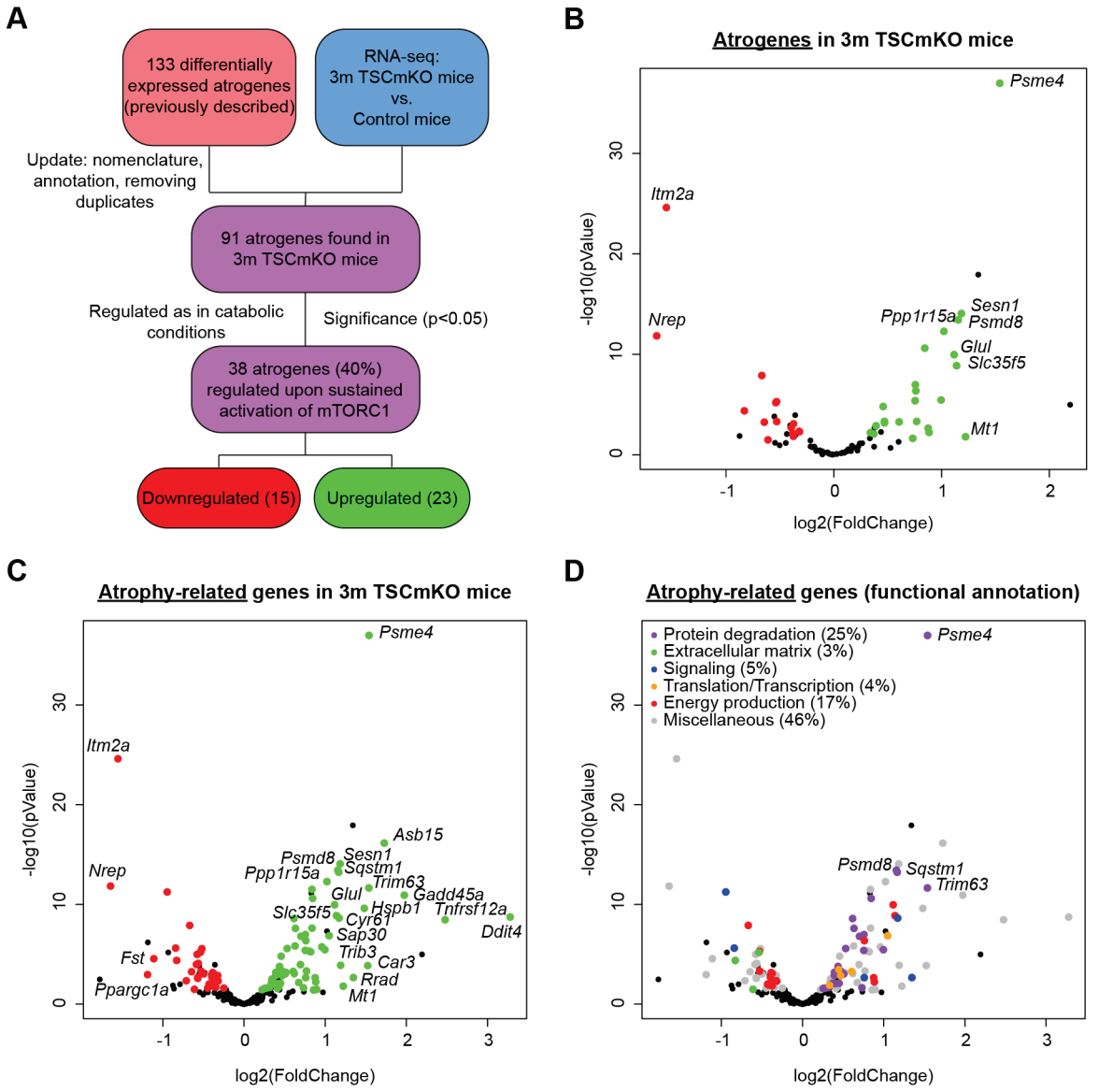

Figure 1. Young TSCmKO mice display an atrophy-related gene expression signature.

(A) Identification of mTORC1-dependent atrogenes, comparing published mRNA expression data of atrogenes with RNA-sequencing data obtained from *extensor digitorum longus* (EDL) muscles from female, 3-month-old TSCmKO mice and Control littermates (n=5). **(B)** Volcano plot of previously described atrogenes found expressed in young TSCmKO mice. Colored circles indicate significantly (p<0.05), differentially expressed (DE) genes (green=upregulated, red=downregulated) between young TSCmKO mice and Control littermates, which are similarly regulated as in other types of muscle atrophy. Genes DE in young TSCmKO mice twofold or more, are labeled by their gene name. **(C)** Volcano plot of atrophy-related genes found expressed in young TSCmKO mice. Genes DE in young TSCmKO mice twofold or more, are labeled by their gene name. **(D)** Volcano plot of atrophy-related genes found expressed in young TSCmKO mice. Genes involved in protein degradation are labeled by their gene name.

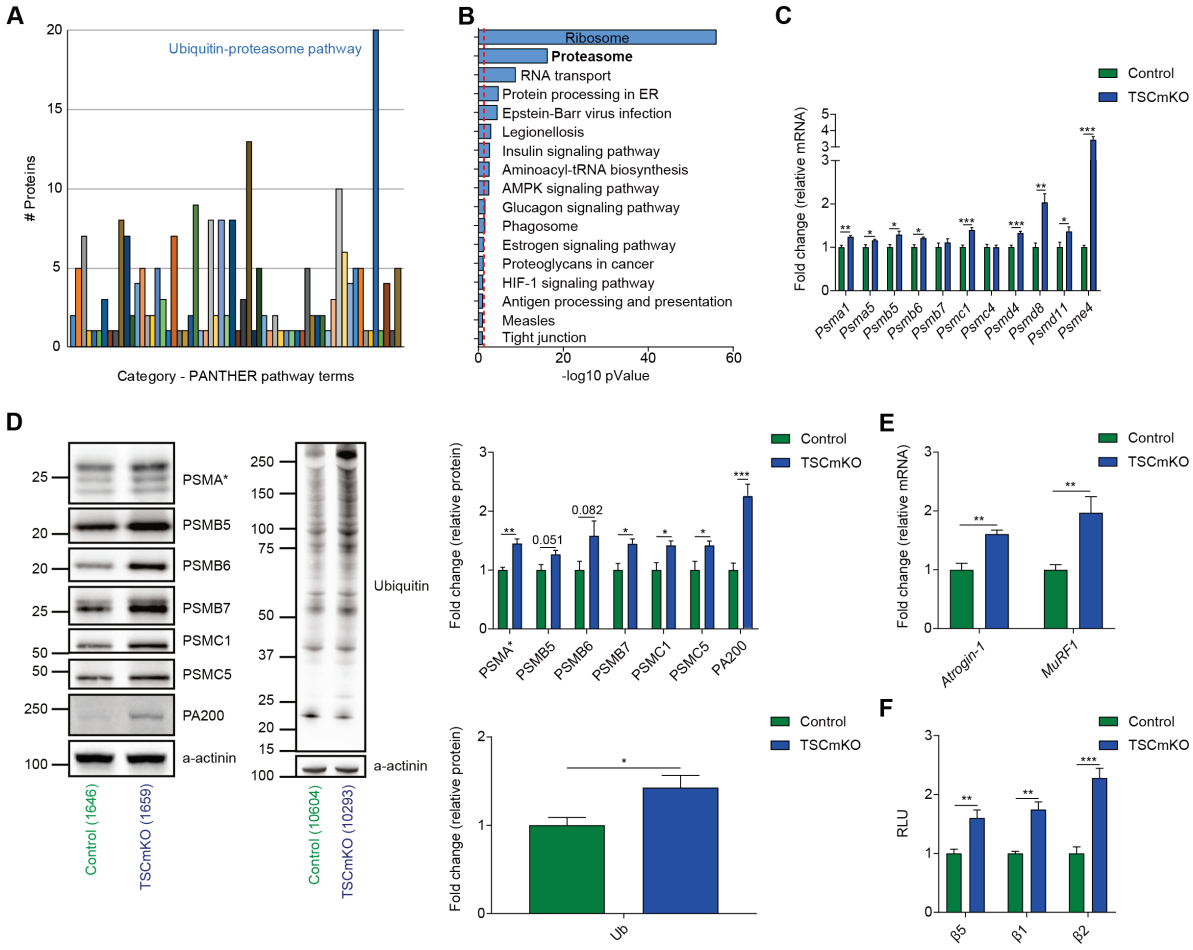

Figure 2. Ubiquitin proteasome system is enriched in young TSCmKO mice.

Significantly ($p<0.05$), differentially expressed (DE) proteins were obtained from proteomics data from *tibialis anterior* (TA) muscles of 3-month-old, male TSCmKO mice and Control littermates (n=4). **(A)** Bar diagram illustrates PANTHER pathway enrichment analysis done with DE proteins. **(B)** DAVID enrichment analysis algorithms were applied on DE proteins to determine the most enriched KEGG pathways. **(C, E)** Relative transcript expression was quantified by RT-qPCR in TA muscle from 2-month-old, female TSCmKO and Control mice, n=5. Transcript encoding β-tubulin was used as reference. **(D)** Western blot analysis of proteasomal subunits (PSM) in TA muscles from 2-month-old, female TSCmKO and Control mice, n=5. Western blot analysis of ubiquitinylated proteins in *gastrocnemius* (GAST) muscles from 3-month-old, male TSCmKO and Control mice, n=6. **(F)** Luciferase-based proteasome activity measurement in lysates of *extensor digitorum longus* (EDL) muscles from 4-month-old, male TSCmKO and Control mice, n=4. Data represent means ± SEM, ***$p \leq 0.001$, **$p \leq 0.01$, *$p \leq 0.05$, Student's t test.

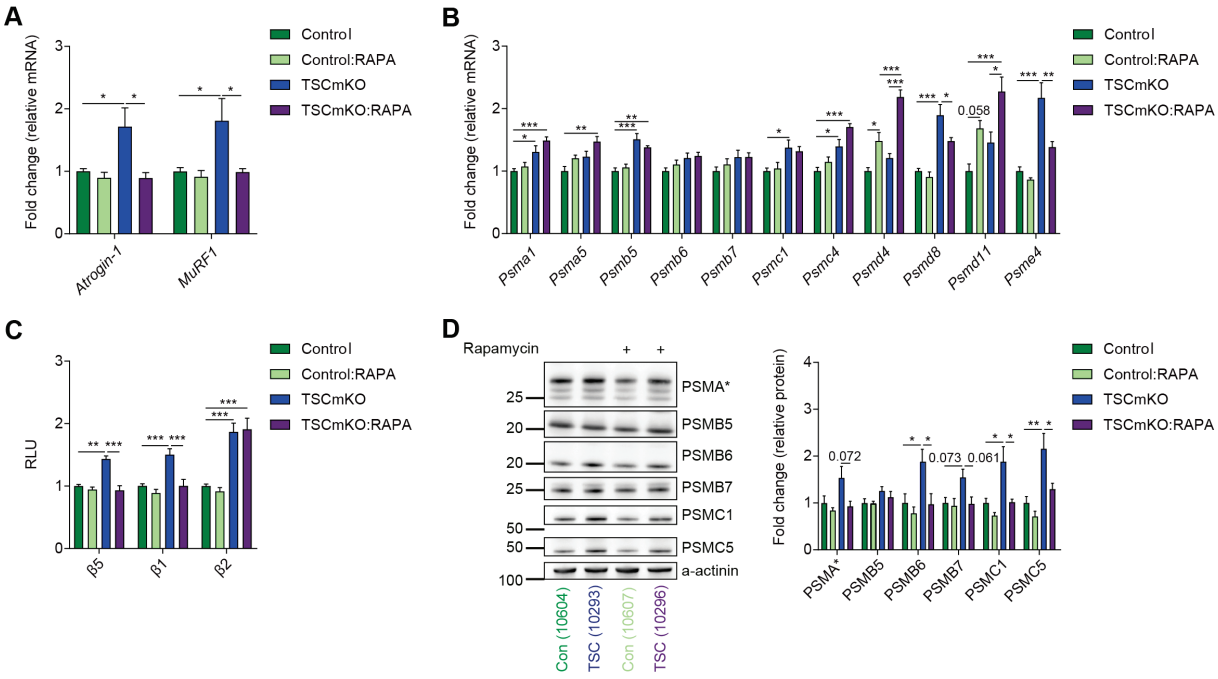

Figure 3. Short-term inhibition with rapamycin reverses the increased UPS in TSCmKO mice.

3-month-old Control and TSCmKO mice were treated with rapamycin (RAPA) or vehicle for 3 days. **(A, B)** Relative transcript expression was quantified by RT-qPCR in *gastrocnemius* (GAST) muscle, n=5 (Control:RAPA), n = 6 (Control, TSCmKO, TSCmKO:RAPA). Transcript encoding β-actin was used as reference. **(C)** Luciferase-based proteasome activity measurement in lysates of *plantaris* (PLA) muscle, n=5 (Control:RAPA), n = 6 (Control, TSCmKO, TSCmKO:RAPA. **(D)** Western blot analysis of proteasomal subunits (PSM) in *tibialis anterior* (TA) muscle, n=4 (Control:RAPA), n = 6 (Control, TSCmKO, TSCmKO:RAPA). Data represent means ± SEM, ***p ≤ 0.001, **p ≤ 0.01, *p ≤ 0.05, One-way ANOVA test.

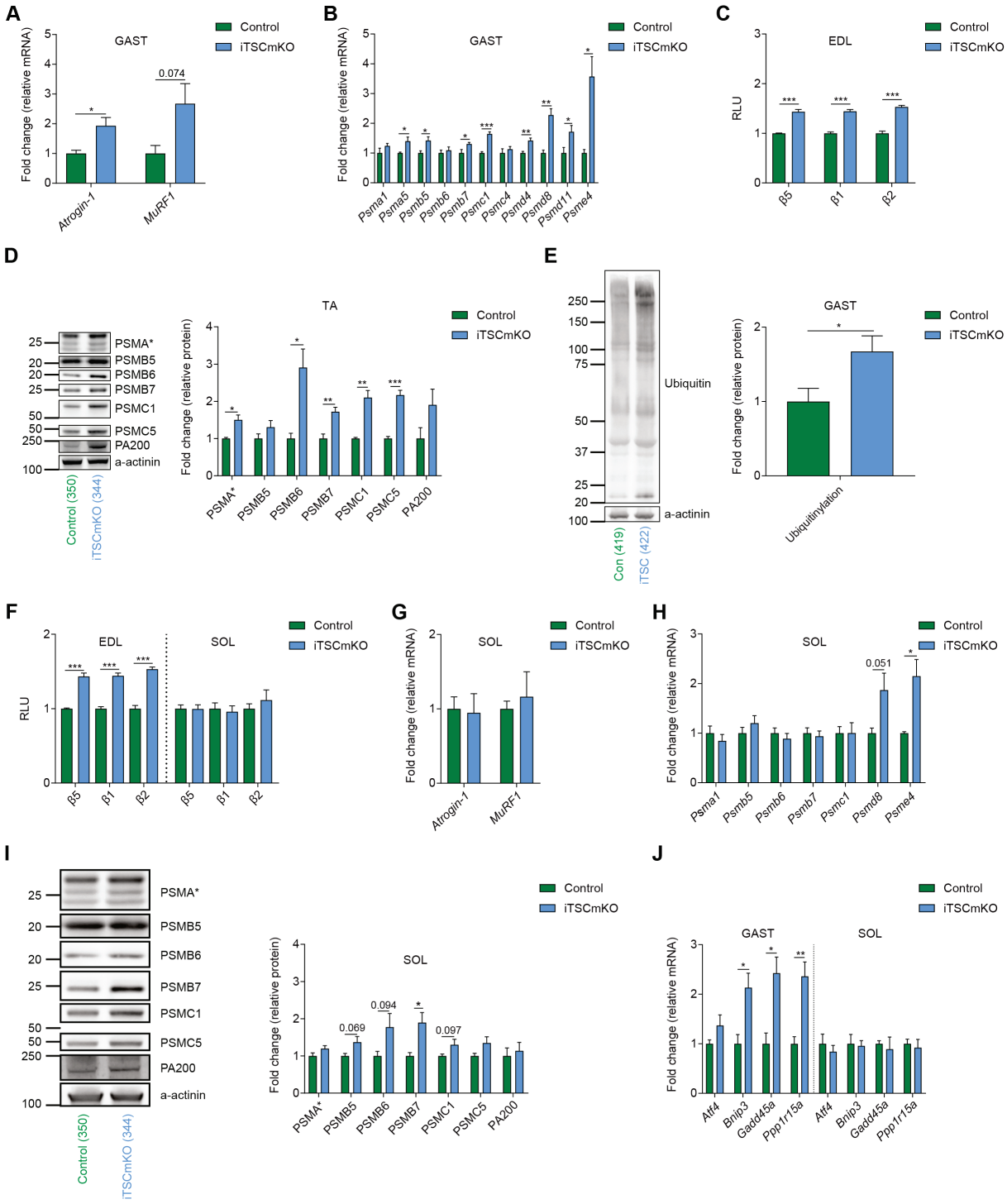

Figure 4. Activation of mTORC1 for 21 days is sufficient to increase the UPS in most adult muscles but not in *soleus*.

In 3-month-old mice, *Tsc1* deletion was induced in skeletal muscle (iTSCmKO mice) and mice were examined 21 days later. **(A, B, J)** Relative transcript expression was quantified by RT-qPCR in *gastrocnemius* (GAST) muscle, n=5 (iTSCmKO), n=4 (Control). Transcript encoding β-tubulin was used as reference. **(C)** Luciferase-based proteasome activity measurement in lysates of *extensor digitorum longus* (EDL) muscle, n=4. **(D)** Western blot analysis of proteasomal subunits (PSM) in *tibialis anterior* (TA) muscle, n=4. **(E)** Western blot analysis of

ubiquitinylated proteins in GAST muscle, n=5 (iTSCmKO), n=4 (Control). The slow-twitch muscle *soleus* (SOL) is hypertrophic in iTSCmKO mice and displays no increase of the UPS. **(F)** Luciferase-based proteasome activity measurement in lysates of EDL and SOL muscle, n=4 (EDL), n=4 (SOL, Control), n=5 (SOL, iTSCmKO). **(G, H, J)** Relative transcript expression was quantified by RT-qPCR in SOL muscle, n=4. Transcript encoding β-actin was used as reference. **(I)** Western blot analysis of PSM in SOL muscle, n=4. Data represent means ± SEM, ***p ≤ 0.001, **p ≤ 0.01, *p ≤ 0.05, Student's t test.

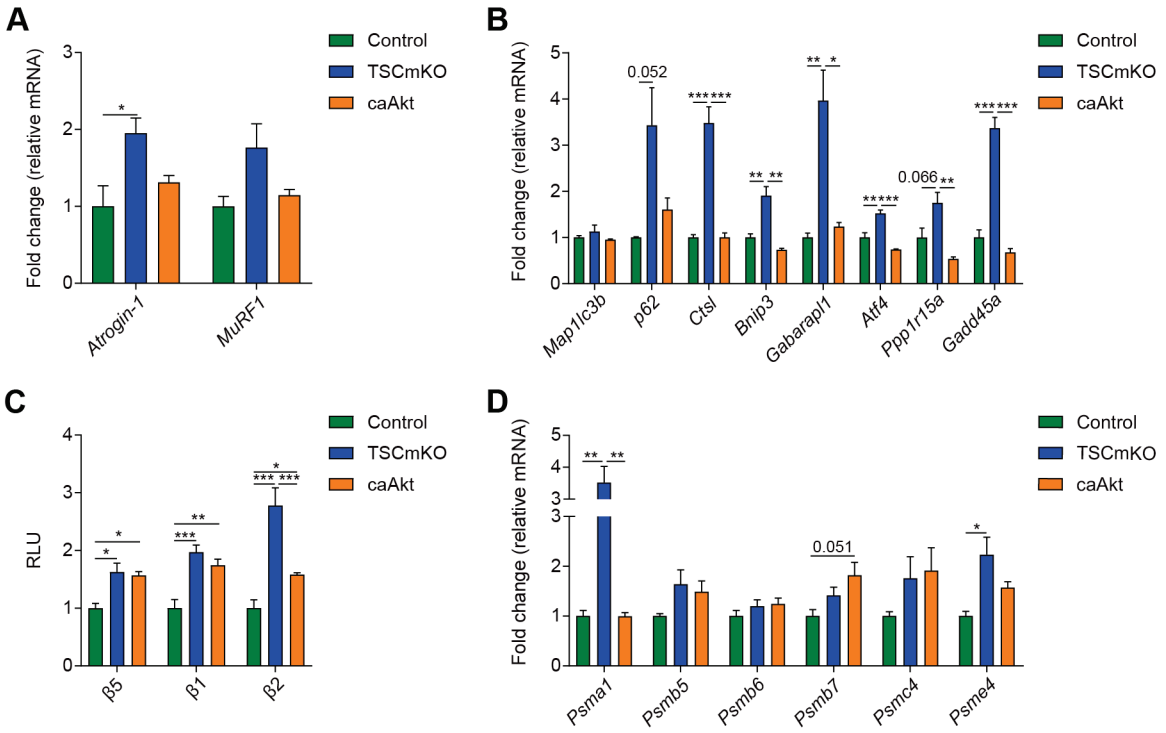

Figure 5. Constitutive activation of Akt induces proteasome activity similarly as in TSCmKO mice.

10-month-old Control, TSCmKO and caAkt mice were treated every 72 h with tamoxifen to induce a constitutive active form of Akt (caAkt mice) for 14 days. **(A, B, D)** Relative transcript expression was quantified by RT-qPCR in *gastrocnemius* (GAST) muscle, n=4 (TSCmKO), n=3 (caAkt, Control). Transcripts encoding the TATA box binding protein (TBP) was used as reference. **(C)** Luciferase-based proteasome activity measurement in lysates of *plantaris* (PLA) muscle, n=3 (caAkt, TSCmKO), n=4 (Control). Data represent means ± SEM, ***p ≤ 0.001, **p ≤ 0.01, *p ≤ 0.05, One-way ANOVA test.

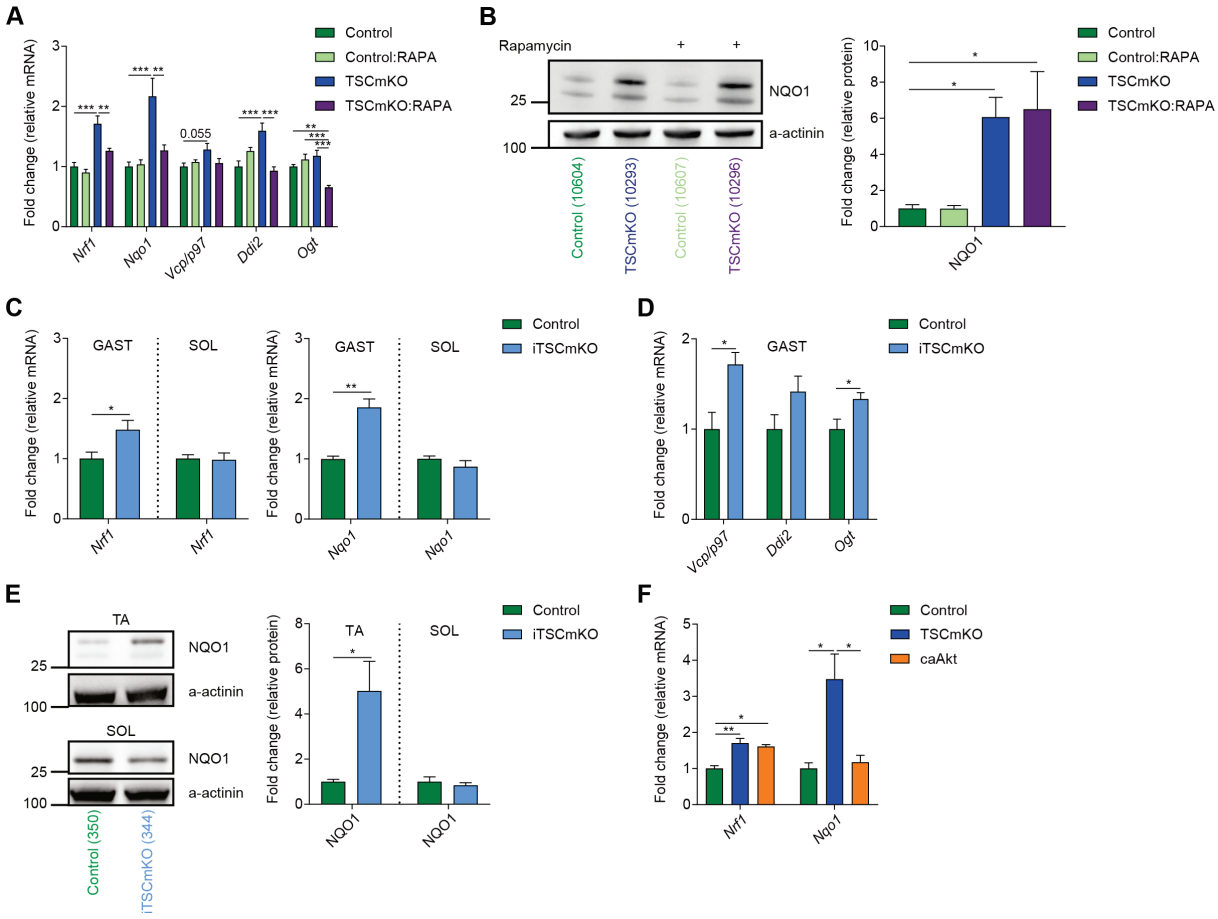

Figure 6. Nrf1 is a key mediator of mTORC1-induced UPS.

3-month-old Control and TSCmKO mice were treated with rapamycin (RAPA) or vehicle for 3 days. **(A)** Relative transcript expression was quantified by RT-qPCR in *gastrocnemius* (GAST) muscle, n=5 (Control:RAPA), n = 6 (Control, TSCmKO, TSCmKO:RAPA). Transcript encoding β-actin was used as reference. **(B)** Western blot analysis of NQO1 in *tibialis anterior* (TA) muscle, n=4 (Control:RAPA), n = 6 (Control, TSCmKO, TSCmKO:RAPA). In 3-month-old mice, *Tsc1* deletion was induced in skeletal muscle (iTSCmKO mice) and mice were examined 21 days later. **(C)** Relative transcript expression was quantified by RT-qPCR in GAST or *soleus* (SOL) muscle, n=5 (GAST iTSCmKO), n=4 (GAST Control, SOL Control, SOL iTSCmKO). Transcripts encoding β-tubulin (GAST) or β-actin (SOL) were used as reference. **(D)** Relative transcript expression was quantified by RT-qPCR in GAST muscle, n=5 (iTSCmKO), n=4 (Control). Transcript encoding β-tubulin was used as reference. **(E)** Western blot analysis of NQO1 in TA or SOL muscle, n=4. 10-month-old Control, TSCmKO and caAkt mice were treated every 72 h with tamoxifen to induce a constitutive active form of Akt (caAkt mice) for 14 days. **(F)** Relative transcript expression was quantified by RT-qPCR in GAST muscle, n=4 (TSCmKO), n=3 (caAkt, Control). Transcripts encoding TBP was used as reference. Data represent means ± SEM, ***p ≤ 0.001, **p ≤ 0.01, *p ≤ 0.05, Student's t test (if two groups were compared), One-way ANOVA test (if more than two groups were compared).

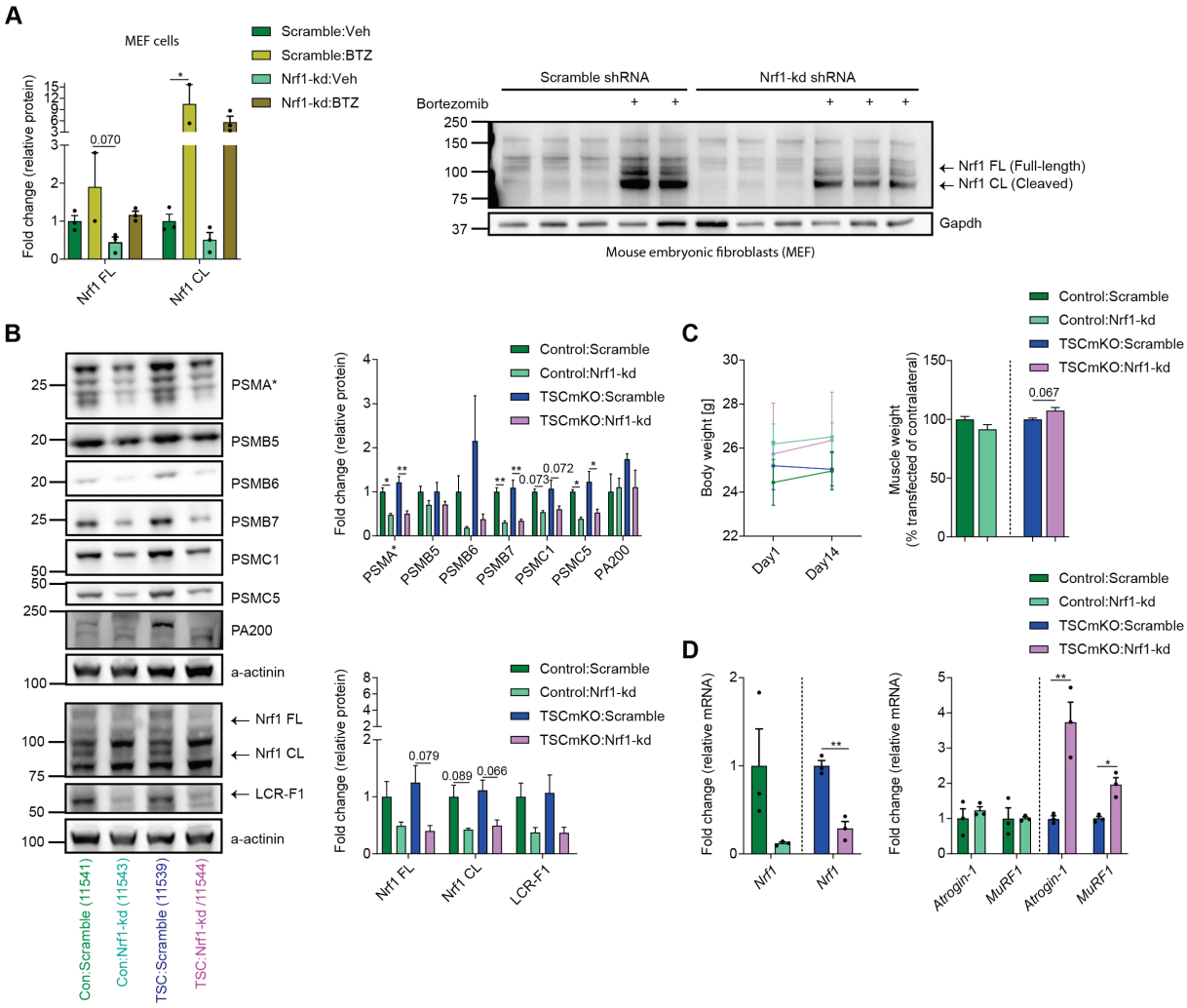

Figure 7. Inactivation of Nrf1 in TSCmKO mice decreases the expression of PSM genes.

(A) Western blot analysis of mouse embryonic fibroblasts (MEFs), transfected with plasmids driving the expression of a shRNA directed to Nrf1 (Nrf1-kd shRNA) or to a scramble sequence (Scramble shRNA), and treated with bortezomib (BTZ) in the last 4 hours before lysis. Nrf1 CL = Cleaved Nrf1; Nrf1 FL = Full-length Nrf1. *Tibialis anterior* (TA) muscle of 3-month-old Control and TSCmKO mice was electroporated with plasmids driving scramble or Nrf1-kd shRNA. Muscles were analyzed 2 weeks later. **(B)** Western blot analysis of proteasomal subunits (PSM), Nrf1 FL, Nrf1 CL and LCR-F1 (Nrf1β) in electroporated TA muscle, n=3. **(C)** *Left:* Delta of body weight between electroporated and the contralateral, sham-treated muscle, n=3. *Right:* Relative muscle weight ratio between electroporated and the contralateral, sham-treated muscle, n=3. **(D)** Relative transcript expression was quantified by RT-qPCR in electroporated TA muscles, n=3. Transcript encoding Desmin (DES) was used as reference. Data represent means ± SEM, ***p ≤ 0.001, **p ≤ 0.01, *p ≤ 0.05, Student's t test (if two groups were compared), One-way ANOVA test (if more than two groups were compared).

Supplemental data

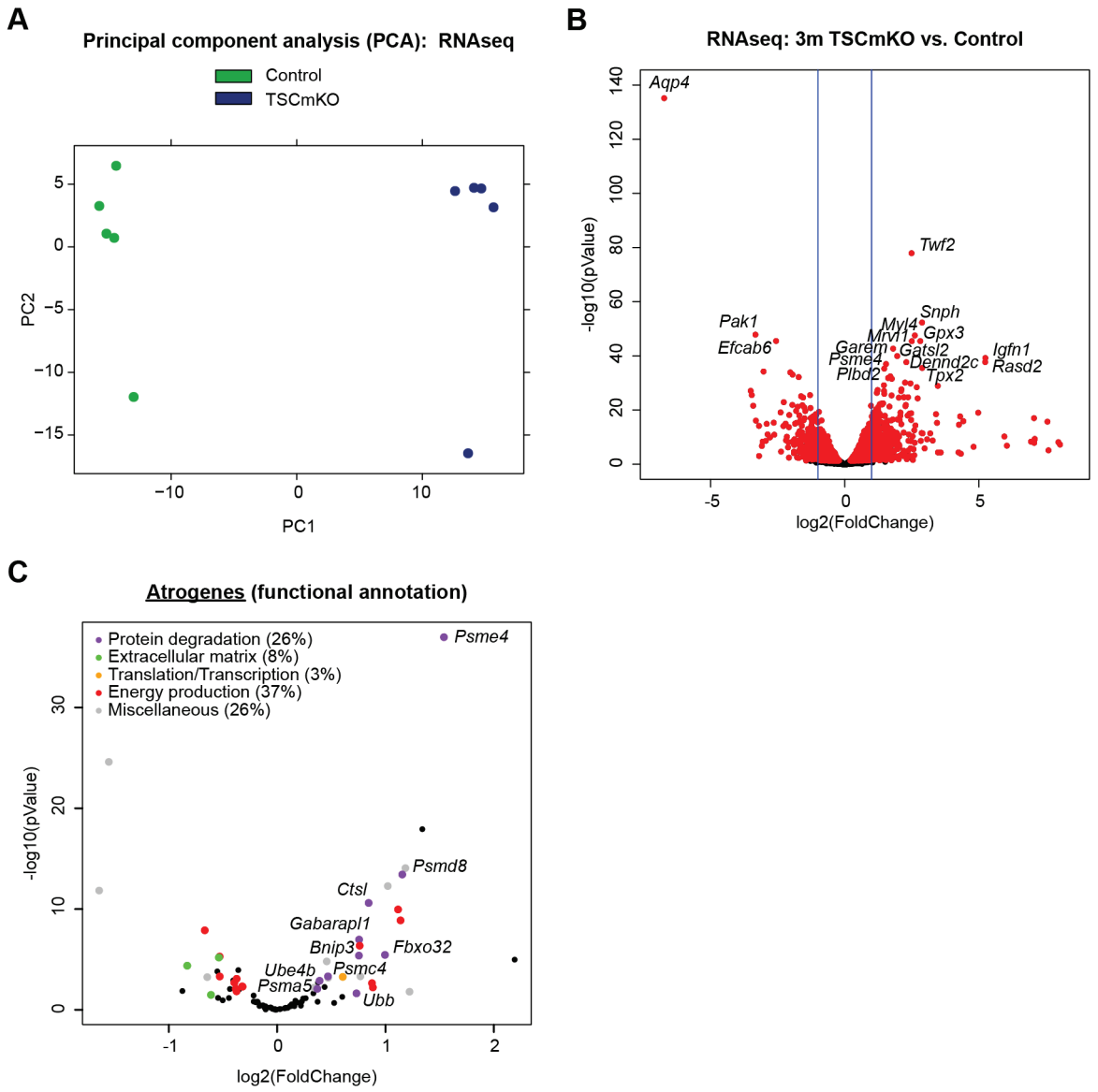

Figure S1. Young TSCmKO mice display an atrophy-related gene expression signature.

(A) Principal component analysis (PCA) of RNA-seq data obtained from *extensor digitorum longus* (EDL) muscles of 3-month-old TSCmKO mice and Control littermates (n=5). Plotting principal component 1 (PC1) versus principal component 2 (PC2) illustrates the clear genotype specific differentiation of TSCmKO mice and Control littermates. **(B)** Volcano plot of all genes expressed in TSCmKO mice and Control littermates. Red circles indicate significantly ($p<0.05$), DE genes. Blue lines represent a fold-change of +/- 2. The 15 most significantly, DE genes are labeled by their gene name. **(C)** Volcano plot of previously described atrogenes found expressed in young TSCmKO mice. Genes involved in protein degradation are labeled by their gene name.

A

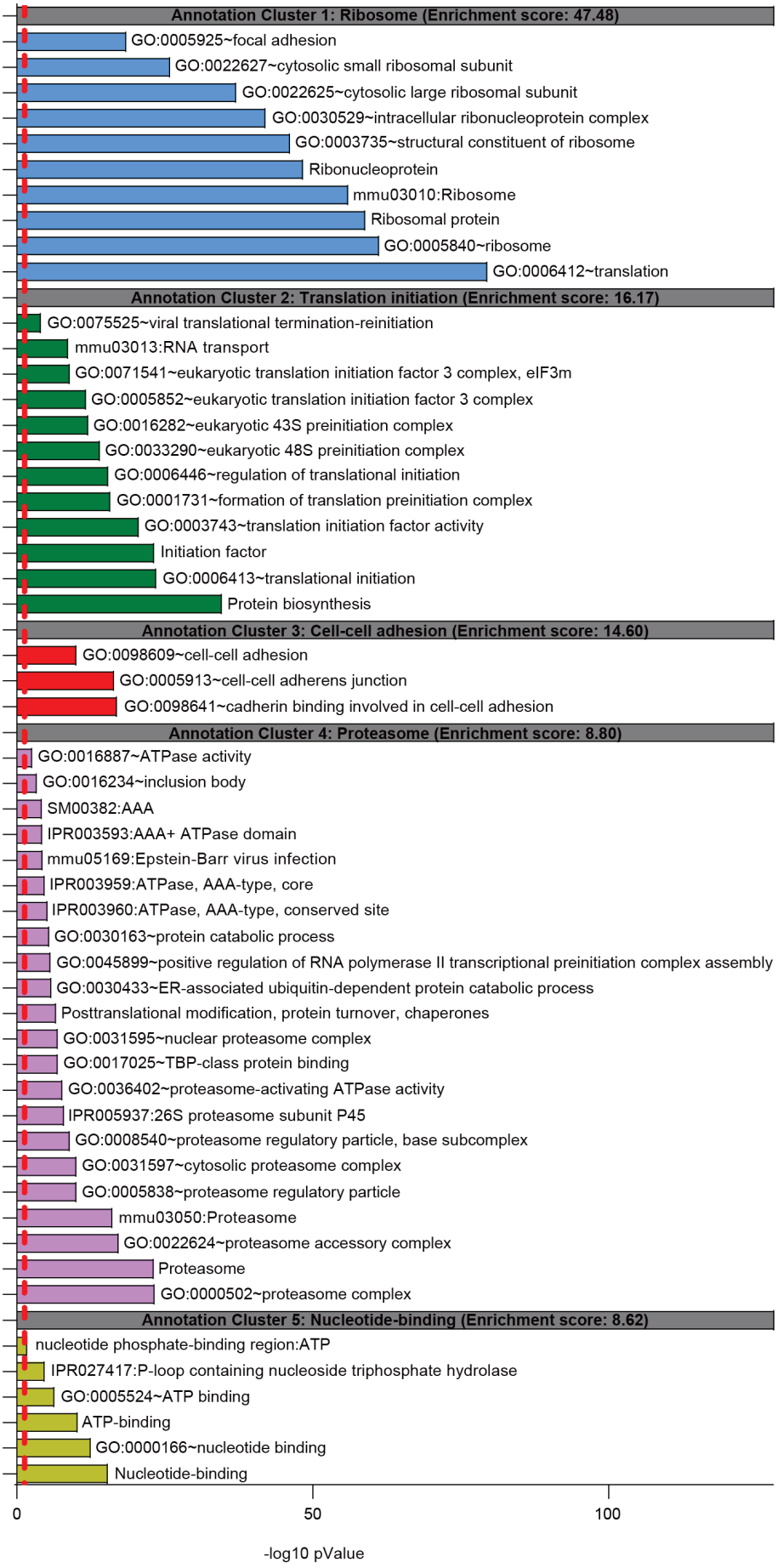
Annotation Cluster 1: Ribosome (Enrichment score: 47.48)
GO:0005925~focal adhesion
GO:0022627~cytosolic small ribosomal subunit
GO:0022625~cytosolic large ribosomal subunit
GO:0030529~intracellular ribonucleoprotein complex
GO:0003735~structural constituent of ribosome
Ribonucleoprotein
mmu03010:Ribosome
Ribosomal protein
GO:0005840~ribosome
GO:0006412~translation
Annotation Cluster 2: Translation initiation (Enrichment score: 16.17)
GO:0075525~viral translational termination-reinitiation
mmu03013:RNA transport
GO:0071541~eukaryotic translation initiation factor 3 complex, eIF3m
GO:0005852~eukaryotic translation initiation factor 3 complex
GO:0016282~eukaryotic 43S preinitiation complex
GO:0033290~eukaryotic 48S preinitiation complex
GO:0006446~regulation of translational initiation
GO:0001731~formation of translation preinitiation complex
GO:0003743~translation initiation factor activity
Initiation factor
GO:0006413~translational initiation
Protein biosynthesis
Annotation Cluster 3: Cell-cell adhesion (Enrichment score: 14.60)
GO:0098609~cell-cell adhesion
GO:0005913~cell-cell adherens junction
GO:0098641~cadherin binding involved in cell-cell adhesion
Annotation Cluster 4: Proteasome (Enrichment score: 8.80)
GO:0016887~ATPase activity
GO:0016234~inclusion body
SM00382:AAA
IPR003593:AAA+ ATPase domain
mmu05169:Epstein-Barr virus infection
IPR003959:ATPase, AAA-type, core
IPR003960:ATPase, AAA-type, conserved site
GO:0030163~protein catabolic process
GO:0045899~positive regulation of RNA polymerase II transcriptional preinitiation complex assembly
GO:0030433~ER-associated ubiquitin-dependent protein catabolic process
Posttranslational modification, protein turnover, chaperones
GO:0031595~nuclear proteasome complex
GO:0017025~TBP-class protein binding
GO:0036402~proteasome-activating ATPase activity
IPR005937:26S proteasome subunit P45
GO:0008540~proteasome regulatory particle, base subcomplex
GO:0031597~cytosolic proteasome complex
GO:0005838~proteasome regulatory particle
mmu03050:Proteasome
GO:0022624~proteasome accessory complex
Proteasome
GO:0000502~proteasome complex
Annotation Cluster 5: Nucleotide-binding (Enrichment score: 8.62)
nucleotide phosphate-binding region:ATP
IPR027417:P-loop containing nucleoside triphosphate hydrolase
GO:0005524~ATP binding
ATP-binding
GO:0000166~nucleotide binding
Nucleotide-binding
0
50
100
-log10 pValue

Figure S2. Ubiquitin proteasome system is enriched in young TSCmKO mice.

(A) Significantly ($p<0.05$) DE proteins were obtained from proteomics data from *tibialis anterior* (TA) muscles of 3-month-old, male TSCmKO mice and Control littermates (n=4). DAVID enrichment algorithms were applied on all DE proteins to calculate functional annotation clustering.

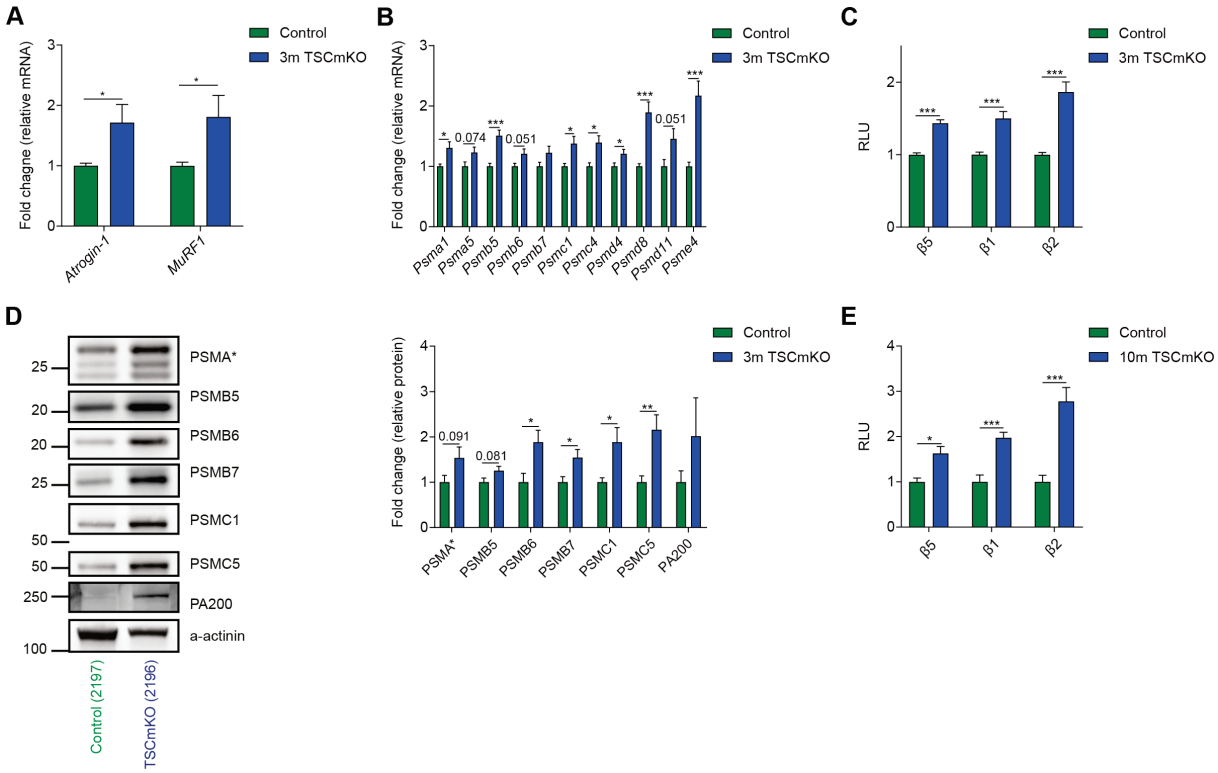

Figure S3. Ubiquitin proteasome system is enriched in young TSCmKO mice.

(A, B) Relative transcript expression was quantified by RT-qPCR in *gastrocnemius* (GAST) muscle from 3-month-old, male TSCmKO and Control mice (n=6). Transcript encoding β-actin was used as reference. **(C)** Luciferase-based proteasome activity measurement in lysates of *plantaris* (PLA) muscles from 3-month-old, male TSCmKO and Control mice (n=6). **(D)** Western blot analysis of proteasomal subunits (PSM) in *tibialis anterior* (TA) muscles from 3-month-old, male TSCmKO and Control mice (n=6). **(E)** Luciferase-based proteasome activity measurement in lysates of PLA muscles from 10-month-old, male TSCmKO (n=3) and Control mice (n=4). Data represent means ± SEM, ***p ≤ 0.001, **p ≤ 0.01, *p ≤ 0.05, Student's t test.

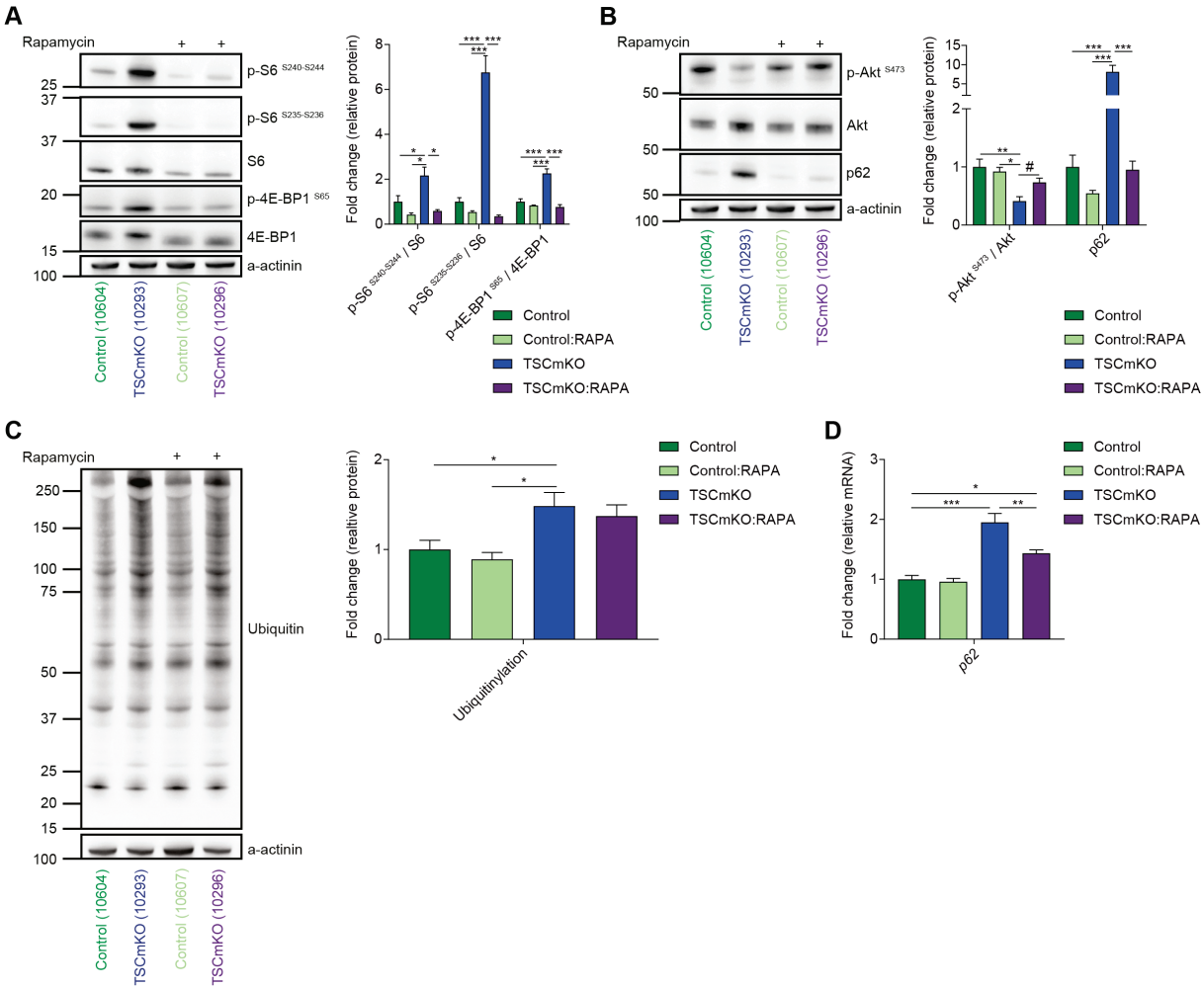

Figure S4. Short-term inhibition with rapamycin reverses the increased UPS in TSCmKO mice.

3-month-old Control and TSCmKO mice were treated with rapamycin (RAPA) or vehicle for 3 days. **(A, B)** Western blot analysis of mTORC1-Akt-signaling in *tibialis anterior* (TA) muscle, n=4 (Control:RAPA), n = 6 (Control, TSCmKO, TSCmKO:RAPA). **(C)** Western blot analysis of ubiquitinylated proteins in TA muscles, n=4 (Control:RAPA), n = 6 (Control, TSCmKO, TSCmKO:RAPA). **(D)** Relative transcript expression was quantified by RT-qPCR in *gastrocnemius* (GAST) muscle, n=5 (Control:RAPA), n = 6 (Control, TSCmKO, TSCmKO:RAPA). Transcript encoding β-actin was used as reference. Data represent means ± SEM, ***p ≤ 0.001, **p ≤ 0.01, *p ≤ 0.05, One-way ANOVA test.

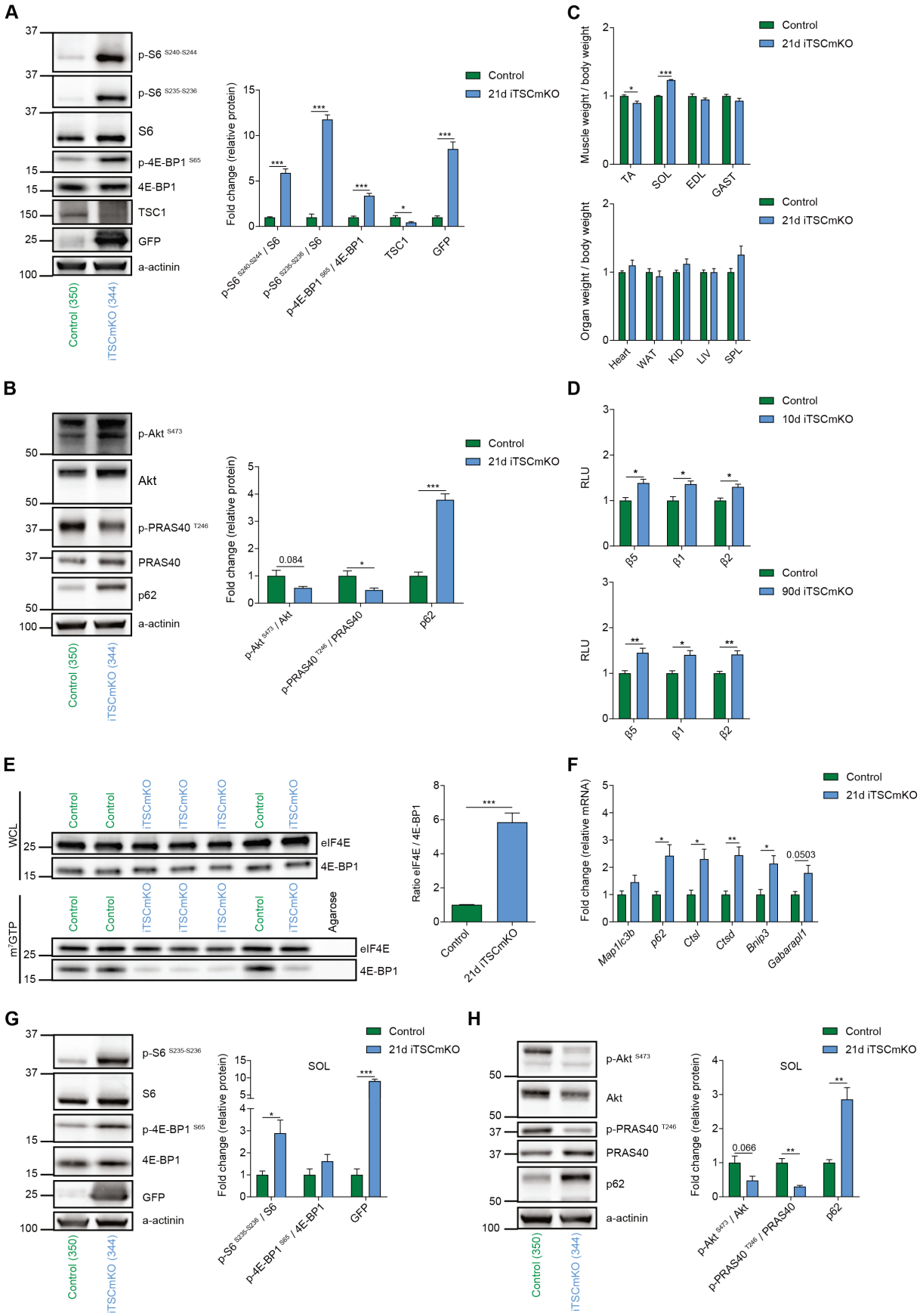
A
p-S6 S240-S244
p-S6 S235-S236
S6
p-4E-BP1 S65
4E-BP1
TSC1
GFP
a-actinin
Control (350)
iTSCmKO (344)
Fold change (relative protein)
Control
21d iTSCmKO
p-S6 S240-S244 / S6
p-S6 S235-S236 / S6
p-4E-BP1 S65 / 4E-BP1
TSC1
GFP
B
p-Akt S473
Akt
p-PRAS40 T246
PRAS40
p62
a-actinin
0.084
p-Akt S473 / Akt
p-PRAS40 T246 / PRAS40
C
Muscle weight / body weight
TA
SOL
EDL
GAST
Organ weight / body weight
Heart
WAT
KID
LIV
SPL
D
RLU
10d iTSCmKO
90d iTSCmKO
β5
β1
β2
E
WCL
m7GTP
Agarose
eIF4E
4E-BP1
Ratio eIF4E / 4E-BP1
F
Fold change (relative mRNA)
0.0503
Map1lc3b
p62
Ctsl
Ctsd
Bnip3
Gabarapl1
G
SOL
H
0.066

Figure S5. Activation of mTORC1 for 21 days is sufficient to increase the UPS in most adult muscles but not in *soleus*.

In 3-month-old mice, *Tsc1* deletion was induced in skeletal muscle (iTSCmKO mice) and mice were examined 10, 21 or 90 days later, as indicated. **(A, B)** Western blot analysis of mTORC1-Akt-signaling in *tibialis anterior* (TA) muscle, n=4. **(C)** Relative muscle and organ weight, n=4. **(D)** Luciferase-based proteasome activity measurement in lysates of *extensor digitorum longus* (EDL) muscles from 10-day and 90-day iTSCmKO mice, n=3 (10d Control), n=5 (10d iTSCmKO), n=4 (90d Control, 90d iTSCmKO). **(E)** Analysis of translation initiation using m^7GTP binding assay in *gastrocnemius* (GAST) muscle, WCL = whole-cell-lysates, n=3 (Control), n=4 (iTSCmKO). **(F)** Relative transcript expression was quantified by RT-qPCR in GAST muscle, n=4 (Control), n=5 (iTSCmKO). Transcript encoding β-tubulin was used as reference. **(G, H)** Western blot analysis of mTORC1/Akt-signaling in *soleus* (SOL) muscle, n=4. Data represent means ± SEM, ***p ≤ 0.001, **p ≤ 0.01, *p ≤ 0.05, Student's t test.

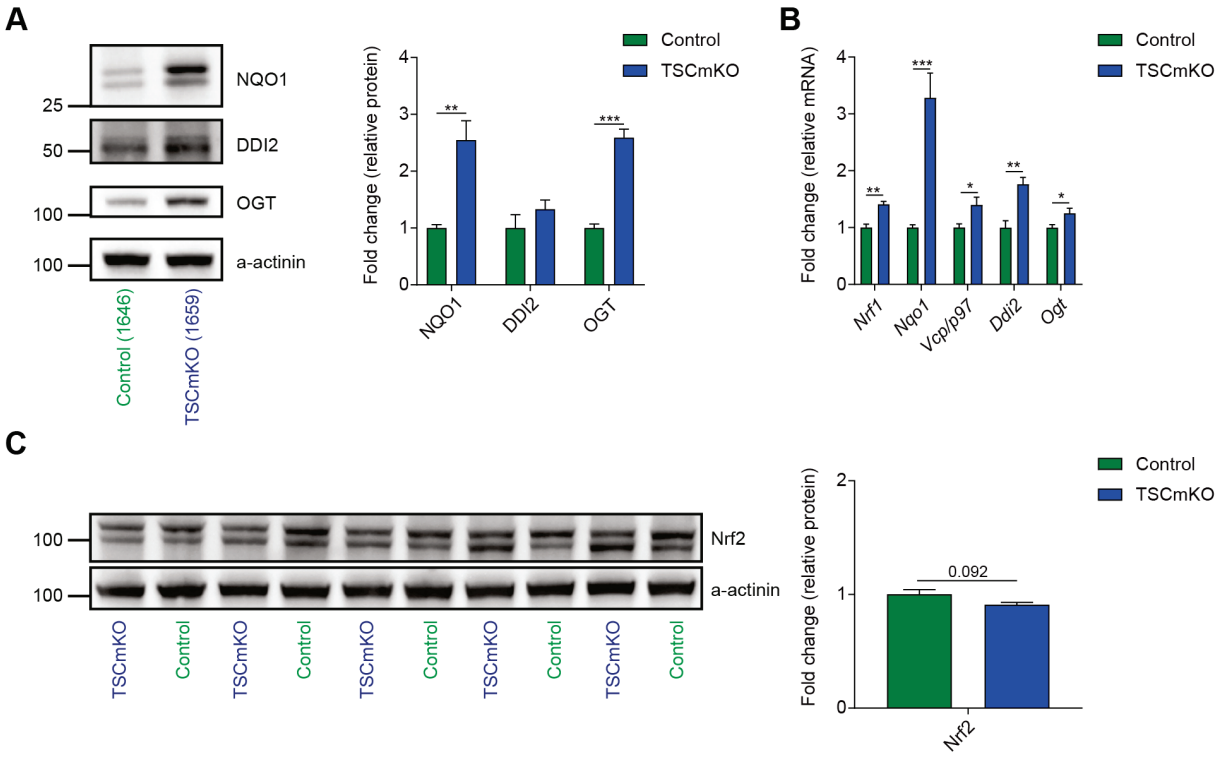

Figure S6. Nrf1 is a key mediator of mTORC1-induced UPS.

(A) Western blot analysis of NQO1, DDI2 and OGT in tibialis anterior (TA) muscles from 2-month-old, female TSCmKO and Control mice, n=5. **(B)** Relative transcript expression was quantified by RT-qPCR in TA muscle from 2-month-old, female TSCmKO and Control mice, n=5. Transcript encoding β-tubulin was used as reference. **(C)** Western blot analysis of Nrf2 in TA muscles from 2-month-old, female TSCmKO and Control mice, n=5. Data represent means ± SEM, ***p ≤ 0.001, **p ≤ 0.01, *p ≤ 0.05, Student's t test.

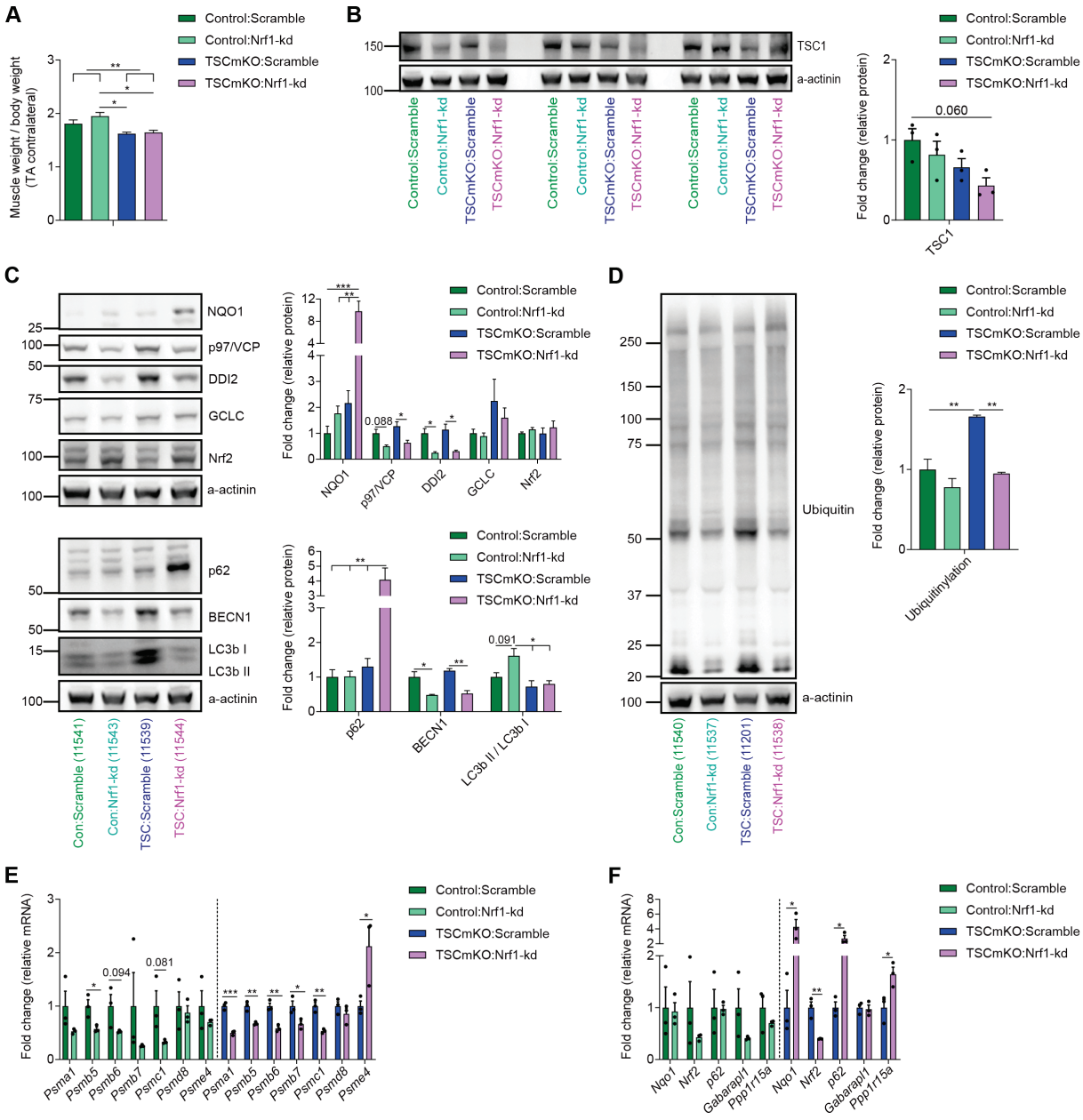

Figure S7. Inactivation of Nrf1 in TSCmKO mice decreases the expression of PSM genes.

Tibialis anterior (TA) muscle of 3-month-old Control and TSCmKO mice was electroporated with plasmids driving scramble or Nrf1-kd shRNA. Muscles were analyzed 2 weeks later. **(B, C)** Western blot analysis of TSC1, proposed targets of Nrf1 and proteins involved in autophagy-lysosomal degradation in electroporated TA muscle, n=3. **(D)** Western blot analysis of ubiquitinylated proteins in electroporated TA muscle, n=3. **(E, F)** Relative transcript expression was quantified by RT-qPCR in electroporated TA muscles, n=3. Transcript encoding Desmin was used as reference. Data represent means ± SEM, ***p ≤ 0.001, **p ≤ 0.01, *p ≤ 0.05, Student's t test (if two groups were compared), One-way ANOVA test (if more than two groups were compared).

Gene Symbol	Reference	Category	as atrogene	FC: TSCmKO vs. Control	PValue
Atp5a1	Lecker et al. (2004)	Energy production	Decreased	0.772	0.00083482
Dera	Lecker et al. (2004)	Energy production	Increased	1.845	0.006017387
Dlat	Lecker et al. (2004)	Energy production	Decreased	0.800	0.004699766
Eno3	Lecker et al. (2004)	Energy production	Decreased	0.760	0.002031758
Glul	Lecker et al. (2004)	Energy production	Increased	2.168	1.09583E-10
Gpd1	Lecker et al. (2004)	Energy production	Decreased	0.768	0.008314873
Ldha	Lecker et al. (2004)	Energy production	Decreased	0.629	1.28988E-08
Ndufs1	Lecker et al. (2004)	Energy production	Decreased	0.692	5.17327E-06
Pgam2	Lecker et al. (2004)	Energy production	Decreased	0.771	0.01473967
Sat1	Lecker et al. (2004)	Energy production	Increased	1.695	4.34812E-07
Slc25a26	Lecker et al. (2004)	Energy production	Decreased	0.693	0.000494468
Slc35f5	Lecker et al. (2004)	Energy production	Increased	2.202	1.34076E-09
Slc7a8	Lecker et al. (2004)	Energy production	Increased	1.835	0.002277851
Tpi1	Lecker et al. (2004)	Energy production	Decreased	0.802	0.005044593
Fn1	Lecker et al. (2004)	Extracellular matrix	Decreased	0.655	0.033173145
Igfbp5	Lecker et al. (2004)	Extracellular matrix	Decreased	0.563	4.20694E-05
Srl	Lecker et al. (2004)	Extracellular matrix	Decreased	0.689	6.46397E-06
Fam134b	Lecker et al. (2004)	Miscellaneous	Increased	1.704	0.000481954
Hectd1	Lecker et al. (2004)	Miscellaneous	Increased	1.373	1.58486E-05
Itm2a	Lecker et al. (2004)	Miscellaneous	Decreased	0.341	2.47776E-25
Mt1	Lecker et al. (2004)	Miscellaneous	Increased	2.333	0.016068802
Nptn	Lecker et al. (2004)	Miscellaneous	Increased	1.265	0.006382659
Nrep	Lecker et al. (2004)	Miscellaneous	Decreased	0.320	1.46442E-12
Ppp1r15a	Lecker et al. (2004)	Miscellaneous	Increased	2.030	5.22626E-13
Sesn1	Lecker et al. (2004)	Miscellaneous	Increased	2.272	8.65483E-15
Tfrc	Lecker et al. (2004)	Miscellaneous	Decreased	0.639	0.000571293
Txnl1	Lecker et al. (2004)	Miscellaneous	Increased	1.386	0.00066842
Bnip3	Lecker et al. (2004)	Protein degradation	Increased	1.687	4.1557E-06
Ctsl	Lecker et al. (2004)	Protein degradation	Increased	1.796	2.47539E-11
Fbxo32	Lecker et al. (2004)	Protein degradation	Increased	1.994	3.55098E-06
Gabarapl1	Lecker et al. (2004)	Protein degradation	Increased	1.689	1.07322E-07
Psma5	Lecker et al. (2004)	Protein degradation	Increased	1.293	0.008270969
Psmc4	Lecker et al. (2004)	Protein degradation	Increased	1.384	0.000480621
Psmd8	Lecker et al. (2004)	Protein degradation	Increased	2.227	3.71704E-14
Psme4	Lecker et al. (2004)	Protein degradation	Increased	2.907	1.03993E-37
Ubb	Lecker et al. (2004)	Protein degradation	Increased	1.661	0.023369007
Ube4b	Lecker et al. (2004)	Protein degradation	Increased	1.312	0.001313838
Eif4ebp1	Lecker et al. (2004)	Translation	Increased	1.522	0.000538631

Table S1. DE genes (TSCmKO vs. Control), previously described as atrogenes.

Identification of mTORC1-dependent atrogenes, comparing published mRNA expression data of atrogenes with RNA-sequencing data obtained from *extensor digitorum longus* (EDL) muscles from female, 3-month-old TSCmKO mice and Control littermates (n=5). Table of previously described atrogenes found expressed in young TSCmKO mice, which are similarly regulated as in other types of muscle atrophy (indicated in column “as atrogene”).

Gene Symbol	Reference	Category	as atrogene	FC: TSCmKO vs. Control	PValue	Direction
Ampd3	Lecker et al. (2004)	Energy production	Increased	1.164	0.38831336	No
Atp5a1	Lecker et al. (2004)	Energy production	Decreased	0.772	0.00083482	Yes
Ckmt2	Lecker et al. (2004)	Energy production	Decreased	1.056	0.626484025	No
Cox7b	Sacheck et al. (2007)	Energy production	Decreased	1.051	0.73402195	No
Dera	Lecker et al. (2004)	Energy production	Increased	1.845	0.006017387	Yes
Dlat	Lecker et al. (2004)	Energy production	Decreased	0.800	0.004699766	Yes
Eno3	Lecker et al. (2004)	Energy production	Decreased	0.760	0.002031758	Yes
Gclm	Sacheck et al. (2007)	Energy production	Increased	1.073	0.465862491	No
Glul	Lecker et al. (2004)	Energy production	Increased	2.168	1.09583E-10	Yes
Gpd1	Lecker et al. (2004)	Energy production	Decreased	0.768	0.008314873	Yes
Hadh	Sacheck et al. (2007)	Energy production	Decreased	0.891	0.261879895	No
Idh3b	Sacheck et al. (2007)	Energy production	Decreased	0.749	0.012297508	Yes
Impdh2	Lecker et al. (2004)	Energy production	Increased	0.739	0.008613491	Opposite
Kctd9	Lecker et al. (2004)	Energy production	Increased	0.784	0.009665123	Opposite
Ldha	Lecker et al. (2004)	Energy production	Decreased	0.629	1.28988E-08	Yes
Mdh1	Lecker et al. (2004)	Energy production	Decreased	1.100	0.353706328	No
Ndufa5	Sacheck et al. (2007)	Energy production	Decreased	0.742	0.010223395	Yes
Ndufb5	Lecker et al. (2004)	Energy production	Decreased	1.070	0.636153621	No
Ndufb8	Lecker et al. (2004)	Energy production	Decreased	1.200	0.071159872	No
Ndufs1	Lecker et al. (2004)	Energy production	Decreased	0.692	5.17327E-06	Yes
Ndufv2	Lecker et al. (2004)	Energy production	Decreased	0.872	0.177964839	No
Oxct1	Lecker et al. (2004)	Energy production	Decreased	1.299	0.001993086	Opposite
Pfkfb3	Lecker et al. (2004)	Energy production	Increased	1.440	0.208317063	No
Pgam2	Lecker et al. (2004)	Energy production	Decreased	0.771	0.01473967	Yes
Phkg1	Lecker et al. (2004)	Energy production	Decreased	0.884	0.172463855	No
Sat1	Lecker et al. (2004)	Energy production	Increased	1.695	4.34812E-07	Yes
Slc25a26	Lecker et al. (2004)	Energy production	Decreased	0.693	0.000494468	Yes
Slc35f5	Lecker et al. (2004)	Energy production	Increased	2.202	1.34076E-09	Yes
Slc3a1	Sacheck et al. (2007)	Energy production	Increased	0.722	0.0593756	No
Slc7a8	Lecker et al. (2004)	Energy production	Increased	1.835	0.002277851	Yes
Tpi1	Lecker et al. (2004)	Energy production	Decreased	0.802	0.005044593	Yes
Uqcrc2	Sacheck et al. (2007)	Energy production	Decreased	0.765	0.000701771	Yes
Col15a1	Lecker et al. (2004)	Extracellular matrix	Decreased	0.928	0.582998902	No
Col1a1	Lecker et al. (2004)	Extracellular matrix	Decreased	0.685	0.065231847	No
Col3a1	Lecker et al. (2004)	Extracellular matrix	Decreased	0.923	0.598449306	No
Col5a2	Lecker et al. (2004)	Extracellular matrix	Decreased	0.895	0.352859889	No
Fbn1	Lecker et al. (2004)	Extracellular matrix	Decreased	0.735	0.067117416	No
Fn1	Lecker et al. (2004)	Extracellular matrix	Decreased	0.655	0.033173145	Yes
Igfbp5	Lecker et al. (2004)	Extracellular matrix	Decreased	0.563	4.20694E-05	Yes
Lgals1	Lecker et al. (2004)	Extracellular matrix	Decreased	1.355	0.005441938	Opposite
Postn	Lecker et al. (2004)	Extracellular matrix	Decreased	0.706	0.113889861	No
Smoc2	Lecker et al. (2004)	Extracellular matrix	Decreased	1.058	0.637320122	No
Srl	Lecker et al. (2004)	Extracellular matrix	Decreased	0.689	6.46397E-06	Yes
Aco2	Raffaello et al. (2006)	Miscellaneous	Decreased	1.034	0.676217745	No
Actn3	Raffaello et al. (2006)	Miscellaneous	Increased	0.917	0.460427268	No
Adss	Raffaello et al. (2006)	Miscellaneous	Decreased	0.766	0.016490552	Yes
Ak1	Raffaello et al. (2006)	Miscellaneous	Decreased	0.698	2.79561E-06	Yes
Apln	Coelho et al. (2019)	Miscellaneous	Increased	0.579	0.010344633	Opposite
Asb15	Coelho et al. (2019)	Miscellaneous	Increased	3.312	7.17011E-17	Yes
Atp2a1	Raffaello et al. (2006)	Miscellaneous	Decreased	0.786	0.020388257	Yes
Atp5b	Raffaello et al. (2006)	Miscellaneous	Decreased	0.889	0.115238536	No
Bcat2	Shimizu et al. (2011)	Miscellaneous	Increased	1.766	5.76154E-06	Yes
Bin1	Raffaello et al. (2006)	Miscellaneous	Increased	1.167	0.036377463	Yes
Cald1	Raffaello et al. (2006)	Miscellaneous	Decreased	0.709	0.000964215	Yes
Cap2	Sacheck et al. (2007)	Miscellaneous	Increased	1.269	0.0031167	Yes
Car3	Raffaello et al. (2006)	Miscellaneous	Increased	2.875	0.00013848	Yes
Cd68	Sacheck et al. (2007)	Miscellaneous	Increased	1.811	0.038466052	Yes
Cebpb	Schakman et al. (2008)	Miscellaneous	Increased	1.331	0.027296303	Yes
Cggbp1	Raffaello et al. (2006)	Miscellaneous	Decreased	1.070	0.35854888	No
Chchd10	Raffaello et al. (2006)	Miscellaneous	Decreased	0.986	0.880580117	No
Chrna1	Sacheck et al. (2007)	Miscellaneous	Increased	0.783	0.009504591	Opposite
Cpe	Lecker et al. (2004)	Miscellaneous	Decreased	2.532	1.18252E-18	Opposite
Cryab	Raffaello et al. (2006)	Miscellaneous	Increased	0.905	0.385363655	No
Cs	Raffaello et al. (2006)	Miscellaneous	Decreased	0.799	0.001384295	Yes
Csnk2a2	Lecker et al. (2004)	Miscellaneous	Increased	1.136	0.182987498	No
Csrp3	Raffaello et al. (2006)	Miscellaneous	Increased	1.859	0.034243374	Yes
Ctso	Raffaello et al. (2006)	Miscellaneous	Decreased	0.677	8.35026E-05	Yes
Ddit4	Shimizu et al. (2011)	Miscellaneous	Increased	9.700	1.86346E-09	Yes
Dhrs7c	Raffaello et al. (2006)	Miscellaneous	Decreased	0.670	1.05494E-05	Yes
Dusp5	Coelho et al. (2019)	Miscellaneous	Increased	1.119	0.807201442	No

Dysf	Sacheck et al. (2007)	Miscellaneous	Increased	1.059	0.610991092	No
Eef1a1	Raffaello et al. (2006)	Miscellaneous	Increased	0.862	0.189121727	No
eIF4E3	Soares et al. (2014)	Miscellaneous	Decreased	1.345	0.002107236	Opposite
Ep300	Schakman et al. (2008)	Miscellaneous	Increased	1.032	0.689880821	No
Fam134b	Lecker et al. (2004)	Miscellaneous	Increased	1.704	0.000481954	Yes
Fhl1	Raffaello et al. (2006)	Miscellaneous	Increased	1.147	0.463284408	No
Fst	Schiaffino et al. (2013)	Miscellaneous	Decreased	0.463	2.84293E-05	Yes
Fth1	Raffaello et al. (2006)	Miscellaneous	Increased	1.786	3.18599E-12	Yes
Gadd45a	Raffaello et al. (2006)	Miscellaneous	Increased	3.928	1.1915E-11	Yes
Gstm1	Raffaello et al. (2006)	Miscellaneous	Increased	0.992	0.929999747	No
H3f3a	Raffaello et al. (2006)	Miscellaneous	Increased	0.903	0.404957632	No
Hectd1	Lecker et al. (2004)	Miscellaneous	Increased	1.373	1.58486E-05	Yes
Hes6	Raffaello et al. (2006)	Miscellaneous	Decreased	2.031	4.95818E-08	Opposite
Hmox1	Kang et al. (2013)	Miscellaneous	Increased	1.596	0.006936233	Yes
Hopx	Coelho et al. (2019)	Miscellaneous	Decreased	0.933	0.623848781	No
Hspb1	Raffaello et al. (2006)	Miscellaneous	Increased	2.792	2.51072E-10	Yes
Ifrd1	Lecker et al. (2004)	Miscellaneous	Increased	1.117	0.429392576	No
Igf1	Coelho et al. (2019)	Miscellaneous	Decreased	0.611	0.004585933	Yes
Igfbp3	Coelho et al. (2019)	Miscellaneous	Increased	1.346	0.018578147	Yes
Itm2a	Lecker et al. (2004)	Miscellaneous	Decreased	0.341	2.47776E-25	Yes
Jph2	Lecker et al. (2004)	Miscellaneous	Decreased	1.261	0.023089985	Opposite
Kcnn3	Sacheck et al. (2007)	Miscellaneous	Increased	1.943	1.84182E-06	Yes
Kif21b	Sacheck et al. (2007)	Miscellaneous	Decreased	1.469	0.074344807	No
Klf15	Coelho et al. (2019)	Miscellaneous	Increased	1.535	0.000877052	Yes
Klhl38	Coelho et al. (2019)	Miscellaneous	Increased	1.246	0.093665245	No
Larp7	Raffaello et al. (2006)	Miscellaneous	Decreased	0.983	0.847942237	No
Ldb3	Lecker et al. (2004)	Miscellaneous	Decreased	1.018	0.836238007	No
Lpin1	Lecker et al. (2004)	Miscellaneous	Increased	0.861	0.151153513	No
Lpp	Raffaello et al. (2006)	Miscellaneous	Increased	0.860	0.089639333	No
Luc7l3	Sacheck et al. (2007)	Miscellaneous	Decreased	0.932	0.443688011	No
Map1lc3a	Raffaello et al. (2006)	Miscellaneous	Increased	1.546	1.50194E-06	Yes
Mb	Raffaello et al. (2006)	Miscellaneous	Increased	0.851	0.249883454	No
Mbnl1	Raffaello et al. (2006)	Miscellaneous	Decreased	1.060	0.449247942	No
Mbtd1	Raffaello et al. (2006)	Miscellaneous	Decreased	0.874	0.156738318	No
Mdh2	Raffaello et al. (2006)	Miscellaneous	Decreased	0.995	0.963469091	No
Mkl1	Coelho et al. (2019)	Miscellaneous	Increased	0.948	0.697651339	No
Mmp14	Raffaello et al. (2006)	Miscellaneous	Increased	0.826	0.137235476	No
Mstn	Schiaffino et al. (2013)	Miscellaneous	Increased	0.938	0.669427386	No
Mt1	Lecker et al. (2004)	Miscellaneous	Increased	2.333	0.016068802	Yes
mt-Co1	Raffaello et al. (2006)	Miscellaneous	Decreased	0.947	0.615225242	No
mt-Cytb	Raffaello et al. (2006)	Miscellaneous	Decreased	0.896	0.388008783	No
mt-Nd2	Raffaello et al. (2006)	Miscellaneous	Decreased	0.970	0.818536604	No
mt-Nd5	Raffaello et al. (2006)	Miscellaneous	Decreased	0.666	0.000107085	Yes
Mybpc1	Raffaello et al. (2006)	Miscellaneous	Decreased	0.962	0.719353331	No
Mybpc2	Raffaello et al. (2006)	Miscellaneous	Decreased	0.674	0.002652255	Yes
Mybph	Raffaello et al. (2006)	Miscellaneous	Increased	0.292	0.003384344	Opposite
Myh4	Raffaello et al. (2006)	Miscellaneous	Decreased	0.867	0.315484196	No
Myl12a	Raffaello et al. (2006)	Miscellaneous	Increased	1.745	4.95958E-06	Yes
Myl2	Lecker et al. (2004)	Miscellaneous	Decreased	4.570	1.04916E-05	Opposite
Myom2	Raffaello et al. (2006)	Miscellaneous	Decreased	1.050	0.692661649	No
Myoz1	Raffaello et al. (2006)	Miscellaneous	Decreased	0.876	0.093446236	No
Ncam1	Sacheck et al. (2007)	Miscellaneous	Increased	0.858	0.332660521	No
Nedd4	McClung et al. (2010)	Miscellaneous	Increased	0.963	0.631656764	No
Nptn	Lecker et al. (2004)	Miscellaneous	Increased	1.265	0.006382659	Yes
Nr1d1	Mayeuf-Louchart et al. (2017)	Miscellaneous	Decreased	1.069	0.634223225	No
Nrep	Lecker et al. (2004)	Miscellaneous	Decreased	0.320	1.46442E-12	Yes
Pdcd10	Soares et al. (2014)	Miscellaneous	Decreased	1.046	0.638777982	No
Pdk4	Schakman et al. (2008)	Miscellaneous	Increased	1.666	0.058119185	No
Pgf	Coelho et al. (2019)	Miscellaneous	Decreased	1.270	0.455643324	No
Pi15	Coelho et al. (2019)	Miscellaneous	Decreased	0.673	0.002164032	Yes
Pik3c3	Schiaffino et al. (2013)	Miscellaneous	Increased	0.926	0.45080135	No
Pik3ip1	Coelho et al. (2019)	Miscellaneous	Increased	1.787	2.4321E-08	Yes
Por	Sacheck et al. (2007)	Miscellaneous	Increased	1.038	0.708727788	No
Ppargc1a	Wang et al. (2016)	Miscellaneous	Decreased	0.439	0.001114996	Yes
Ppp1r15a	Lecker et al. (2004)	Miscellaneous	Increased	2.030	5.22626E-13	Yes
Prnp	Sacheck et al. (2007)	Miscellaneous	Increased	1.154	0.127525651	No
Ptges3	Lecker et al. (2004)	Miscellaneous	Increased	0.682	0.000155724	Opposite
Pvalb	Lecker et al. (2004)	Miscellaneous	Decreased	0.929	0.45201604	No
Pygm	Raffaello et al. (2006)	Miscellaneous	Decreased	0.851	0.091416563	No
Rpl3	Raffaello et al. (2006)	Miscellaneous	Increased	0.962	0.733378031	No
Rplp0	Raffaello et al. (2006)	Miscellaneous	Increased	1.429	0.00067187	Yes
Rplp2	Raffaello et al. (2006)	Miscellaneous	Increased	0.895	0.460539409	No
Rps18	Raffaello et al. (2006)	Miscellaneous	Increased	0.777	0.074997948	No

Rps20	Raffaello et al. (2006)	Miscellaneous	Increased	0.960	0.684467534	No
S1pr2	Pierucci et al. (2018)	Miscellaneous	Increased	1.051	0.811661646	No
Sesn1	Lecker et al. (2004)	Miscellaneous	Increased	2.272	8.65483E-15	Yes
Sh3glb1	Lecker et al. (2004)	Miscellaneous	Decreased	0.962	0.601217438	No
Slc25a4	Raffaello et al. (2006)	Miscellaneous	Decreased	0.766	0.000775653	Yes
Sln	Sacheck et al. (2007)	Miscellaneous	Increased	0.902	0.763342753	No
Smpx	Raffaello et al. (2006)	Miscellaneous	Increased	0.890	0.323925335	No
Spns2	Pierucci et al. (2018)	Miscellaneous	Increased	1.154	0.348541319	No
Tfrc	Lecker et al. (2004)	Miscellaneous	Decreased	0.639	0.000571293	Yes
Tnfrsf12a	Hindi et al. (2013)	Miscellaneous	Increased	5.565	3.47268E-09	Yes
Tnfsf12	Hindi et al. (2013)	Miscellaneous	Increased	1.619	0.000110984	Yes
Trib3	Choi et al. (2019)	Miscellaneous	Increased	2.282	0.000129242	Yes
Ttn	Raffaello et al. (2006)	Miscellaneous	Decreased	0.733	0.025587052	Yes
Txnl1	Lecker et al. (2004)	Miscellaneous	Increased	1.386	0.00066842	Yes
Vdac1	Raffaello et al. (2006)	Miscellaneous	Decreased	0.842	0.025290137	Yes
Asb2	Bello et al. (2009)	Protein degradation	Increased	1.321	0.009001682	Yes
Becn1	Mammucari et a. (2017)	Protein degradation	Increased	1.354	0.000168687	Yes
Bnip3	Lecker et al. (2004)	Protein degradation	Increased	1.687	4.1557E-06	Yes
Cblb	Abe et al. (2013)	Protein degradation	Increased	0.898	0.232509032	No
Ctsl	Lecker et al. (2004)	Protein degradation	Increased	1.796	2.47539E-11	Yes
Fbxo21	Milan et al. (2015)	Protein degradation	Increased	1.001	0.997889878	No
Fbxo30	Sartori et al. (2013)	Protein degradation	Increased	1.626	1.60955E-07	Yes
Fbxo31	Milan et al. (2015)	Protein degradation	Increased	1.206	0.026383022	Yes
Fbxo32	Lecker et al. (2004)	Protein degradation	Increased	1.994	3.55098E-06	Yes
Fbxo40	Shi et al. (2011)	Protein degradation	Increased	1.551	2.55245E-08	Yes
Fbxw7	Shin et al. (2018)	Protein degradation	Increased	0.974	0.753865897	No
Gabarapl1	Lecker et al. (2004)	Protein degradation	Increased	1.689	1.07322E-07	Yes
Itch	Milan et al. (2015)	Protein degradation	Increased	1.092	0.211436357	No
Map1lc3b	Lecker et al. (2004)	Protein degradation	Increased	0.914	0.36067096	No
Mdm2	Ramos et al. (2017)	Protein degradation	Increased	1.313	0.000652836	Yes
Mul1	Lokireddy et al. (2012)*	Protein degradation	Increased	1.193	0.027112398	Yes
Nsfl1c	Piccirillo et al. (2012)	Protein degradation	Increased	1.262	0.077212307	No
Psma1	Lecker et al. (2004)	Protein degradation	Increased	1.095	0.42336849	No
Psma5	Lecker et al. (2004)	Protein degradation	Increased	1.293	0.008270969	Yes
Psmb3	Lecker et al. (2004)	Protein degradation	Increased	1.048	0.713956947	No
Psmb4	Lecker et al. (2004)	Protein degradation	Increased	1.097	0.286246068	No
Psmc4	Lecker et al. (2004)	Protein degradation	Increased	1.384	0.000480621	Yes
Psmd11	Lecker et al. (2004)	Protein degradation	Increased	1.171	0.15167781	No
Psmd8	Lecker et al. (2004)	Protein degradation	Increased	2.227	3.71704E-14	Yes
Psme4	Lecker et al. (2004)	Protein degradation	Increased	2.907	1.03993E-37	Yes
Rps27a	Lecker et al. (2004)	Protein degradation	Increased	1.517	0.051734756	No
Sqstm1	Milan et al. (2015)	Protein degradation	Increased	2.244	5.98994E-14	Yes
Traf6	Paul et al. (2010)	Protein degradation	Increased	1.533	2.61125E-09	Yes
Trim32	Kudryashova et al. (2005)	Protein degradation	Increased	1.422	0.000957328	Yes
Trim54	Centner et al. (2001)	Protein degradation	Increased	1.243	0.02174058	Yes
Trim55	Centner et al. (2001)	Protein degradation	Increased	1.174	0.076953289	No
Trim63	Bodine et al. (2001)	Protein degradation	Increased	2.904	2.25452E-12	Yes
Uba52	Lecker et al. (2004)	Protein degradation	Increased	0.990	0.966865453	No
Ubb	Lecker et al. (2004)	Protein degradation	Increased	1.661	0.023369007	Yes
Ubc	Lecker et al. (2004)	Protein degradation	Increased	0.983	0.909831012	No
Ube2j1	Lecker et al. (2004)	Protein degradation	Increased	0.989	0.869643757	No
Ube3b	Kerksick et al. (2013)	Protein degradation	Increased	1.445	2.67442E-06	Yes
Ube4b	Lecker et al. (2004)	Protein degradation	Increased	1.312	0.001313838	Yes
Usp14	Lecker et al. (2004)	Protein degradation	Increased	1.085	0.433941799	No
Vcp	Piccirillo et al. (2012)	Protein degradation	Increased	1.366	0.008145317	Yes
Acvr2b	Magnusson et al. (2005)	Signaling	Decreased	1.116	0.376621915	No
Adam19	Magnusson et al. (2005)	Signaling	Increased	0.846	0.218395967	No
Cacng1	Magnusson et al. (2005)	Signaling	Increased	0.683	0.000879977	Opposite
Camk2d	Magnusson et al. (2005)	Signaling	Increased	0.716	0.000737603	Opposite
Cd82	Magnusson et al. (2005)	Signaling	Increased	0.524	6.67257E-06	Opposite
Cdkn1a	Magnusson et al. (2005)	Signaling	Increased	1.693	0.002236232	Yes
Ctgf	Magnusson et al. (2005)	Signaling	Increased	1.017	0.933616501	No
Cyr61	Magnusson et al. (2005)	Signaling	Increased	2.252	2.38375E-09	Yes
Frat2	Magnusson et al. (2005)	Signaling	Decreased	0.558	2.45013E-06	Yes
Fzd9	Magnusson et al. (2005)	Signaling	Decreased	1.354	0.036636756	Opposite
Kcna7	Magnusson et al. (2005)	Signaling	Decreased	1.171	0.243068306	No
Kcnj12	Magnusson et al. (2005)	Signaling	Decreased	1.054	0.61204453	No
Maged1	Magnusson et al. (2005)	Signaling	Increased	0.934	0.460836399	No
Mt2	Magnusson et al. (2005)	Signaling	Increased	1.962	0.06660961	No
Pick1	Magnusson et al. (2005)	Signaling	Decreased	1.777	7.50285E-12	Opposite
Ptp4a3	Magnusson et al. (2005)	Signaling	Decreased	0.923	0.334983044	No
Ramp1	Magnusson et al. (2005)	Signaling	Decreased	0.815	0.082733961	No
Rrad	Magnusson et al. (2005)	Signaling	Increased	2.544	0.002218105	Yes

Timp1	Magnusson et al. (2005)	Signaling	Increased	1.111	0.718537876	No
Vegfa	Magnusson et al. (2005)	Signaling	Decreased	0.519	5.70648E-12	Yes
Atf4	Lecker et al. (2004)	Transcription	Increased	0.957	0.593093155	No
Atf6b	Sacheck et al. (2007)	Transcription	Increased	1.384	0.001401524	Yes
Carm1	Sacheck et al. (2007)	Transcription	Increased	0.951	0.597099318	No
Cdr2	Magnusson et al. (2005)	Transcription	Increased	1.155	0.450692469	No
Eftud2	Sacheck et al. (2007)	Transcription	Increased	1.259	0.013000071	Yes
Ezh1	Lecker et al. (2004)	Transcription	Increased	1.124	0.126129871	No
Foxo1	Lecker et al. (2004)	Transcription	Increased	0.893	0.416926684	No
Foxo3	Ikeda et al. (2016)	Transcription	Increased	1.362	0.000350273	Yes
Id2	Magnusson et al. (2005)	Transcription	Increased	0.803	0.178071666	No
Junb	Lecker et al. (2004)	Transcription	Decreased	1.296	0.158282182	No
Maf	Lecker et al. (2004)	Transcription	Decreased	0.971	0.811361363	No
Max	Lecker et al. (2004)	Transcription	Increased	1.020	0.835456848	No
Myc	Magnusson et al. (2005)	Transcription	Increased	0.440	6.50308E-07	Opposite
Myog	Sacheck et al. (2007)	Transcription	Increased	0.550	0.028922574	Opposite
Nfe2l2	Lecker et al. (2004)	Transcription	Increased	1.181	0.075743435	No
Nr4a1	Magnusson et al. (2005)	Transcription	Decreased	0.840	0.41505349	No
Ppp5c	Sacheck et al. (2007)	Transcription	Increased	1.005	0.971384063	No
Prmt1	Magnusson et al. (2005)	Transcription	Increased	0.901	0.27035962	No
Rb1	Magnusson et al. (2005)	Transcription	Increased	1.024	0.765237484	No
Sap30	Magnusson et al. (2005)	Transcription	Increased	2.068	1.40071E-07	Yes
Srcap	Lecker et al. (2004)	Transcription	Decreased	0.996	0.961149347	No
Tgif1	Lecker et al. (2004)	Transcription	Increased	0.929	0.919115536	No
Zbtb16	Magnusson et al. (2005)	Transcription	Decreased	0.977	0.833279877	No
Ddx42	Lecker et al. (2004)	Translation	Increased	0.860	0.038221699	Opposite
Ddx6	Sacheck et al. (2007)	Translation	Increased	0.778	0.003429638	Opposite
Eif4a2	Lecker et al. (2004)	Translation	Increased	0.755	0.001221286	Opposite
Eif4ebp1	Lecker et al. (2004)	Translation	Increased	1.522	0.000538631	Yes
Eif4g2	Lecker et al. (2004)	Translation	Increased	0.780	0.000114349	Opposite
Ncl	Lecker et al. (2004)	Translation	Increased	0.881	0.154441289	No
Rpl12	Lecker et al. (2004)	Translation	Increased	0.545	0.013551729	Opposite
Rrp9	Sacheck et al. (2007)	Translation	Increased	1.169	0.150852367	No

Table S2. Unsupervised list of atrophy-related genes (01.01.2019)

Unsupervised list of atrophy-related genes found in literature, compared with RNA-sequencing data obtained from *extensor digitorum longus* (EDL) muscles from female, 3-month-old TSCmKO mice and Control littermates (n=5). Table of atrophy-related genes found expressed in young TSCmKO mice. Reference marked with asterisk (*) was retracted (but not regarding the findings that describe Mul1 as atrophy-related gene).

Gene Symbol	Reference	Category	as atrogene	FC: TSCmKO vs. Control	PValue
Ldha	Lecker et al. (2004)	Energy production	Decreased	0.629	1.28988E-08
Ndufs1	Lecker et al. (2004)	Energy production	Decreased	0.692	5.17327E-06
Slc25a26	Lecker et al. (2004)	Energy production	Decreased	0.693	0.000494468
Eno3	Lecker et al. (2004)	Energy production	Decreased	0.760	0.002031758
Gpd1	Lecker et al. (2004)	Energy production	Decreased	0.768	0.008314873
Pgam2	Lecker et al. (2004)	Energy production	Decreased	0.771	0.01473967
Atp5a1	Lecker et al. (2004)	Energy production	Decreased	0.772	0.00083482
Dlat	Lecker et al. (2004)	Energy production	Decreased	0.800	0.004699766
Tpi1	Lecker et al. (2004)	Energy production	Decreased	0.802	0.005044593
Slc35f5	Lecker et al. (2004)	Energy production	Increased	2.202	1.34076E-09
Glul	Lecker et al. (2004)	Energy production	Increased	2.168	1.09583E-10
Dera	Lecker et al. (2004)	Energy production	Increased	1.845	0.006017387
Slc7a8	Lecker et al. (2004)	Energy production	Increased	1.835	0.002277851
Sat1	Lecker et al. (2004)	Energy production	Increased	1.695	4.34812E-07
Ndufa5	Sacheck et al. (2007)	Energy production	Decreased	0.742	0.010223395
Idh3b	Sacheck et al. (2007)	Energy production	Decreased	0.749	0.012297508
Uqcrc2	Sacheck et al. (2007)	Energy production	Decreased	0.765	0.000701771
Igfbp5	Lecker et al. (2004)	Extracellular matrix	Decreased	0.563	4.20694E-05
Fn1	Lecker et al. (2004)	Extracellular matrix	Decreased	0.655	0.033173145
Srl	Lecker et al. (2004)	Extracellular matrix	Decreased	0.689	6.46397E-06
Bcat2	Shimizu et al. (2011)	Miscellaneous	Increased	1.766	5.76154E-06
Nrep	Lecker et al. (2004)	Miscellaneous	Decreased	0.320	1.46442E-12
Itm2a	Lecker et al. (2004)	Miscellaneous	Decreased	0.341	2.47776E-25
Tfrc	Lecker et al. (2004)	Miscellaneous	Decreased	0.639	0.000571293
Mt1	Lecker et al. (2004)	Miscellaneous	Increased	2.333	0.016068802
Sesn1	Lecker et al. (2004)	Miscellaneous	Increased	2.272	8.65483E-15
Ppp1r15a	Lecker et al. (2004)	Miscellaneous	Increased	2.030	5.22626E-13
Fam134b	Lecker et al. (2004)	Miscellaneous	Increased	1.704	0.000481954
Txnl1	Lecker et al. (2004)	Miscellaneous	Increased	1.386	0.00066842
Hectd1	Lecker et al. (2004)	Miscellaneous	Increased	1.373	1.58486E-05
Nptn	Lecker et al. (2004)	Miscellaneous	Increased	1.265	0.006382659
Igf1	Coelho et al. (2019)	Miscellaneous	Decreased	0.611	0.004585933
Pi15	Coelho et al. (2019)	Miscellaneous	Decreased	0.673	0.002164032
Asb15	Coelho et al. (2019)	Miscellaneous	Increased	3.312	7.17011E-17
Pik3ip1	Coelho et al. (2019)	Miscellaneous	Increased	1.787	2.4321E-08
Igfbp3	Coelho et al. (2019)	Miscellaneous	Increased	1.346	0.018578147
mt-Nd5	Raffaello et al. (2006)	Miscellaneous	Decreased	0.666	0.000107085
Dhrs7c	Raffaello et al. (2006)	Miscellaneous	Decreased	0.670	1.05494E-05
Mybpc2	Raffaello et al. (2006)	Miscellaneous	Decreased	0.674	0.002652255
Ctso	Raffaello et al. (2006)	Miscellaneous	Decreased	0.677	8.35026E-05
Ak1	Raffaello et al. (2006)	Miscellaneous	Decreased	0.698	2.79561E-06
Cald1	Raffaello et al. (2006)	Miscellaneous	Decreased	0.709	0.000964215
Ttn	Raffaello et al. (2006)	Miscellaneous	Decreased	0.733	0.025587052
Slc25a4	Raffaello et al. (2006)	Miscellaneous	Decreased	0.766	0.000775653
Adss	Raffaello et al. (2006)	Miscellaneous	Decreased	0.766	0.016490552
Atp2a1	Raffaello et al. (2006)	Miscellaneous	Decreased	0.786	0.020388257
Cs	Raffaello et al. (2006)	Miscellaneous	Decreased	0.799	0.001384295
Vdac1	Raffaello et al. (2006)	Miscellaneous	Decreased	0.842	0.025290137
Gadd45a	Raffaello et al. (2006)	Miscellaneous	Increased	3.928	1.1915E-11
Car3	Raffaello et al. (2006)	Miscellaneous	Increased	2.875	0.00013848
Hspb1	Raffaello et al. (2006)	Miscellaneous	Increased	2.792	2.51072E-10
Csrp3	Raffaello et al. (2006)	Miscellaneous	Increased	1.859	0.034243374
Fth1	Raffaello et al. (2006)	Miscellaneous	Increased	1.786	3.18599E-12
Myl12a	Raffaello et al. (2006)	Miscellaneous	Increased	1.745	4.95958E-06
Rplp0	Raffaello et al. (2006)	Miscellaneous	Increased	1.429	0.00067187
Bin1	Raffaello et al. (2006)	Miscellaneous	Increased	1.167	0.036377463

Cebpb	Schakman et al. (2008)	Miscellaneous	Increased	1.331	0.027296303
Ppargc1a	Wang et al. (2016)	Miscellaneous	Decreased	0.439	0.001114996
Fst	Schiaffino et al. (2013)	Miscellaneous	Decreased	0.463	2.84293E-05
Kcnn3	Sacheck et al. (2007)	Miscellaneous	Increased	1.943	1.84182E-06
Cd68	Sacheck et al. (2007)	Miscellaneous	Increased	1.811	0.038466052
Cap2	Sacheck et al. (2007)	Miscellaneous	Increased	1.269	0.0031167
Hmox1	Kang et al. (2013)	Miscellaneous	Increased	1.596	0.006936233
Tnfrsf12a	Hindi et al. (2013)	Miscellaneous	Increased	5.565	3.47268E-09
Tnfsf12	Hindi et al. (2013)	Miscellaneous	Increased	1.619	0.000110984
Trib3	Choi et al. (2019)	Miscellaneous	Increased	2.282	0.000129242
Klf15	Coelho et al. (2019)	Miscellaneous	Increased	1.535	0.000877052
Ddit4	Shimizu et al. (2011)	Miscellaneous	Increased	9.700	1.86346E-09
Map1lc3a	Raffaello et al. (2006)	Protein degradation	Increased	1.546	1.50194E-06
Mul1	Lokireddy et al. (2012)*	Protein degradation	Increased	1.193	0.027112398
Gabarapl1	Lecker et al. (2004)	Protein degradation	Increased	1.689	1.07322E-07
Bnip3	Lecker et al. (2004)	Protein degradation	Increased	1.687	4.1557E-06
Becn1	Mammucari et a. (2017)	Protein degradation	Increased	1.354	0.000168687
Sqstm1	Milan et al. (2015)	Protein degradation	Increased	2.244	5.98994E-14
Vcp	Piccirillo et al. (2012)	Protein degradation	Increased	1.366	0.008145317
Trim63	Bodine et al. (2001)	Protein degradation	Increased	2.904	2.25452E-12
Trim54	Centner et al. (2001)	Protein degradation	Increased	1.243	0.02174058
Ube3b	Kerksick et al. (2013)	Protein degradation	Increased	1.445	2.67442E-06
Trim32	Kudryashova et al. (2005)	Protein degradation	Increased	1.422	0.000957328
Psme4	Lecker et al. (2004)	Protein degradation	Increased	2.907	1.03993E-37
Psmd8	Lecker et al. (2004)	Protein degradation	Increased	2.227	3.71704E-14
Fbxo32	Lecker et al. (2004)	Protein degradation	Increased	1.994	3.55098E-06
Ctsl	Lecker et al. (2004)	Protein degradation	Increased	1.796	2.47539E-11
Ubb	Lecker et al. (2004)	Protein degradation	Increased	1.661	0.023369007
Psmc4	Lecker et al. (2004)	Protein degradation	Increased	1.384	0.000480621
Ube4b	Lecker et al. (2004)	Protein degradation	Increased	1.312	0.001313838
Psma5	Lecker et al. (2004)	Protein degradation	Increased	1.293	0.008270969
Traf6	Paul et al. (2010)	Protein degradation	Increased	1.533	2.61125E-09
Mdm2	Ramos et al. (2017)	Protein degradation	Increased	1.313	0.000652836
Fbxo30	Sartori et al. (2013)	Protein degradation	Increased	1.626	1.60955E-07
Asb2	Bello et al. (2009)	Protein degradation	Increased	1.321	0.009001682
Fbxo31	Milan et al. (2015)	Protein degradation	Increased	1.206	0.026383022
Fbxo40	Shi et al. (2011)	Protein degradation	Increased	1.551	2.55245E-08
Foxo3	Ikeda et al. (2016)	Protein degradation	Increased	1.362	0.000350273
Vegfa	Magnusson et al. (2005)	Signaling	Decreased	0.519	5.70648E-12
Frat2	Magnusson et al. (2005)	Signaling	Decreased	0.558	2.45013E-06
Rrad	Magnusson et al. (2005)	Signaling	Increased	2.544	0.002218105
Cyr61	Magnusson et al. (2005)	Signaling	Increased	2.252	2.38375E-09
Cdkn1a	Magnusson et al. (2005)	Signaling	Increased	1.693	0.002236232
Sap30	Magnusson et al. (2005)	Transcription	Increased	2.068	1.40071E-07
Atf6b	Sacheck et al. (2007)	Transcription	Increased	1.384	0.001401524
Eftud2	Sacheck et al. (2007)	Transcription	Increased	1.259	0.013000071
Eif4ebp1	Lecker et al. (2004)	Translation	Increased	1.522	0.000538631

Table S3. DE genes (TSCmKO vs. Control), found as atrophy-related genes

Identification of mTORC1-dependent atrophy-related genes, comparing a unsupervised list of atrophy-related genes with RNA-sequencing data obtained from *extensor digitorum longus* (EDL) muscles from female, 3-month-old TSCmKO mice and Control littermates (n=5). Table of previously described atrophy-related genes found expressed in young TSCmKO mice, which are similarly regulated as in other types of muscle atrophy (indicated in column “as atrogene”). Reference marked with asterisk (*) was retracted (but not regarding the findings that describe Mul1 as atrophy-related gene).

Gene	Forward primer	Reverse primer
Actb (B-actin)	CAGCTTCTTTGCAGCTCCTT	GCAGCGATATCGTCATCCA
Atf4	AGCAAAACAAGACAGCAGCC	ACTCTCTTCTTCCCCCTTGC
Bnip3	TTCCACTAGCACCTTCTGATGA	GAACACCGCATTTACAGAACAA
Ctsd	CGTCTTGCTGCTCATTCTCGGCC	GCCGCCCACCTCCGTCATAGT
Ctsl	GTGGACTGTTCTCACGCTCA	TCCGTCCTTCGCTTCATAGG
Ddi2	TGAACGGGCATCCTGTGAAA	AATTGAGAAGGAGCACGCCA
Des	GAGGTTGTCAGCGAGGCTAC	CTTCAGGAGGCAGTGAGGAC
Fbxo32 (Atrogin-1)	CTCTGTACCATGCCGTTCCT	GGCTGCTGAACAGATTCTCC
Gabarapl1	CATCGTGGAGAAGGCTCCTA	ATACAGCTGGCCCATGGTAG
Gadd45a	CCGAAAGGATGGACACGGTG	TTATCGGGGTCTACGTTGAGC
Map1lc3b (LC3b)	CACTGCTCTGTCTTGTGTAGGTTG	TCGTTGTGCCTTTATTAGTGCATC
MuRF1 (Trim63)	ACCTGCTGGTGGAAAACA	AGGAGCAAGTAGGCACCTCA
Nfe2l1 (Nrf1)	CCCTACTCACCCAGTCAGTATG	CATCGTGCGAGGAATGAGGA
Nfe2l2 (Nrf2)	GCCCACATTCCCAAACAAGAT	CCAGAGAGCTATTGAGGGACTG
Nqo1	TTCTCTGGCCGATTCAGAG	GGCTGCTTGGAGCAAAATAG
Ogt	TTCGGGAATCACCCTACTTCA	TACCATCATCCGGGCTCAA
Ppp1r15a (Gadd34)	GACCCCTCCAACTCTCCTTC	CTTCCTCAGCCTCAGCATTC
Psma1	CCTCAGGGCAGGATTCATCAA	GAGCGGCAAGCTCTGACTG
Psma5	AGCAATTGGCTCTGCTTCAG	GCATTCAGCTTCTCCTCCAT
Psmb5	AGGAGCCGCGAATCGAAATG	CCAGAAGGTACGGGTTGATCTC
Psmb6	CTGGGAAAACCGGGAAGTCTC	GAGTCCGCTCCTAGAACCAC
Psmb7	GTGTCGGTGTTTCAGCCAC	TCCGCTTCCAAGACAGCATT
Psmc1	AAGGGGGTCATTCTCTACGG	AAGCTCTGAGCCAACCACTC
Psmc4	TGGTCATCGGTCAGTTCTTG	CGGTCGATGGTACTCAGGAT

Psmd11	AGGCAGACAGAAGCATTGAAA	GGTCCAAAATCCCATGAAACT
Psmd4	TCTCCTATTCTGGCTGGTGAA	CATGCTGCTTAGGTCTGGAAG
Psmd8	GCCTCAATCTCCTCTTCCTGCTATC	GTCTGTCATCTTTTTGGGTGTGC
Psme4	AGCGTCAACAAGATAAGAATGCT	GCCCGATTCCTATATGCTCAAA
Sqstm1 (p62)	AGGGAACACAGCAAGCTCAT	GACTCAGCTGTAGGGCAAGG
Tbp	TGCTGTTGGTGATTGTTGGT	CTGGCTTGTGTGGGAAAGAT
Tubb (B-tubulin)	GAAGCTGACCACACCCACCT	TGAAGAAGTGCAGGCGTGGG
Vcp (p97)	GGTTGGGGTTAGAGCAGCTT	GCGACTAATCAAACGACGGC

Table S4: Primers used for quantitative PCR analysis

Protein	Ab No	Company	Dilution
4E-BP1	#9452	Cell Signaling Technology	1:1000
4E-BP1 p-S65	#9451	Cell Signaling Technology	1:1000
a-actinin	A7732	Sigma	1:5000
Akt	#9272	Cell Signaling Technology	1:1000
Akt p-S473	#9271	Cell Signaling Technology	1:1000
BECN1	#3495	Cell Signaling Technology	1:1000
DDI2	ab197081	Abcam	1:2000
eIF4E	#2067	Cell Signaling Technology	1:1000
GAPDH	#2118	Cell Signaling Technology	1:5000
GCLC	ab41463	Abcam	1:1000
GFP	11 814 460 001	Roche	1:1000
LC3B	#2775	Cell Signaling Technology	1:1000
Ubiquitin	BML-PW8810	Enzo	1:500
NFE2L1 (Nrf1)	#8052	Cell Signaling Technology	1:1000
NFE2L2 (Nrf2)	#12721	Cell Signaling Technology	1:1000
NQO1	ab2346	Abcam	1:5000
OGT	#24083	Cell Signaling Technology	1:1000
SQSTM1 (p62)	GP62-C	Progen	1:1000
PA200	18799-1-AP	Proteintech	1:500
PRAS40	#2610	Cell Signaling Technology	1:1000
PRAS40 p-T246	#2997	Cell Signaling Technology	1:1000
PSMA* (PSMA1,2,3,5,6,7)	BML-PW8195	Enzo	1:1000
PSMB5	ab3330	Abcam	1:1000
PSMB6	#13267	Cell Signaling Technology	1:1000

PSMB7	#13207	Cell Signaling Technology	1:1000
PSMC1	ab140450	Abcam	1:2000
PSMC5	ab140450	Abcam	1:2000
S6	#2217	Cell Signaling Technology	1:1000
S6 p-S235-S236	#2211	Cell Signaling Technology	1:1000
S6 p-S240-S244	#5364	Cell Signaling Technology	1:1000
TSC1	A300-316A	Bethyl	1:5000
VCP (p97)	#2648	Cell Signaling Technology	1:1000

Table S5: Primary antibodies used for immunoblotting

<u>Part 2</u> - “Proteasome inhibition in Control and TSCmKO mice”

Proteasome inhibition has mainly been studied in the context of cancer treatment and neurodegenerative diseases because of its anti-inflammatory activity and its ability to induce cellular apoptosis and to shift the equilibrium of proteostasis towards cell death (Manasanch and Orlowski, 2017). Currently, the three proteasome inhibitors bortezomib (BTZ), carfilzomib and ixazomib are approved for the treatment of adult patients with multiple myeloma (Adams and Kauffman, 2004; Meng et al., 1999; Richardson et al., 2014; Richardson et al., 2015; Richardson et al., 2005; Richardson et al., 2010; Wang et al., 2013). In parallel to the studies in cancer treatment, proteasome inhibitors were tested to counteract muscle atrophy by reducing accelerated protein degradation. Indeed, several *in vivo* studies reported beneficial effects on muscle proteostasis and atrophy by applying proteasome inhibitors on distinct catabolic states, such as sepsis, hindlimb casting and unloading, denervation, immobilization or in animal models for muscular dystrophies (Beehler et al., 2006; Carmignac et al., 2011; Caron et al., 2011; Fischer et al., 2000; Jamart et al., 2011; Korner et al., 2014; Krawiec et al., 2005; Supinski et al., 2009; Vargas and Lang, 2008). Although it was shown that BTZ affects muscle proteostasis and at least can partially prevent muscle wasting in animal models, its use was never approved in patients for treatment of muscle atrophy. In addition, clinical trials with BTZ for the treatment of cancer cachexia have not shown consistent results (Madeddu and Mantovani, 2009; Penna et al., 2016).

In this thesis, we investigated the role of mTORC1 in regulating muscle proteostasis and we identified the mTORC1-Nrf1-signaling as an important mediator of increasing proteasomal biosynthesis and inducing the UPS. To elucidate the role of the 26S proteasome in this mechanism and to test if proteasome inhibition is sufficient to attenuate muscle atrophy in TSCmKO mice, we recently started to explore the usage of BTZ in skeletal muscle. BTZ belongs to the proteasome inhibitor group of boronates, dipeptidyl boronic acids, which reversibly bind and inhibit the β5 catalytic enzyme of the 26S proteasome (Adams et al., 1998).

Unfortunately, there is not much data about the efficacy and the duration of effect of BTZ in murine skeletal muscle. Therefore, we first tested the response of BTZ (1 mg/kg) to the proteasome activity in skeletal muscles of Control mice. Confirming proper application and successful targeting of skeletal muscle, we found a 50% reduction in β5-activity 6 hours after BTZ treatment in lysates of *plantaris* (PLA) muscle (**Figure 4A**). Interestingly, β5-activity was completely restored after 48 hours (**Figure 4A**). Surprisingly, we found an even more pronounced inhibition of the β1-activity, with 75% reduction after 6 hours maintained over 72 hours ending still with more than 50% reduction (**Figure 4A**). Finally, β2 activity was not affected by proteasome inhibition using BTZ (**Figure 4A**).

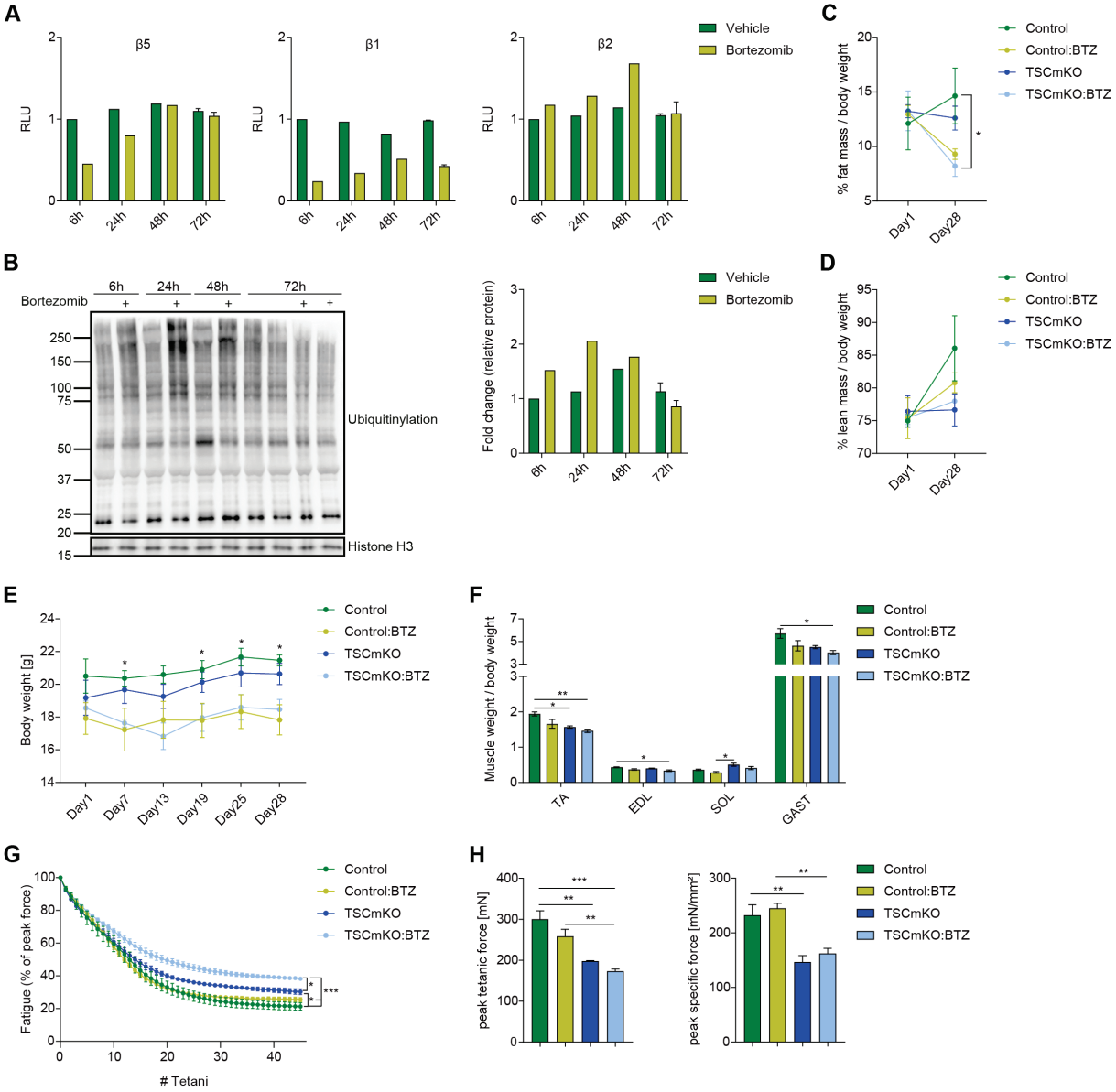

Figure 4. Proteasome inhibition using bortezomib in skeletal muscle of Control and TSCmKO mice.

3-month-old Control mice were treated once with bortezomib (BTZ) or vehicle and have been dissected after 6, 24, 48 or 72 hours. **(A)** Luciferase-based proteasome activity measurement in lysates of *extensor digitorum longus* (EDL) muscles. **(B)** Western blot analysis of ubiquitinylated proteins in *tibialis anterior* (TA) muscles. 3-month-old TSCmKO and Control mice were treated every 72 h with BTZ or vehicle for 4 weeks, n=3. **(C)** Progression of relative fat mass between start and end of the treatment. **(D)** Progression of relative lean mass between start and end of the treatment. **(E)** Body weight was measured every 6th day and at the last day of treatment. Asterisk indicating where body weight was significantly different between Control and Control:BTZ. **(F)** Relative muscle weight after BTZ treatment. **(G)** Muscle fatigue depicted in percentage of peak force for each contraction (tetani). Asterisk indicating significance levels at the last contraction. **(H)** Peak tetanic force (absolute force) and peak specific force (absolute force normalized to cross-sectional area) after BTZ treatment. Data represent means ± SEM, ***p ≤ 0.001, **p ≤ 0.01, *p ≤ 0.05, Student's t test (if two groups were compared), One-way ANOVA test (if more than two groups were compared), Two-way ANOVA test (if multiple time points and more than two groups were compared).

Accumulation of ubiquitinylated proteins is a direct and functional indication for proteasome inhibition. We found the strongest accumulation of ubiquitinylated proteins 24 hours after the BTZ treatment (**Figure 4B**). These findings lead to the assumption that decreased proteasome activity precedes the accumulation of ubiquitinylated proteins, and that decreased β5-activity is required and as well the limiting factor, for proteasomal degradation in skeletal muscle. These preliminary experiments were performed with n=1 (6 h, 24 h and 48 h) and with n=2 (72 h) to study the response of BTZ prior to a long-term treatment in Control and TSCmKO mice. Therefore, higher n number would be necessary to make statistics and to make conclusive statements.

To test if proteasome inhibition is sufficient to attenuate muscle atrophy in TSCmKO mice, we subjected young TSCmKO and Control mice to a 4-week proteasome inhibition using BTZ (1 mg/kg, every 72 hours, intraperitoneally injections). Both, Control and TSCmKO mice, lost body mass upon proteasome inhibition, due to a strong decrease in fat mass (**Figure 4C, 4E**). Lean mass showed a trend to be decreased in Control mice but not in TSCmKO mice with BTZ (**Figure 5D**). We found a trend to decreased relative muscle weight in TSCmKO and Control mice with BTZ (**Figure 4F**). As we previously showed, peak tetanic and specific force were significantly decreased in TSCmKO mice (Castets et al., 2013) and we did rather observe a trend to decreased than improved tetanic force after the BTZ treatment in Control and TSCmKO mice (**Figure 4H**). Nevertheless, we found a weak trend to increased peak specific force in TSCmKO mice with BTZ compared to vehicle-treated TSCmKO mice (**Figure 4H**). Because absolute force was rather decreased and specific force shows a trend to be increased, we assume alterations to the cross-sectional area of TSCmKO mice treated with BTZ. Interestingly, we found a significant improvement in fatigue resistance of young TSCmKO mice compared to Control littermates, and even more improved fatigue resistance upon proteasome inhibition in TSCmKO mice but not in Control mice (**Figure 4G**). This is on one side an indication for more oxidative fibers and on the other hand, it could mean that fast fibers are less atrophic. Altogether, these data suggest rather mild changes to the muscle histology and physiology in Control and TSCmKO mice after 4 weeks of BTZ treatment. Important to note is, that we performed this experiments with n=3, which is not enough statistical power to properly analyze histological and physiological data. Moreover, we will have to analyze fiber size and cross-sectional area, fiber type distribution and the ubiquitin-proteasome system. Since Nrf1 was described as a key-driver of the “bounce-back” response upon proteasome inhibition (Radhakrishnan et al., 2010; Sha and Goldberg, 2014; Steffen et al., 2010), it will be interesting to test how Nrf1 is regulated in skeletal muscle of Control and TSCmKO mice. Therefore, Nrf1-activity could also explain a rather mild response to the BTZ treatment, assuming continual restoration of proteasome function, due to newly synthesized proteasomal subunits.

In addition, we assume that proteasome inhibition using BTZ (1 mg/kg) in skeletal muscle, completely blocks proteasome degradation only during the first 24 hours. Therefore, in a 72-hours treatment during 4 weeks there will be alternating states of active and inhibited proteasome degradation. Finally, the increase of the UPS in TSCmKO mice is relatively mild compared to other catabolic conditions, such as starvation or denervation. We assume that a mild increase of the UPS, over days and month, is the reason for the atrophy in TSCmKO mice. Therefore, proteasome inhibition in alternating states of active and inactive degradation during four weeks may lead to marginally improvements in muscle mass but might also be a good option for therapeutic strategies. Even though longer treatment durations are difficult to perform because of the whole-body adverse effects of proteasome inhibitors, there might be possibilities to dampen, but not inactivate, proteasome degradation.

Results - Part 2 - Material and Methods

Mice

All mice were maintained in a licensed animal facility with a fixed 12 h dark-light cycle and were allowed for food and water *ad libitum*. All animal studies were performed under the guidelines and the law of the Swiss authorities and were regularly controlled and approved by the veterinary office.

Animal experiments

In some experiments mice were intraperitoneally injected with bortezomib (BTZ; 1 mg/kg; Selleck Chemicals) diluted in saline every 72 hours for four consecutive weeks. This mice were weighed before each injection. For the time course study of BTZ in skeletal muscle, BTZ (1 mg/kg; Selleck Chemicals) diluted in saline was once intraperitoneally injected.

In vitro muscle force

In vitro force measurements of *extensor digitorum longus* (EDL) muscles were conducted as described previously (Bentzinger et al., 2008). Muscle fatigue was measured by repeated stimulation (number of contractions) at 200 Hz every 8 s and then recorded by using the Aurora Scientific Inc. Model 610A Dynamic Muscle Control Software. Graph displays maximal peak force of each contraction.

Ubiquitinylation analysis

Dissected muscle was rapidly frozen in liquid nitrogen. Frozen muscles were pulverized on a metal plate chilled in liquid nitrogen and directly snap-frozen as pellet in liquid nitrogen.

Samples were lysed in cold Ub-lysis-buffer (1 mM EDTA, 25 µM MG 132, 50 mM N-ethylmaleimide, 50 mM TrisHCl pH 8.0, 150 mM NaCl, 1% NP-40, 0.5% sodium deoxycholate, 0.1% SDS, ddH_2O) supplemented with phosphatase and protease inhibitor cocktail tablets (Roche), incubated on a rotating wheel for 2 h at 4°C and sonicated twice for 10 s. Afterwards, the lysate was centrifuged at 16,000 g for 20 min at 4°C. Supernatant (cleared lysates) were used to determine total protein amount using the Pierce BCA Protein Assay Kit (Thermo Fisher Scientific) according to manufacturer’s protocol. Immunoblotting was performed as described above.

Proteasome activity assay

Proteasome activity assay was adapted from a protocol described previously (Strucksberg et al., 2010). Briefly, dissected EDL muscles were rinsed in ice-cold PBS, immediately cut into 5-6 pieces and directly lysed in ice-cold PBS-E (5 mM EDTA pH 8.0, PBS pH 7.2) and sonicated two times for 10 s. Afterwards, the lysate was centrifuged at 13,000 g for 5 min at 4°C. Supernatant (cleared lysates) were used to determine total protein amount using the Pierce BCA Protein Assay Kit (Thermo Fisher Scientific) according to manufacturer’s protocol. Three individual luciferase-based Proteasome-Glo™ Assay Systems (Promega) were used to measure the activity of each peptidase of the proteasome. Assay was performed on white, 96-well microplates (greiner BIO-ONE) and luminescence was measured with Infinite M1000 (Tecan). Human, purified 20S proteasome (Enzo Life Sciences, BML-PW8720) was used as positive control. Proteasome inhibitor MG 132 (50 µM, TOCRIS Biotechne) was used for measuring non-proteasomal activity in this assay, which was used for background subtraction.

Statistical analysis

Data are presented as the mean value and the respective standard error of the mean (SEM, error bars). Student’s t test was used when two groups were compared to evaluate statistical significance. One-way or two-way analysis of variance (ANOVA) test with Tukey’s correction for multiple comparisons were used to compare more than two groups. A confidence level of 0.05 was accepted for statistical significance.

***Part 3* - “Proteasome activity in sarcopenia”**

Similar to what we observe in TSCmKO mice, the muscle loss that is characteristic for sarcopenia develops slowly and gradually over time (Cohen et al., 2015). However, this process is strongly accelerated in TSCmKO mice, as these mice undergo many symptoms of precocious sarcopenia (Bentzinger et al., 2013; Castets et al., 2013; Guridi et al., 2015).

In this thesis we investigated the role of mTORC1 in regulating muscle proteostasis and we identified the mechanism that sustained active mTORC1 induces the ubiquitin-proteasome system (UPS) *via* the transcriptional regulator Nrf1. Both, the mTORC1 signaling as well as the UPS are considered as potential treatment targets in sarcopenia (Cohen et al., 2015; Yoon, 2017). The role of mTORC1 activity in sarcopenia is still controversially discussed. Several studies described reduced mTORC1 activity and decreased protein synthesis rates as the main reason for muscle wasting in the elderly (Cuthbertson et al., 2005; Leger et al., 2008; Pallafacchina et al., 2002). However, recent studies observed hyper-phosphorylation of mTORC1 in aged human muscles, but also in muscles of aged mice and rats (Joseph et al., 2019; Markofski et al., 2015; White et al., 2016). Importantly, a recent study reported beneficial effects for mTORC1 inhibition on muscle wasting in aged rats (Joseph et al., 2019).

Since muscles of TSCmKO mice and sarcopenic muscles share many common characteristics but also share a strong activation of the mTORC1-signaling, we wondered if the UPS is induced in sarcopenic muscles as well. For that reason, we measured proteasome activity for all three catalytic enzymes of the 26S proteasome in *plantaris* muscles of young, 8-month-old mice and compared them with *plantaris* muscles of sarcopenic, 28-month-old mice. Chymotrypsin-like (β5) activity was not altered between 8- and 28-month-old mice (**Figure 5A**). We found caspase-like (β1) activity significantly decreased and trypsin-like (β2) activity significantly increased in 28-month-old, sarcopenic mice compared to young 8-month-old mice (**Figure 5A**). Therefore, we found ambiguous results about the proteasome activity in sarcopenic mice. There is a thin line between normally aged muscles and sarcopenic muscles, which somewhen rapidly start to loose muscle mass. By normalizing the body weight to the muscle weight, we calculated a factor that is representative for the relative muscle wasting of the *plantaris* in a particular mouse. We found in the 28-month-old mice a separation of four mice with a mild or no muscle wasting, similar to young mice and a group of four mice with strong muscle wasting (**Figure 5B, 5C, 5D**). By correlating this wasting factor with the proteasome activity revealed that the decrease in β1-activity was specific for muscles with mild wasting (**Figure 5C**). Instead, muscles with stronger wasting displayed similar proteasome activity as found in muscles of young mice (**Figure 5C**). Similar correlation was obtained for β5-activity (**Figure 5B**).

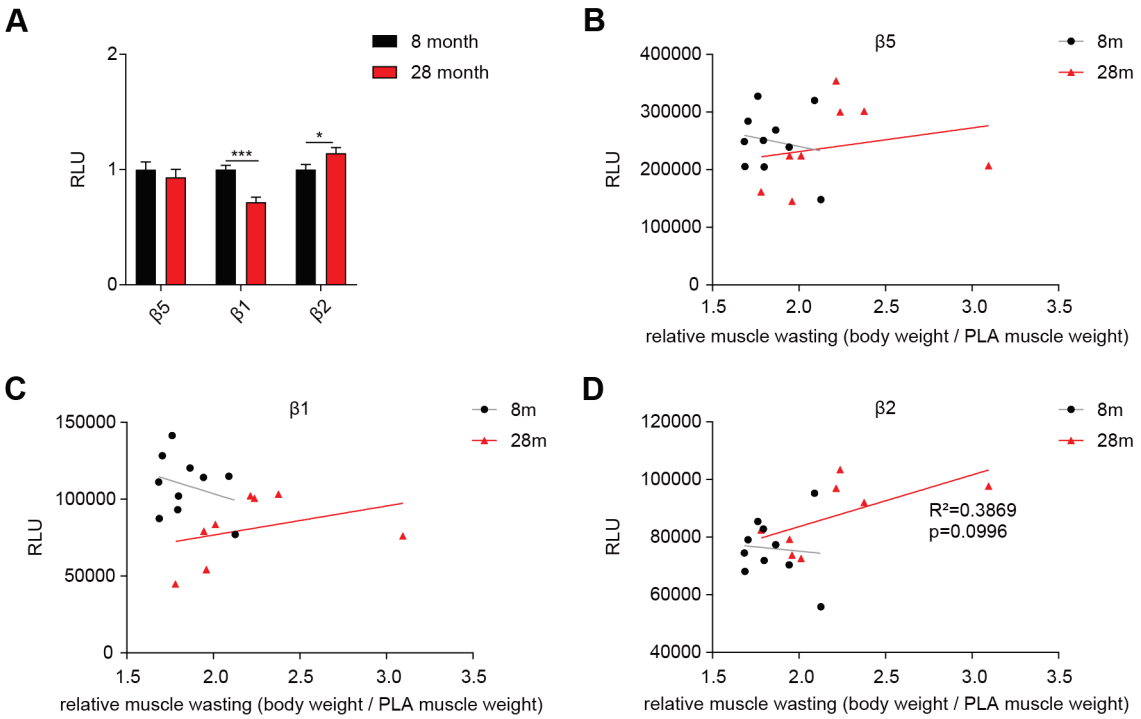

Figure 5. Proteasome activity in sarcopenic muscles

Proteasome activity was measured in *plantaris* (PLA) muscle of young 8-month-old, aged 24-month-old and sarcopenic 28-month-old mice. **(A)** Luciferase-based proteasome activity measurement in lysates of PLA muscles, n=10 (8 month, 24 month), n=8 (28 month). **(B)** Linear regression and correlation of proteasome activity and relative muscle wasting for β5-activity, n=10 (8 month, 24 month), n=8 (28 month). **(C)** Linear regression and correlation of proteasome activity and relative muscle wasting for β1-activity, n=10 (8 month, 24 month), n=8 (28 month). **(D)** Linear regression and correlation of proteasome activity and relative muscle wasting for β2-activity, n=10 (8 month, 24 month), n=8 (28 month). Data represent means ± SEM, ***p ≤ 0.001, **p ≤ 0.01, *p ≤ 0.05, Student's t test (if two groups were compared), Pearson correlation coefficients (if correlation was analyzed).

The significant increase found for β2-activity in 28-month-old mice compared with 8-month-old mice is also due to muscles, which undergo stronger wasting (**Figure 5D**). Surprisingly, we almost found significant correlation for β2-activity and the muscle wasting in 28-month-old, sarcopenic mice (**Figure 5D**). Interestingly, β2-activity of the 26S proteasome was also slightly stronger increased in young TSCmKO mice (**Manuscript Figure 2F**) and even more stronger increased in 10-month-old TSCmKO mice (**Manuscript Figure S3E**) with muscles displaying strong muscle wasting and myopathy (Castets et al., 2013). Moreover, β2-activity was not reversed in young TSCmKO mice treated with rapamycin for 3 days (**Manuscript Figure 3C**). In contrast, muscles with constitutive activation of Akt, which are hypertrophic and have no signs of muscle wasting or myopathy, had a normal, mild activation of β2-activity as observed for β1- and β5-activity (**Manuscript Figure 5C**). Altogether, our data demonstrates that β2-activity of the proteasome is characteristically increased in muscles undergoing wasting, atrophy, myopathy and sarcopenia. Since we measure proteasome activity in lysates of muscle tissue, one explanation for this observation could be the invasion of muscle fibers by other cell

types (i.e. inflammatory cells), which may display distinct proteasome activity than muscle fibers. To make a statement about the activity of the UPS in sarcopenia and whether mTORC1 regulates the UPS in sarcopenic muscles or not would need further investigations. However, our results clearly demonstrate that proteasome activity is not similarly increased as in TSCmKO mice. Nevertheless, sarcopenic muscles, characterized by pronounced muscle wasting show a clear trend for increased proteasome β2-activity.

Besides, it would be interesting to test if Nrf1 regulates proteasomal biosynthesis in sarcopenic muscles. Dampening of the Nrf1-activity could be a possibility to make muscle proteostasis more sensitive for proteasome inhibition. Unfortunately, there is no approach for using proteasome inhibitors in sarcopenia. On the other hand, many aging studies reported a decrease of PSM genes, proteasome function and the UPS with age in different tissues and organs (Chondrogianni and Gonos, 2005; Dahlmann, 2007; Gaczynska et al., 2001; Lee et al., 1999; Lee et al., 2000; Tonoki et al., 2009). Overexpression or activating Nrf1 might contribute to restore proteasomal function with age. Particularly, in age-related neurodegenerative disorders, such as Alzheimer’s (Keck et al., 2003), Parkinson’s (McNaught et al., 2003) or Huntington’s disease (Seo et al., 2004), malfunctioning of the UPS could be overcome by activating Nrf1.

Results - Part 3 - Material and Methods

Mice

All mice were maintained in a licensed animal facility with a fixed 12 h dark-light cycle and were allowed for food and water *ad libitum*. All mice of the aging study were fed with a semi-purified diet called AIN93M (KLIBA NAFAG). All animal studies were performed under the guidelines and the law of the Swiss authorities and were regularly controlled and approved by the veterinary office.

Proteasome activity assay

Proteasome activity assay was adapted from a protocol described previously (Strucksberg et al., 2010). Briefly, dissected *plantaris* (PLA) muscles were rinsed in ice-cold PBS, immediately cut into 5-6 pieces and directly lysed in ice-cold PBS-E (5 mM EDTA pH 8.0, PBS pH 7.2) and sonicated two times for 10 s. Afterwards, the lysate was centrifuged at 13,000 g for 5 min at 4°C. Supernatant (cleared lysates) were used to determine total protein amount using the Pierce BCA Protein Assay Kit (Thermo Fisher Scientific) according to manufacturer’s protocol. Three individual luciferase-based Proteasome-Glo™ Assay Systems (Promega) were used to measure the activity of each peptidase of the proteasome. Assay was performed on white, 96-well microplates (greiner BIO-ONE) and luminescence was measured with Infinite M1000

(Tecan). Human, purified 20S proteasome (Enzo Life Sciences, BML-PW8720) was used as positive control. Proteasome inhibitor MG 132 (50 µM, TOCRIS Biotechne) was used for measuring non-proteasomal activity in this assay, which was used for background subtraction.

Statistical analysis

All experiments were performed on a minimum of n (number of individual experiments) ≥3 independent biological samples. In all graphs, data are presented as the mean value and the respective standard error of the mean (SEM, error bars). Student’s t test was used when two groups were compared to evaluate statistical significance. Pearson correlation was used to statistically analyze correlation betwenn proteasome activity and muscle wasting. A confidence level of 0.05 was accepted for statistical significance.

7. Conclusions and future prospects

Activation of mTORC1 in skeletal muscle is generally associated with growth, increasing translation and protein synthesis, promoting anabolism and mediating hypertrophy. In contrast, sustained activation of mTORC1 in skeletal muscles was previously shown to cause a blockage in autophagy induction and muscle atrophy, resulting in a severe muscle wasting and myopathy.

In this thesis, mice with a muscle-specific ablation of TSC1 (TSCmKO mice), which leads to sustained activation of mTORC1, were used as a model to explore the role of mTORC1 in regulating muscle proteostasis. It was demonstrated that TSCmKO mice express a large set of atrophy-related genes, mainly involved in protein degradation processes. This strong, atrophic response in transcriptional regulation, highlighted the importance to explore new mechanisms of how mTORC1 controls catabolic processes to regulate muscle proteostasis. This thesis revealed that sustained activation of mTORC1 leads to an overall induction of the ubiquitin-proteasome system (UPS). This induction includes ubiquitin-E3-ligases, ubiquitinylation, transcriptional activation of proteasomal biosynthesis and increased proteasome activity. However, if the increase of the UPS also effectively increases overall protein degradation rates, remains to be tested. This would be essential for associating induced UPS activity with muscle atrophy.

Furthermore, distinct interventions were used to identify the prerequisites and to dissect the mechanism leading to an increased UPS in TSCmKO mice. It was demonstrated that short-term treatment with rapamycin hinders the induction of the UPS, and that short-term activation of mTORC1 during 21 days is sufficient to induce it. The identification of a new mechanism regulating muscle proteostasis revealed that an mTORC1-dependent activation of the UPS is mediated by the transcription factor Nrf1. Taken together, it appears that sustained activation of mTORC1-signaling induces the UPS *via* two separate catabolic processes: First, by transcriptionally inducing proteasomal biosynthesis mediated through Nrf1. Second, by the feedback mechanism leading to deceased Akt activity and increased FoxO transcription factor activity, which results in the activation of an atrophy-related gene program, increased expression of various ubiquitin-E3-ligases and increased ubiquitinylation. Further investigations are needed to ascertain if the increase of Nrf1 is regulated in an mTORC1-direct manner or if it is increased as an acute response to a secondary consequence, such as increased protein synthesis, blocked autophagy induction or accumulation of misfolded proteins and increased ER-stress. In either case, it remains to elucidate if mTORC1 regulates Nrf1 *via* SREBF1 or by a completely unknown, new mechanism.

This thesis further demonstrated that the slow-twitch muscle *soleus* strongly varies in the response to sustained activation of mTORC1. Similar to fast-twitch muscles, the *soleus* muscle

of TSCmKO mice displays increased protein synthesis but in contrast no activation of the UPS. Why Nrf1 as well as FoxO transcription factors were not induced in the *soleus* muscles of TSCmKO mice, remains obscure and needs further investigations. One possible explanation for the “FoxO-part” would be that the status of Akt phosphorylation is not the limiting factor of FoxO phosphorylation in these muscles. FoxO was also shown to be regulated by post-translational modifications, such as acetylation, ubiquitinylation and methylation. Similarly, one possible explanation for the “Nrf1-part” would be that one of the post-translational regulators of Nrf1 (i.e. p97, OGT, DDI2), which were shown in this thesis to be regulated in an mTORC1-dependent way in fast-twitch muscles, repress the activity of Nrf1 in the *soleus*. Nevertheless, this would not explain the absence of the transcriptional increase of *Nrf1* observed in fast-twitch muscles. Another possibility is, that the basal activity of mTORC1 and the rates in protein synthesis are highly different between slow and fast-twitch muscles and therefore a potential threshold to induce a catabolic response could be completely different.

In addition, this thesis showed that inactivation of Nrf1 for two weeks in TSCmKO mice strongly decreases the expression of proteasomal subunits and shows a trend for increased muscle weight. These results have to be confirmed in TSCmKO mice with prolonged inactivation of Nrf1. We hypothesize that prolonged inactivation of Nrf1 will result in an attenuation of the muscle atrophy in TSCmKO mice, which in parallel will demonstrate that an mTORC1-Nrf1-dependent increase of the UPS causes muscle atrophy in TSCmKO mice.

Increased Nrf1-activtiy is generally directly associated with an evolutionary conserved response mechanism upon proteasome perturbation to increase proteasomal biosynthesis and to maintain cellular proteostasis. Thus, Nrf1 received significant medical relevance as regulator of this important compensatory response that promotes tumor cell survival and attenuates therapeutic efficacy. Therefore, active Nrf1 in muscle might reduce the efficacy of proteasome inhibitors in the treatment of muscle wasting, as for example seen in sarcopenia. Indeed, this thesis demonstrated that TSCmKO mice show neither an attenuation of muscle atrophy nor an improvement of muscle function after bortezomib treatment. Nevertheless, extensive experiments are necessary to completely characterize the application of bortezomib in TSCmKO mice. Particularly, describing the role of Nrf1, in muscles of TSCmKO mice, in mediating proteasomal biosynthesis upon bortezomib treatment, would be interesting for future therapeutic strategies.

The results presented in this thesis unraveled a new mechanism of how mTORC1 regulates the ubiquitin-proteasome system. In addition, these findings may lead to the thorough characterization of Nrf1 as a new possible target to slow-down the massive muscle wasting observed in cachexia or sarcopenia.

8. References

Adams, J., Behnke, M., Chen, S., Cruickshank, A.A., Dick, L.R., Grenier, L., Klunder, J.M., Ma, Y.T., Plamondon, L., and Stein, R.L. (1998). Potent and selective inhibitors of the proteasome: dipeptidyl boronic acids. Bioorg Med Chem Lett *8*, 333-338.

Adams, J., and Kauffman, M. (2004). Development of the proteasome inhibitor Velcade (Bortezomib). Cancer Invest *22*, 304-311.

Adams, J., Palombella, V.J., Sausville, E.A., Johnson, J., Destree, A., Lazarus, D.D., Maas, J., Pien, C.S., Prakash, S., and Elliott, P.J. (1999). Proteasome inhibitors: a novel class of potent and effective antitumor agents. Cancer Res *59*, 2615-2622.

Alessi, D.R., James, S.R., Downes, C.P., Holmes, A.B., Gaffney, P.R., Reese, C.B., and Cohen, P. (1997). Characterization of a 3-phosphoinositide-dependent protein kinase which phosphorylates and activates protein kinase Balpha. Curr Biol *7*, 261-269.

Alsina, M., Trudel, S., Furman, R.R., Rosen, P.J., O'Connor, O.A., Comenzo, R.L., Wong, A., Kunkel, L.A., Molineaux, C.J., and Goy, A. (2012). A phase I single-agent study of twice-weekly consecutive-day dosing of the proteasome inhibitor carfilzomib in patients with relapsed or refractory multiple myeloma or lymphoma. Clin Cancer Res *18*, 4830-4840.

Altun, M., Besche, H.C., Overkleeft, H.S., Piccirillo, R., Edelmann, M.J., Kessler, B.M., Goldberg, A.L., and Ulfhake, B. (2010). Muscle wasting in aged, sarcopenic rats is associated with enhanced activity of the ubiquitin proteasome pathway. J Biol Chem *285*, 39597-39608.

Augusto, V.P., C.;Campos,G. (2004). Skeletal muscle fiber types in C57BL6J mice. Brazilian journal of morphological sciences *21*, 6.

Bar-Peled, L., Chantranupong, L., Cherniack, A.D., Chen, W.W., Ottina, K.A., Grabiner, B.C., Spear, E.D., Carter, S.L., Meyerson, M., and Sabatini, D.M. (2013). A Tumor suppressor complex with GAP activity for the Rag GTPases that signal amino acid sufficiency to mTORC1. Science *340*, 1100-1106.

Bar-Peled, L., Schweitzer, L.D., Zoncu, R., and Sabatini, D.M. (2012). Ragulator is a GEF for the rag GTPases that signal amino acid levels to mTORC1. Cell *150*, 1196-1208.

Barany, M. (1967). ATPase activity of myosin correlated with speed of muscle shortening. J Gen Physiol *50*, Suppl:197-218.

Barnard, R.J., Edgerton, V.R., Furukawa, T., and Peter, J.B. (1971). Histochemical, biochemical, and contractile properties of red, white, and intermediate fibers. Am J Physiol *220*, 410-414.

Barthelme, D., Jauregui, R., and Sauer, R.T. (2015). An ALS disease mutation in Cdc48/p97 impairs 20S proteasome binding and proteolytic communication. Protein Sci *24*, 1521-1527.

Barthelme, D., and Sauer, R.T. (2012). Identification of the Cdc48*20S proteasome as an ancient AAA+ proteolytic machine. Science *337*, 843-846.

Beehler, B.C., Sleph, P.G., Benmassaoud, L., and Grover, G.J. (2006). Reduction of skeletal muscle atrophy by a proteasome inhibitor in a rat model of denervation. Exp Biol Med (Maywood) *231*, 335-341.

Bentzinger, C.F., Lin, S., Romanino, K., Castets, P., Guridi, M., Summermatter, S., Handschin, C., Tintignac, L.A., Hall, M.N., and Ruegg, M.A. (2013). Differential response of skeletal muscles to mTORC1 signaling during atrophy and hypertrophy. Skeletal Muscle *3*, 6.

Bentzinger, C.F., Romanino, K., Cloetta, D., Lin, S., Mascarenhas, J.B., Oliveri, F., Xia, J., Casanova, E., Costa, C.F., Brink, M.*, et al.* (2008). Skeletal muscle-specific ablation of raptor, but not of rictor, causes metabolic changes and results in muscle dystrophy. Cell Metab *8*, 411-424.

Biswas, M., and Chan, J.Y. (2010). Role of Nrf1 in antioxidant response element-mediated gene expression and beyond. Toxicol Appl Pharmacol *244*, 16-20.

Biswas, M., Phan, D., Watanabe, M., and Chan, J.Y. (2011). The Fbw7 tumor suppressor regulates nuclear factor E2-related factor 1 transcription factor turnover through proteasome-mediated proteolysis. J Biol Chem *286*, 39282-39289.

Bodine, S.C., Stitt, T.N., Gonzalez, M., Kline, W.O., Stover, G.L., Bauerlein, R., Zlotchenko, E., Scrimgeour, A., Lawrence, J.C., Glass, D.J.*, et al.* (2001). Akt/mTOR pathway is a crucial regulator of skeletal muscle hypertrophy and can prevent muscle atrophy in vivo. Nat Cell Biol *3*, 1014-1019.

Brooke, M.H., and Kaiser, K.K. (1970). Three "myosin adenosine triphosphatase" systems: the nature of their pH lability and sulfhydryl dependence. J Histochem Cytochem *18*, 670-672.

Brown, E.J., Albers, M.W., Shin, T.B., Ichikawa, K., Keith, C.T., Lane, W.S., and Schreiber, S.L. (1994). A mammalian protein targeted by G1-arresting rapamycin-receptor complex. Nature *369*, 756-758.

Buchberger, A., Schindelin, H., and Hanzelmann, P. (2015). Control of p97 function by cofactor binding. FEBS Lett *589*, 2578-2589.

Bugno, M., Daniel, M., Chepelev, N.L., and Willmore, W.G. (2015). Changing gears in Nrf1 research, from mechanisms of regulation to its role in disease and prevention. Biochim Biophys Acta *1849*, 1260-1276.

Buller, A.J., Eccles, J.C., and Eccles, R.M. (1960). Differentiation of fast and slow muscles in the cat hind limb. J Physiol *150*, 399-416.

Burke, R.E., Levine, D.N., and Zajac, F.E., 3rd (1971). Mammalian motor units: physiological-histochemical correlation in three types in cat gastrocnemius. Science *174*, 709-712.

Cafferkey, R., Young, P.R., McLaughlin, M.M., Bergsma, D.J., Koltin, Y., Sathe, G.M., Faucette, L., Eng, W.K., Johnson, R.K., and Livi, G.P. (1993). Dominant missense mutations in a novel yeast protein related to mammalian phosphatidylinositol 3-kinase and VPS34 abrogate rapamycin cytotoxicity. Mol Cell Biol *13*, 6012-6023.

Calderon, J.C., Bolanos, P., and Caputo, C. (2014). The excitation-contraction coupling mechanism in skeletal muscle. Biophys Rev *6*, 133-160.

Carmignac, V., Quere, R., and Durbeej, M. (2011). Proteasome inhibition improves the muscle of laminin alpha2 chain-deficient mice. Hum Mol Genet *20*, 541-552.

Caron, A.Z., Haroun, S., Leblanc, E., Trensz, F., Guindi, C., Amrani, A., and Grenier, G. (2011). The proteasome inhibitor MG132 reduces immobilization-induced skeletal muscle atrophy in mice. BMC Musculoskelet Disord *12*, 185.

Castets, P., Lin, S., Rion, N., Di Fulvio, S., Romanino, K., Guridi, M., Frank, S., Tintignac, L.A., Sinnreich, M., and Ruegg, M.A. (2013). Sustained activation of mTORC1 in skeletal muscle inhibits constitutive and starvation-induced autophagy and causes a severe, late-onset myopathy. Cell Metab *17*, 731-744.

Chai, R.J., Vukovic, J., Dunlop, S., Grounds, M.D., and Shavlakadze, T. (2011). Striking denervation of neuromuscular junctions without lumbar motoneuron loss in geriatric mouse muscle. PLoS One *6*, e28090.

Chan, J.Y., Kwong, M., Lu, R., Chang, J., Wang, B., Yen, T.S., and Kan, Y.W. (1998). Targeted disruption of the ubiquitous CNC-bZIP transcription factor, Nrf-1, results in anemia and embryonic lethality in mice. Embo J *17*, 1779-1787.

Chan, K., Lu, R., Chang, J.C., and Kan, Y.W. (1996). NRF2, a member of the NFE2 family of transcription factors, is not essential for murine erythropoiesis, growth, and development. Proc Natl Acad Sci U S A *93*, 13943-13948.

Chantranupong, L., Scaria, S.M., Saxton, R.A., Gygi, M.P., Shen, K., Wyant, G.A., Wang, T., Harper, J.W., Gygi, S.P., and Sabatini, D.M. (2016). The CASTOR Proteins Are Arginine Sensors for the mTORC1 Pathway. Cell.

Chantranupong, L., Wolfson, R.L., Orozco, J.M., Saxton, R.A., Scaria, S.M., Bar-Peled, L., Spooner, E., Isasa, M., Gygi, S.P., and Sabatini, D.M. (2014). The Sestrins Interact with GATOR2 to Negatively Regulate the Amino-Acid-Sensing Pathway Upstream of mTORC1. Cell Rep *9*, 1-8.

Chondrogianni, N., and Gonos, E.S. (2005). Proteasome dysfunction in mammalian aging: steps and factors involved. Exp Gerontol *40*, 931-938.

Ciciliot, S., Rossi, A.C., Dyar, K.A., Blaauw, B., and Schiaffino, S. (2013). Muscle type and fiber type specificity in muscle wasting. Int J Biochem Cell Biol *45*, 2191-2199.

Cohen, S., Nathan, J.A., and Goldberg, A.L. (2015). Muscle wasting in disease: molecular mechanisms and promising therapies. Nat Rev Drug Discov *14*, 58-74.

Combaret, L., Dardevet, D., Bechet, D., Taillandier, D., Mosoni, L., and Attaix, D. (2009). Skeletal muscle proteolysis in aging. Curr Opin Clin Nutr Metab Care *12*, 37-41.

Cosqueric, G., Sebag, A., Ducolombier, C., Thomas, C., Piette, F., and Weill-Engerer, S. (2006). Sarcopenia is predictive of nosocomial infection in care of the elderly. Br J Nutr *96*, 895-901.

Coyle, E.F., Sidossis, L.S., Horowitz, J.F., and Beltz, J.D. (1992). Cycling efficiency is related to the percentage of type I muscle fibers. Med Sci Sports Exerc *24*, 782-788.

Craiu, A., Gaczynska, M., Akopian, T., Gramm, C.F., Fenteany, G., Goldberg, A.L., and Rock, K.L. (1997). Lactacystin and clasto-lactacystin beta-lactone modify multiple proteasome beta-subunits and inhibit intracellular protein degradation and major histocompatibility complex class I antigen presentation. J Biol Chem *272*, 13437-13445.

Crow, M.T., and Kushmerick, M.J. (1982). Chemical energetics of slow- and fast-twitch muscles of the mouse. J Gen Physiol *79*, 147-166.

Cuthbertson, D., Smith, K., Babraj, J., Leese, G., Waddell, T., Atherton, P., Wackerhage, H., Taylor, P.M., and Rennie, M.J. (2005). Anabolic signaling deficits underlie amino acid resistance of wasting, aging muscle. Faseb J *19*, 422-424.

Dahlmann, B. (2007). Role of proteasomes in disease. BMC Biochem *8 Suppl 1*, S3.

Deschenes, M.R., Roby, M.A., Eason, M.K., and Harris, M.B. (2010). Remodeling of the neuromuscular junction precedes sarcopenia related alterations in myofibers. Exp Gerontol *45*, 389-393.

Diaz-Villanueva, J.F., Diaz-Molina, R., and Garcia-Gonzalez, V. (2015). Protein Folding and Mechanisms of Proteostasis. Int J Mol Sci *16*, 17193-17230.

Dibble, C.C., and Manning, B.D. (2013). Signal integration by mTORC1 coordinates nutrient input with biosynthetic output. Nat Cell Biol *15*, 555-564.

Dikic, I. (2017). Proteasomal and Autophagic Degradation Systems. Annu Rev Biochem *86*, 193-224.

Ding, Q., Martin, S., Dimayuga, E., Bruce-Keller, A.J., and Keller, J.N. (2006). LMP2 knock-out mice have reduced proteasome activities and increased levels of oxidatively damaged proteins. Antioxid Redox Signal *8*, 130-135.

Duvel, K., Yecies, J.L., Menon, S., Raman, P., Lipovsky, A.I., Souza, A.L., Triantafellow, E., Ma, Q., Gorski, R., Cleaver, S.*, et al.* (2010). Activation of a metabolic gene regulatory network downstream of mTOR complex 1. Mol Cell *39*, 171-183.

Evans, W.J., Morley, J.E., Argiles, J., Bales, C., Baracos, V., Guttridge, D., Jatoi, A., Kalantar-Zadeh, K., Lochs, H., Mantovani, G.*, et al.* (2008). Cachexia: a new definition. Clin Nutr *27*, 793-799.

Fardini, Y., Dehennaut, V., Lefebvre, T., and Issad, T. (2013). O-GlcNAcylation: A New Cancer Hallmark? Front Endocrinol (Lausanne) *4*, 99.

Fenteany, G., Standaert, R.F., Lane, W.S., Choi, S., Corey, E.J., and Schreiber, S.L. (1995). Inhibition of proteasome activities and subunit-specific amino-terminal threonine modification by lactacystin. Science *268*, 726-731.

Fielding, R.A., Vellas, B., Evans, W.J., Bhasin, S., Morley, J.E., Newman, A.B., Abellan van Kan, G., Andrieu, S., Bauer, J., Breuille, D.*, et al.* (2011). Sarcopenia: an undiagnosed condition in older adults. Current consensus definition: prevalence, etiology, and consequences. International working group on sarcopenia. J Am Med Dir Assoc *12*, 249-256.

Finley, D., Chen, X., and Walters, K.J. (2016). Gates, Channels, and Switches: Elements of the Proteasome Machine. Trends Biochem Sci *41*, 77-93.

Fischer, D., Gang, G., Pritts, T., and Hasselgren, P.O. (2000). Sepsis-induced muscle proteolysis is prevented by a proteasome inhibitor in vivo. Biochem Biophys Res Commun *270*, 215-221.

Frankland-Searby, S., and Bhaumik, S.R. (2012). The 26S proteasome complex: an attractive target for cancer therapy. Biochim Biophys Acta *1825*, 64-76.

Fu, H., Sadis, S., Rubin, D.M., Glickman, M., van Nocker, S., Finley, D., and Vierstra, R.D. (1998). Multiubiquitin chain binding and protein degradation are mediated by distinct domains within the 26 S proteasome subunit Mcb1. J Biol Chem *273*, 1970-1981.

Furrer, R., and Handschin, C. (2019). Muscle Wasting Diseases: Novel Targets and Treatments. Annu Rev Pharmacol Toxicol *59*, 315-339.

Gaczynska, M., Osmulski, P.A., and Ward, W.F. (2001). Caretaker or undertaker? The role of the proteasome in aging. Mech Ageing Dev *122*, 235-254.

Ganley, I.G., Lam du, H., Wang, J., Ding, X., Chen, S., and Jiang, X. (2009). ULK1.ATG13.FIP200 complex mediates mTOR signaling and is essential for autophagy. J Biol Chem *284*, 12297-12305.

Gentry, B.A., Ferreira, J.A., Phillips, C.L., and Brown, M. (2011). Hindlimb skeletal muscle function in myostatin-deficient mice. Muscle Nerve *43*, 49-57.

Greer, E.L., and Brunet, A. (2008). FOXO transcription factors in ageing and cancer. Acta Physiol (Oxf) *192*, 19-28.

Groll, M., Bajorek, M., Kohler, A., Moroder, L., Rubin, D.M., Huber, R., Glickman, M.H., and Finley, D. (2000). A gated channel into the proteasome core particle. Nat Struct Biol *7*, 1062-1067.

Guridi, M., Tintignac, L.A., Lin, S., Kupr, B., Castets, P., and Ruegg, M.A. (2015). Activation of mTORC1 in skeletal muscle regulates whole-body metabolism through FGF21. Sci Signal *8*, ra113.

Hamalainen, N., and Pette, D. (1995). Patterns of myosin isoforms in mammalian skeletal muscle fibres. Microsc Res Tech *30*, 381-389.

Han, J.W., Valdez, J.L., Ho, D.V., Lee, C.S., Kim, H.M., Wang, X., Huang, L., and Chan, J.Y. (2017). Nuclear factor-erythroid-2 related transcription factor-1 (Nrf1) is regulated by O-GlcNAc transferase. Free Radic Biol Med *110*, 196-205.

Handschin, C., Chin, S., Li, P., Liu, F., Maratos-Flier, E., Lebrasseur, N.K., Yan, Z., and Spiegelman, B.M. (2007). Skeletal muscle fiber-type switching, exercise intolerance, and myopathy in PGC-1alpha muscle-specific knock-out animals. J Biol Chem *282*, 30014-30021.

Hanson, P.I., and Whiteheart, S.W. (2005). AAA+ proteins: have engine, will work. Nat Rev Mol Cell Biol *6*, 519-529.

Hara, T., Takamura, A., Kishi, C., Iemura, S., Natsume, T., Guan, J.L., and Mizushima, N. (2008). FIP200, a ULK-interacting protein, is required for autophagosome formation in mammalian cells. J Cell Biol *181*, 497-510.

Harrington, L.S., Findlay, G.M., Gray, A., Tolkacheva, T., Wigfield, S., Rebholz, H., Barnett, J., Leslie, N.R., Cheng, S., Shepherd, P.R.*, et al.* (2004). The TSC1-2 tumor suppressor controls insulin-PI3K signaling via regulation of IRS proteins. J Cell Biol *166*, 213-223.

Hayes, J.D., Ellis, E.M., Neal, G.E., Harrison, D.J., and Manson, M.M. (1999). Cellular response to cancer chemopreventive agents: contribution of the antioxidant responsive element to the adaptive response to oxidative and chemical stress. Biochem Soc Symp *64*, 141-168.

He, C., and Levine, B. (2010). The Beclin 1 interactome. Curr Opin Cell Biol *22*, 140-149.

Horowitz, J.F., Sidossis, L.S., and Coyle, E.F. (1994). High efficiency of type I muscle fibers improves performance. Int J Sports Med *15*, 152-157.

Hosokawa, N., Sasaki, T., Iemura, S., Natsume, T., Hara, T., and Mizushima, N. (2009). Atg101, a novel mammalian autophagy protein interacting with Atg13. Autophagy *5*, 973-979.

Husnjak, K., Elsasser, S., Zhang, N., Chen, X., Randles, L., Shi, Y., Hofmann, K., Walters, K.J., Finley, D., and Dikic, I. (2008). Proteasome subunit Rpn13 is a novel ubiquitin receptor. Nature *453*, 481-488.

Huxley, A.F., and Niedergerke, R. (1954). Structural changes in muscle during contraction; interference microscopy of living muscle fibres. Nature *173*, 971-973.

Huxley, H., and Hanson, J. (1954). Changes in the cross-striations of muscle during contraction and stretch and their structural interpretation. Nature *173*, 973-976.

Ibebunjo, C., Chick, J.M., Kendall, T., Eash, J.K., Li, C., Zhang, Y., Vickers, C., Wu, Z., Clarke, B.A., Shi, J.*, et al.* (2013). Genomic and proteomic profiling reveals reduced mitochondrial function and disruption of the neuromuscular junction driving rat sarcopenia. Mol Cell Biol *33*, 194-212.

Inoki, K., Li, Y., Zhu, T., Wu, J., and Guan, K.L. (2002). TSC2 is phosphorylated and inhibited by Akt and suppresses mTOR signalling. Nat Cell Biol *4*, 648-657.

Itoh, K., Chiba, T., Takahashi, S., Ishii, T., Igarashi, K., Katoh, Y., Oyake, T., Hayashi, N., Satoh, K., Hatayama, I.*, et al.* (1997). An Nrf2/small Maf heterodimer mediates the induction of phase II detoxifying enzyme genes through antioxidant response elements. Biochem Biophys Res Commun *236*, 313-322.

Iwanczyk, J., Sadre-Bazzaz, K., Ferrell, K., Kondrashkina, E., Formosa, T., Hill, C.P., and Ortega, J. (2006). Structure of the Blm10-20 S proteasome complex by cryo-electron microscopy. Insights into the mechanism of activation of mature yeast proteasomes. J Mol Biol *363*, 648-659.

Jaiswal, A.K. (2004). Nrf2 signaling in coordinated activation of antioxidant gene expression. Free Radic Biol Med *36*, 1199-1207.

Jamart, C., Raymackers, J.M., Li An, G., Deldicque, L., and Francaux, M. (2011). Prevention of muscle disuse atrophy by MG132 proteasome inhibitor. Muscle Nerve *43*, 708-716.

Johnson, D.E. (2015). The ubiquitin-proteasome system: opportunities for therapeutic intervention in solid tumors. Endocr Relat Cancer *22*, T1-17.

Joseph, G.A., Wang, S., Zhou, W., Kimble, G., Tse, H., Eash, J., Shavlakadze, T., and Glass, D.J. (2019). Inhibition of mTORC1 signaling in aged rats counteracts the decline in muscle mass and reverses multiple parameters of muscle signaling associated with sarcopenia. 591891.

Jung, J., Genau, H.M., and Behrends, C. (2015). Amino acid dependent mTORC1 regulation by the lysosomal membrane protein SLC38A9. Mol Cell Biol.

Kaestner, K.H., Knochel, W., and Martinez, D.E. (2000). Unified nomenclature for the winged helix/forkhead transcription factors. Genes Dev *14*, 142-146.

Kahn, A.J., and Sandow, A. (1950). The potentiation of muscular contraction by the nitrate-ion. Science *112*, 647-649.

Keck, S., Nitsch, R., Grune, T., and Ullrich, O. (2003). Proteasome inhibition by paired helical filament-tau in brains of patients with Alzheimer's disease. J Neurochem *85*, 115-122.

Khor, B., Bredemeyer, A.L., Huang, C.Y., Turnbull, I.R., Evans, R., Maggi, L.B., Jr., White, J.M., Walker, L.M., Carnes, K., Hess, R.A.*, et al.* (2006). Proteasome activator PA200 is required for normal spermatogenesis. Mol Cell Biol *26*, 2999-3007.

Kikis, E.A., Gidalevitz, T., and Morimoto, R.I. (2010). Protein homeostasis in models of aging and age-related conformational disease. Adv Exp Med Biol *694*, 138-159.

Kim, J., Kundu, M., Viollet, B., and Guan, K.L. (2011). AMPK and mTOR regulate autophagy through direct phosphorylation of Ulk1. Nat Cell Biol *13*, 132-141.

Kim, J., Xing, W., Wergedal, J., Chan, J.Y., and Mohan, S. (2010). Targeted disruption of nuclear factor erythroid-derived 2-like 1 in osteoblasts reduces bone size and bone formation in mice. Physiological Genomics *40*, 100-110.

Kitajima, Y., Tashiro, Y., Suzuki, N., Warita, H., Kato, M., Tateyama, M., Ando, R., Izumi, R., Yamazaki, M., Abe, M.*, et al.* (2014). Proteasome dysfunction induces muscle growth defects and protein aggregation. J Cell Sci *127*, 5204-5217.

Klionsky, D.J., Abdalla, F.C., Abeliovich, H., Abraham, R.T., Acevedo-Arozena, A., Adeli, K., Agholme, L., Agnello, M., Agostinis, P., Aguirre-Ghiso, J.A.*, et al.* (2012). Guidelines for the use and interpretation of assays for monitoring autophagy. Autophagy *8*, 445-544.

Kobayashi, A., Tsukide, T., Miyasaka, T., Morita, T., Mizoroki, T., Saito, Y., Ihara, Y., Takashima, A., Noguchi, N., Fukamizu, A.*, et al.* (2011). Central nervous system-specific deletion of transcription factor Nrf1 causes progressive motor neuronal dysfunction. Genes Cells *16*, 692-703.

Koizumi, S., Hamazaki, J., and Murata, S. (2018). Transcriptional regulation of the 26S proteasome by Nrf1. Proc Jpn Acad Ser B Phys Biol Sci *94*, 325-336.

Koizumi, S., Irie, T., Hirayama, S., Sakurai, Y., Yashiroda, H., Naguro, I., Ichijo, H., Hamazaki, J., and Murata, S. (2016). The aspartyl protease DDI2 activates Nrf1 to compensate for proteasome dysfunction. Elife *5*.

Korde, N., Roschewski, M., Zingone, A., Kwok, M., Manasanch, E.E., Bhutani, M., Tageja, N., Kazandjian, D., Mailankody, S., Wu, P.*, et al.* (2015). Treatment With Carfilzomib-Lenalidomide-Dexamethasone With Lenalidomide Extension in Patients With Smoldering or Newly Diagnosed Multiple Myeloma. JAMA Oncol *1*, 746-754.

Korner, Z., Fontes-Oliveira, C.C., Holmberg, J., Carmignac, V., and Durbeej, M. (2014). Bortezomib partially improves laminin alpha2 chain-deficient muscular dystrophy. Am J Pathol *184*, 1518-1528.

Kraemer, W.J., Patton, J.F., Gordon, S.E., Harman, E.A., Deschenes, M.R., Reynolds, K., Newton, R.U., Triplett, N.T., and Dziados, J.E. (1995). Compatibility of high-intensity strength and endurance training on hormonal and skeletal muscle adaptations. J Appl Physiol (1985) *78*, 976-989.

Krawiec, B.J., Frost, R.A., Vary, T.C., Jefferson, L.S., and Lang, C.H. (2005). Hindlimb casting decreases muscle mass in part by proteasome-dependent proteolysis but independent of protein synthesis. Am J Physiol Endocrinol Metab *289*, E969-980.

Kunz, J., Henriquez, R., Schneider, U., Deuter-Reinhard, M., Movva, N.R., and Hall, M.N. (1993). Target of rapamycin in yeast, TOR2, is an essential phosphatidylinositol kinase homolog required for G1 progression. Cell *73*, 585-596.

Kwak, M.K., Wakabayashi, N., Itoh, K., Motohashi, H., Yamamoto, M., and Kensler, T.W. (2003). Modulation of gene expression by cancer chemopreventive dithiolethiones through the Keap1-Nrf2 pathway. Identification of novel gene clusters for cell survival. J Biol Chem *278*, 8135-8145.

Kwon, D.Y., Motley, W.W., Fischbeck, K.H., and Burnett, B.G. (2011). Increasing expression and decreasing degradation of SMN ameliorate the spinal muscular atrophy phenotype in mice. Hum Mol Genet *20*, 3667-3677.

Lamb, C.A., Yoshimori, T., and Tooze, S.A. (2013). The autophagosome: origins unknown, biogenesis complex. Nat Rev Mol Cell Biol *14*, 759-774.

Laplante, M., and Sabatini, D.M. (2009). mTOR signaling at a glance. J Cell Sci *122*, 3589-3594.

Laplante, M., and Sabatini, D.M. (2012). mTOR signaling in growth control and disease. Cell *149*, 274-293.

Lecker, S.H., Jagoe, R.T., Gilbert, A., Gomes, M., Baracos, V., Bailey, J., Price, S.R., Mitch, W.E., and Goldberg, A.L. (2004). Multiple types of skeletal muscle atrophy involve a common program of changes in gene expression. Faseb J *18*, 39-51.

Lee, C.K., Klopp, R.G., Weindruch, R., and Prolla, T.A. (1999). Gene expression profile of aging and its retardation by caloric restriction. Science *285*, 1390-1393.

Lee, C.K., Weindruch, R., and Prolla, T.A. (2000). Gene-expression profile of the ageing brain in mice. Nat Genet *25*, 294-297.

Lee, C.S., Ho, D.V., and Chan, J.Y. (2013). Nuclear factor-erythroid 2-related factor 1 regulates expression of proteasome genes in hepatocytes and protects against endoplasmic reticulum stress and steatosis in mice. Febs J *280*, 3609-3620.

Lee, C.S., Lee, C., Hu, T., Nguyen, J.M., Zhang, J., Martin, M.V., Vawter, M.P., Huang, E.J., and Chan, J.Y. (2011). Loss of nuclear factor E2-related factor 1 in the brain leads to dysregulation of proteasome gene expression and neurodegeneration. Proc Natl Acad Sci U S A *108*, 8408-8413.

Lee, D.H., and Goldberg, A.L. (1998). Proteasome inhibitors: valuable new tools for cell biologists. Trends Cell Biol *8*, 397-403.

Leger, B., Derave, W., De Bock, K., Hespel, P., and Russell, A.P. (2008). Human sarcopenia reveals an increase in SOCS-3 and myostatin and a reduced efficiency of Akt phosphorylation. Rejuvenation Res *11*, 163-175B.

Leggett, D.S., Hanna, J., Borodovsky, A., Crosas, B., Schmidt, M., Baker, R.T., Walz, T., Ploegh, H., and Finley, D. (2002). Multiple associated proteins regulate proteasome structure and function. Mol Cell *10*, 495-507.

Leuchtmann, A.B., and Handschin, C. (2019). Pharmacological targeting of age-related changes in skeletal muscle tissue. Pharmacol Res.

Leung, L., Kwong, M., Hou, S., Lee, C., and Chan, J.Y. (2003). Deficiency of the Nrf1 and Nrf2 transcription factors results in early embryonic lethality and severe oxidative stress. J Biol Chem *278*, 48021-48029.

Lexell, J. (1995). Human aging, muscle mass, and fiber type composition. J Gerontol A Biol Sci Med Sci *50 Spec No*, 11-16.

Li, X., Matilainen, O., Jin, C., Glover-Cutter, K.M., Holmberg, C.I., and Blackwell, T.K. (2011). Specific SKN-1/Nrf stress responses to perturbations in translation elongation and proteasome activity. PLoS Genet *7*, e1002119.

Lin, J., Wu, H., Tarr, P.T., Zhang, C.Y., Wu, Z., Boss, O., Michael, L.F., Puigserver, P., Isotani, E., Olson, E.N.*, et al.* (2002). Transcriptional co-activator PGC-1 alpha drives the formation of slow-twitch muscle fibres. Nature *418*, 797-801.

Livneh, I., Cohen-Kaplan, V., Cohen-Rosenzweig, C., Avni, N., and Ciechanover, A. (2016). The life cycle of the 26S proteasome: from birth, through regulation and function, and onto its death. Cell Res *26*, 869-885.

Long, X., Lin, Y., Ortiz-Vega, S., Yonezawa, K., and Avruch, J. (2005). Rheb binds and regulates the mTOR kinase. Curr Biol *15*, 702-713.

Lopez, A.D., Tar, K., Krugel, U., Dange, T., Ros, I.G., and Schmidt, M. (2011). Proteasomal degradation of Sfp1 contributes to the repression of ribosome biogenesis during starvation and is mediated by the proteasome activator Blm10. Mol Biol Cell *22*, 528-540.

Lundgren, J., Masson, P., Mirzaei, Z., and Young, P. (2005). Identification and characterization of a Drosophila proteasome regulatory network. Mol Cell Biol *25*, 4662-4675.

Ma, X.M., and Blenis, J. (2009). Molecular mechanisms of mTOR-mediated translational control. Nat Rev Mol Cell Biol *10*, 307-318.

Madeddu, C., and Mantovani, G. (2009). An update on promising agents for the treatment of cancer cachexia. Curr Opin Support Palliat Care *3*, 258-262.

Maiese, K., Chong, Z.Z., and Shang, Y.C. (2008). OutFOXOing disease and disability: the therapeutic potential of targeting FoxO proteins. Trends Mol Med *14*, 219-227.

Maillard, R.A., Chistol, G., Sen, M., Righini, M., Tan, J., Kaiser, C.M., Hodges, C., Martin, A., and Bustamante, C. (2011). ClpX(P) generates mechanical force to unfold and translocate its protein substrates. Cell *145*, 459-469.

Mammucari, C., Milan, G., Romanello, V., Masiero, E., Rudolf, R., Del Piccolo, P., Burden, S.J., Di Lisi, R., Sandri, C., Zhao, J.*, et al.* (2007). FoxO3 controls autophagy in skeletal muscle in vivo. Cell Metab *6*, 458-471.

Manasanch, E.E., and Orlowski, R.Z. (2017). Proteasome inhibitors in cancer therapy. Nat Rev Clin Oncol *14*, 417-433.

Mannhaupt, G., Schnall, R., Karpov, V., Vetter, I., and Feldmann, H. (1999). Rpn4p acts as a transcription factor by binding to PACE, a nonamer box found upstream of 26S proteasomal and other genes in yeast. FEBS Lett *450*, 27-34.

Manning, B.D., Tee, A.R., Logsdon, M.N., Blenis, J., and Cantley, L.C. (2002). Identification of the tuberous sclerosis complex-2 tumor suppressor gene product tuberin as a target of the phosphoinositide 3-kinase/akt pathway. Mol Cell *10*, 151-162.

Markofski, M.M., Dickinson, J.M., Drummond, M.J., Fry, C.S., Fujita, S., Gundermann, D.M., Glynn, E.L., Jennings, K., Paddon-Jones, D., Reidy, P.T.*, et al.* (2015). Effect of age on basal muscle protein synthesis and mTORC1 signaling in a large cohort of young and older men and women. Exp Gerontol *65*, 1-7.

Masiero, E., Agatea, L., Mammucari, C., Blaauw, B., Loro, E., Komatsu, M., Metzger, D., Reggiani, C., Schiaffino, S., and Sandri, M. (2009). Autophagy is required to maintain muscle mass. Cell Metab *10*, 507-515.

McNaught, K.S., Belizaire, R., Isacson, O., Jenner, P., and Olanow, C.W. (2003). Altered proteasomal function in sporadic Parkinson's disease. Exp Neurol *179*, 38-46.

Meiners, S., Heyken, D., Weller, A., Ludwig, A., Stangl, K., Kloetzel, P.M., and Kruger, E. (2003). Inhibition of proteasome activity induces concerted expression of proteasome genes and de novo formation of Mammalian proteasomes. J Biol Chem *278*, 21517-21525.

Meng, L., Mohan, R., Kwok, B.H., Elofsson, M., Sin, N., and Crews, C.M. (1999). Epoxomicin, a potent and selective proteasome inhibitor, exhibits in vivo antiinflammatory activity. Proc Natl Acad Sci U S A *96*, 10403-10408.

Menon, S., Dibble, C.C., Talbott, G., Hoxhaj, G., Valvezan, A.J., Takahashi, H., Cantley, L.C., and Manning, B.D. (2014). Spatial control of the TSC complex integrates insulin and nutrient regulation of mTORC1 at the lysosome. Cell *156*, 771-785.

Meyer, H., Bug, M., and Bremer, S. (2012). Emerging functions of the VCP/p97 AAA-ATPase in the ubiquitin system. Nat Cell Biol *14*, 117-123.

Milan, G., Romanello, V., Pescatore, F., Armani, A., Paik, J.H., Frasson, L., Seydel, A., Zhao, J., Abraham, R., Goldberg, A.L.*, et al.* (2015). Regulation of autophagy and the ubiquitin-proteasome system by the FoxO transcriptional network during muscle atrophy. Nat Commun *6*, 6670.

Mitch, W.E., and Goldberg, A.L. (1996). Mechanisms of muscle wasting. The role of the ubiquitin-proteasome pathway. N Engl J Med *335*, 1897-1905.

Mitsiades, N., Mitsiades, C.S., Poulaki, V., Chauhan, D., Fanourakis, G., Gu, X., Bailey, C., Joseph, M., Libermann, T.A., Treon, S.P.*, et al.* (2002). Molecular sequelae of proteasome inhibition in human multiple myeloma cells. Proc Natl Acad Sci U S A *99*, 14374-14379.

Nguyen, T., Sherratt, P.J., and Pickett, C.B. (2003). Regulatory mechanisms controlling gene expression mediated by the antioxidant response element. Annu Rev Pharmacol Toxicol *43*, 233-260.

Nyquist, K., and Martin, A. (2014). Marching to the beat of the ring: polypeptide translocation by AAA+ proteases. Trends Biochem Sci *39*, 53-60.

Ohtsuji, M., Katsuoka, F., Kobayashi, A., Aburatani, H., Hayes, J.D., and Yamamoto, M. (2008). Nrf1 and Nrf2 play distinct roles in activation of antioxidant response element-dependent genes. J Biol Chem *283*, 33554-33562.

Pallafacchina, G., Calabria, E., Serrano, A.L., Kalhovde, J.M., and Schiaffino, S. (2002). A protein kinase B-dependent and rapamycin-sensitive pathway controls skeletal muscle growth but not fiber type specification. Proc Natl Acad Sci U S A *99*, 9213-9218.

Palombella, V.J., Rando, O.J., Goldberg, A.L., and Maniatis, T. (1994). The ubiquitin-proteasome pathway is required for processing the NF-kappa B1 precursor protein and the activation of NF-kappa B. Cell *78*, 773-785.

Park, S., Pak, J., Jang, I., and Cho, J.W. (2014). Inhibition of mTOR affects protein stability of OGT. Biochem Biophys Res Commun *453*, 208-212.

Penna, F., Bonetto, A., Aversa, Z., Minero, V.G., Rossi Fanelli, F., Costelli, P., and Muscaritoli, M. (2016). Effect of the specific proteasome inhibitor bortezomib on cancer-related muscle wasting. J Cachexia Sarcopenia Muscle *7*, 345-354.

Peter, J.B., Barnard, R.J., Edgerton, V.R., Gillespie, C.A., and Stempel, K.E. (1972). Metabolic profiles of three fiber types of skeletal muscle in guinea pigs and rabbits. Biochemistry *11*, 2627-2633.

Petit, C.S., Roczniak-Ferguson, A., and Ferguson, S.M. (2013). Recruitment of folliculin to lysosomes supports the amino acid-dependent activation of Rag GTPases. J Cell Biol *202*, 1107-1122.

Piccirillo, R., and Goldberg, A.L. (2012). The p97/VCP ATPase is critical in muscle atrophy and the accelerated degradation of muscle proteins. Embo J *31*, 3334-3350.

Pierobon-Bormioli, S., Sartore, S., Libera, L.D., Vitadello, M., and Schiaffino, S. (1981). "Fast" isomyosins and fiber types in mammalian skeletal muscle. J Histochem Cytochem *29*, 1179-1188.

Potter, C.J., Pedraza, L.G., and Xu, T. (2002). Akt regulates growth by directly phosphorylating Tsc2. Nat Cell Biol *4*, 658-665.

Qian, M.X., Pang, Y., Liu, C.H., Haratake, K., Du, B.Y., Ji, D.Y., Wang, G.F., Zhu, Q.Q., Song, W., Yu, Y.*, et al.* (2013). Acetylation-mediated proteasomal degradation of core histones during DNA repair and spermatogenesis. Cell *153*, 1012-1024.

Rabl, J., Smith, D.M., Yu, Y., Chang, S.C., Goldberg, A.L., and Cheng, Y. (2008). Mechanism of gate opening in the 20S proteasome by the proteasomal ATPases. Mol Cell *30*, 360-368.

Radhakrishnan, S.K., den Besten, W., and Deshaies, R.J. (2014). p97-dependent retrotranslocation and proteolytic processing govern formation of active Nrf1 upon proteasome inhibition. Elife *3*, e01856.

Radhakrishnan, S.K., Lee, C.S., Young, P., Beskow, A., Chan, J.Y., and Deshaies, R.J. (2010). Transcription factor Nrf1 mediates the proteasome recovery pathway after proteasome inhibition in mammalian cells. Mol Cell *38*, 17-28.

Rebsamen, M., Pochini, L., Stasyk, T., de Araujo, M.E., Galluccio, M., Kandasamy, R.K., Snijder, B., Fauster, A., Rudashevskaya, E.L., Bruckner, M.*, et al.* (2015). SLC38A9 is a component of the lysosomal amino acid sensing machinery that controls mTORC1. Nature.

Richardson, P.G., Baz, R., Wang, M., Jakubowiak, A.J., Laubach, J.P., Harvey, R.D., Talpaz, M., Berg, D., Liu, G., Yu, J.*, et al.* (2014). Phase 1 study of twice-weekly ixazomib, an oral proteasome inhibitor, in relapsed/refractory multiple myeloma patients. Blood *124*, 1038-1046.

Richardson, P.G., Moreau, P., Laubach, J.P., Gupta, N., Hui, A.M., Anderson, K.C., San Miguel, J.F., and Kumar, S. (2015). The investigational proteasome inhibitor ixazomib for the treatment of multiple myeloma. Future Oncol *11*, 1153-1168.

Richardson, P.G., Sonneveld, P., Schuster, M.W., Irwin, D., Stadtmauer, E.A., Facon, T., Harousseau, J.L., Ben-Yehuda, D., Lonial, S., Goldschmidt, H.*, et al.* (2005). Bortezomib or high-dose dexamethasone for relapsed multiple myeloma. N Engl J Med *352*, 2487-2498.

Richardson, P.G., Weller, E., Lonial, S., Jakubowiak, A.J., Jagannath, S., Raje, N.S., Avigan, D.E., Xie, W., Ghobrial, I.M., Schlossman, R.L.*, et al.* (2010). Lenalidomide, bortezomib, and dexamethasone combination therapy in patients with newly diagnosed multiple myeloma. Blood *116*, 679-686.

Risson, V., Mazelin, L., Roceri, M., Sanchez, H., Moncollin, V., Corneloup, C., Richard-Bulteau, H., Vignaud, A., Baas, D., Defour, A.*, et al.* (2009). Muscle inactivation of mTOR causes metabolic and dystrophin defects leading to severe myopathy. J Cell Biol *187*, 859-874.

Roberts, L.D., Ashmore, T., McNally, B.D., Murfitt, S.A., Fernandez, B.O., Feelisch, M., Lindsay, R., Siervo, M., Williams, E.A., Murray, A.J.*, et al.* (2017). Inorganic Nitrate Mimics Exercise-Stimulated Muscular Fiber-Type Switching and Myokine and gamma-Aminobutyric Acid Release. Diabetes *66*, 674-688.

Rogov, V., Dotsch, V., Johansen, T., and Kirkin, V. (2014). Interactions between autophagy receptors and ubiquitin-like proteins form the molecular basis for selective autophagy. Mol Cell *53*, 167-178.

Ruegg, M.A., and Glass, D.J. (2011). Molecular mechanisms and treatment options for muscle wasting diseases. Annu Rev Pharmacol Toxicol *51*, 373-395.

Rushmore, T.H., Morton, M.R., and Pickett, C.B. (1991). The antioxidant responsive element. Activation by oxidative stress and identification of the DNA consensus sequence required for functional activity. J Biol Chem *266*, 11632-11639.

Sabatini, D.M., Erdjument-Bromage, H., Lui, M., Tempst, P., and Snyder, S.H. (1994). RAFT1: a mammalian protein that binds to FKBP12 in a rapamycin-dependent fashion and is homologous to yeast TORs. Cell *78*, 35-43.

Sabers, C.J., Martin, M.M., Brunn, G.J., Williams, J.M., Dumont, F.J., Wiederrecht, G., and Abraham, R.T. (1995). Isolation of a protein target of the FKBP12-rapamycin complex in mammalian cells. J Biol Chem *270*, 815-822.

Sacheck, J.M., Hyatt, J.P., Raffaello, A., Jagoe, R.T., Roy, R.R., Edgerton, V.R., Lecker, S.H., and Goldberg, A.L. (2007). Rapid disuse and denervation atrophy involve transcriptional changes similar to those of muscle wasting during systemic diseases. Faseb J *21*, 140-155.

Sacheck, J.M., Ohtsuka, A., McLary, S.C., and Goldberg, A.L. (2004). IGF-I stimulates muscle growth by suppressing protein breakdown and expression of atrophy-related ubiquitin ligases, atrogin-1 and MuRF1. Am J Physiol Endocrinol Metab *287*, E591-601.

Sadre-Bazzaz, K., Whitby, F.G., Robinson, H., Formosa, T., and Hill, C.P. (2010). Structure of a Blm10 complex reveals common mechanisms for proteasome binding and gate opening. Mol Cell *37*, 728-735.

Sancak, Y., Bar-Peled, L., Zoncu, R., Markhard, A.L., Nada, S., and Sabatini, D.M. (2010). Ragulator-Rag complex targets mTORC1 to the lysosomal surface and is necessary for its activation by amino acids. Cell *141*, 290-303.

Sancak, Y., Peterson, T.R., Shaul, Y.D., Lindquist, R.A., Thoreen, C.C., Bar-Peled, L., and Sabatini, D.M. (2008). The Rag GTPases bind raptor and mediate amino acid signaling to mTORC1. Science *320*, 1496-1501.

Sancak, Y., Thoreen, C.C., Peterson, T.R., Lindquist, R.A., Kang, S.A., Spooner, E., Carr, S.A., and Sabatini, D.M. (2007). PRAS40 is an insulin-regulated inhibitor of the mTORC1 protein kinase. Mol Cell *25*, 903-915.

Sandow, A. (1952). Excitation-contraction coupling in muscular response. Yale J Biol Med *25*, 176-201.

Sandri, M. (2010). Autophagy in skeletal muscle. FEBS Lett *584*, 1411-1416.

Sandri, M. (2013). Protein breakdown in muscle wasting: role of autophagy-lysosome and ubiquitin-proteasome. Int J Biochem Cell Biol *45*, 2121-2129.

Sandri, M., Sandri, C., Gilbert, A., Skurk, C., Calabria, E., Picard, A., Walsh, K., Schiaffino, S., Lecker, S.H., and Goldberg, A.L. (2004). Foxo transcription factors induce the atrophy-related ubiquitin ligase atrogin-1 and cause skeletal muscle atrophy. Cell *117*, 399-412.

Sartori, R., Schirwis, E., Blaauw, B., Bortolanza, S., Zhao, J., Enzo, E., Stantzou, A., Mouisel, E., Toniolo, L., Ferry, A.*, et al.* (2013). BMP signaling controls muscle mass. Nat Genet *45*, 1309-1318.

Sasaki, K., Hamazaki, J., Koike, M., Hirano, Y., Komatsu, M., Uchiyama, Y., Tanaka, K., and Murata, S. (2010). PAC1 gene knockout reveals an essential role of chaperone-mediated 20S proteasome biogenesis and latent 20S proteasomes in cellular homeostasis. Mol Cell Biol *30*, 3864-3874.

Saxton, R.A., Chantranupong, L., Knockenhauer, K.E., Schwartz, T.U., and Sabatini, D.M. (2016a). Mechanism of arginine sensing by CASTOR1 upstream of mTORC1. Nature.

Saxton, R.A., Knockenhauer, K.E., Wolfson, R.L., Chantranupong, L., Pacold, M.E., Wang, T., Schwartz, T.U., and Sabatini, D.M. (2016b). Structural basis for leucine sensing by the Sestrin2-mTORC1 pathway. Science *351*, 53-58.

Schiaffino, S. (2010). Fibre types in skeletal muscle: a personal account. Acta Physiol (Oxf) *199*, 451-463.

Schiaffino, S. (2011). Fiber Types in Mammalian Skeletal Muscles. Physiology Review.

Scott, W., Stevens, J., and Binder-Macleod, S.A. (2001). Human skeletal muscle fiber type classifications. Phys Ther *81*, 1810-1816.

Sekine, H., Okazaki, K., Kato, K., Alam, M.M., Shima, H., Katsuoka, F., Tsujita, T., Suzuki, N., Kobayashi, A., Igarashi, K.*, et al.* (2018). O-GlcNAcylation Signal Mediates Proteasome Inhibitor Resistance in Cancer Cells by Stabilizing NRF1. Mol Cell Biol.

Seo, H., Sonntag, K.C., and Isacson, O. (2004). Generalized brain and skin proteasome inhibition in Huntington's disease. Ann Neurol *56*, 319-328.

Sha, Z., and Goldberg, A.L. (2014). Proteasome-mediated processing of Nrf1 is essential for coordinate induction of all proteasome subunits and p97. Curr Biol *24*, 1573-1583.

Sha, Z., Schnell, H.M., Ruoff, K., and Goldberg, A. (2018). Rapid induction of p62 and GABARAPL1 upon proteasome inhibition promotes survival before autophagy activation. J Cell Biol.

Shi, Y., Chen, X., Elsasser, S., Stocks, B.B., Tian, G., Lee, B.H., Shi, Y., Zhang, N., de Poot, S.A., Tuebing, F.*, et al.* (2016). Rpn1 provides adjacent receptor sites for substrate binding and deubiquitination by the proteasome. Science *351*.

Shimobayashi, M., and Hall, M.N. (2014). Making new contacts: the mTOR network in metabolism and signalling crosstalk. Nat Rev Mol Cell Biol *15*, 155-162.

Sodi, V.L., Khaku, S., Krutilina, R., Schwab, L.P., Vocadlo, D.J., Seagroves, T.N., and Reginato, M.J. (2015). mTOR/MYC Axis Regulates O-GlcNAc Transferase Expression and O-GlcNAcylation in Breast Cancer. Mol Cancer Res *13*, 923-933.

Stadtmueller, B.M., and Hill, C.P. (2011). Proteasome activators. Mol Cell *41*, 8-19.

Staron, R.S., Karapondo, D.L., Kraemer, W.J., Fry, A.C., Gordon, S.E., Falkel, J.E., Hagerman, F.C., and Hikida, R.S. (1994). Skeletal muscle adaptations during early phase of heavy-resistance training in men and women. J Appl Physiol (1985) *76*, 1247-1255.

Staron, R.S., and Pette, D. (1993). The continuum of pure and hybrid myosin heavy chain-based fibre types in rat skeletal muscle. Histochemistry *100*, 149-153.

Steffen, J., Seeger, M., Koch, A., and Kruger, E. (2010). Proteasomal degradation is transcriptionally controlled by TCF11 via an ERAD-dependent feedback loop. Mol Cell *40*, 147-158.

Stohwasser, R., Kuckelkorn, U., Kraft, R., Kostka, S., and Kloetzel, P.M. (1996). 20S proteasome from LMP7 knock out mice reveals altered proteolytic activities and cleavage site preferences. FEBS Lett *383*, 109-113.

Stokoe, D., Stephens, L.R., Copeland, T., Gaffney, P.R., Reese, C.B., Painter, G.F., Holmes, A.B., McCormick, F., and Hawkins, P.T. (1997). Dual role of phosphatidylinositol-3,4,5-trisphosphate in the activation of protein kinase B. Science *277*, 567-570.

Strucksberg, K.H., Tangavelou, K., Schroder, R., and Clemen, C.S. (2010). Proteasomal activity in skeletal muscle: a matter of assay design, muscle type, and age. Anal Biochem *399*, 225-229.

Supinski, G.S., Vanags, J., and Callahan, L.A. (2009). Effect of proteasome inhibitors on endotoxin-induced diaphragm dysfunction. Am J Physiol Lung Cell Mol Physiol *296*, L994-L1001.

Szentesi, P., Zaremba, R., van Mechelen, W., and Stienen, G.J. (2001). ATP utilization for calcium uptake and force production in different types of human skeletal muscle fibres. J Physiol *531*, 393-403.

Tanahashi, N., Murakami, Y., Minami, Y., Shimbara, N., Hendil, K.B., and Tanaka, K. (2000). Hybrid proteasomes. Induction by interferon-gamma and contribution to ATP-dependent proteolysis. J Biol Chem *275*, 14336-14345.

Tar, K., Dange, T., Yang, C., Yao, Y., Bulteau, A.L., Salcedo, E.F., Braigen, S., Bouillaud, F., Finley, D., and Schmidt, M. (2014). Proteasomes associated with the Blm10 activator protein antagonize mitochondrial fission through degradation of the fission protein Dnm1. J Biol Chem *289*, 12145-12156.

Tomlin, F.M., Gerling-Driessen, U.I.M., Liu, Y.C., Flynn, R.A., Vangala, J.R., Lentz, C.S., Clauder-Muenster, S., Jakob, P., Mueller, W.F., Ordonez-Rueda, D.*, et al.* (2017). Inhibition of NGLY1 Inactivates the Transcription Factor Nrf1 and Potentiates Proteasome Inhibitor Cytotoxicity. ACS Cent Sci *3*, 1143-1155.

Tonoki, A., Kuranaga, E., Tomioka, T., Hamazaki, J., Murata, S., Tanaka, K., and Miura, M. (2009). Genetic evidence linking age-dependent attenuation of the 26S proteasome with the aging process. Mol Cell Biol *29*, 1095-1106.

Tsuchiya, Y., Morita, T., Kim, M., Iemura, S., Natsume, T., Yamamoto, M., and Kobayashi, A. (2011). Dual regulation of the transcriptional activity of Nrf1 by beta-TrCP- and Hrd1-dependent degradation mechanisms. Mol Cell Biol *31*, 4500-4512.

Tsun, Z.Y., Bar-Peled, L., Chantranupong, L., Zoncu, R., Wang, T., Kim, C., Spooner, E., and Sabatini, D.M. (2013). The folliculin tumor suppressor is a GAP for the RagC/D GTPases that signal amino acid levels to mTORC1. Mol Cell *52*, 495-505.

Ustrell, V., Hoffman, L., Pratt, G., and Rechsteiner, M. (2002). PA200, a nuclear proteasome activator involved in DNA repair. Embo J *21*, 3516-3525.

Vander Haar, E., Lee, S.I., Bandhakavi, S., Griffin, T.J., and Kim, D.H. (2007). Insulin signalling to mTOR mediated by the Akt/PKB substrate PRAS40. Nat Cell Biol *9*, 316-323.

Vargas, R., and Lang, C.H. (2008). Alcohol accelerates loss of muscle and impairs recovery of muscle mass resulting from disuse atrophy. Alcohol Clin Exp Res *32*, 128-137.

Verma, R., Aravind, L., Oania, R., McDonald, W.H., Yates, J.R., 3rd, Koonin, E.V., and Deshaies, R.J. (2002). Role of Rpn11 metalloprotease in deubiquitination and degradation by the 26S proteasome. Science *298*, 611-615.

Very, N., Steenackers, A., Dubuquoy, C., Vermuse, J., Dubuquoy, L., Lefebvre, T., and El Yazidi-Belkoura, I. (2018). Cross regulation between mTOR signaling and O-GlcNAcylation. J Bioenerg Biomembr.

Voutsadakis, I.A. (2017). Proteasome expression and activity in cancer and cancer stem cells. Tumour Biol *39*, 1010428317692248.

Wang, C.W., and Klionsky, D.J. (2003). The molecular mechanism of autophagy. Mol Med *9*, 65-76.

Wang, S., Tsun, Z.Y., Wolfson, R.L., Shen, K., Wyant, G.A., Plovanich, M.E., Yuan, E.D., Jones, T.D., Chantranupong, L., Comb, W.*, et al.* (2015). Metabolism. Lysosomal amino acid transporter SLC38A9 signals arginine sufficiency to mTORC1. Science *347*, 188-194.

Wang, Y., and Pessin, J.E. (2013). Mechanisms for fiber-type specificity of skeletal muscle atrophy. Curr Opin Clin Nutr Metab Care *16*, 243-250.

Wang, Z., Yang, J., Kirk, C., Fang, Y., Alsina, M., Badros, A., Papadopoulos, K., Wong, A., Woo, T., Bomba, D.*, et al.* (2013). Clinical pharmacokinetics, metabolism, and drug-drug interaction of carfilzomib. Drug Metab Dispos *41*, 230-237.

Waters, R.E., Rotevatn, S., Li, P., Annex, B.H., and Yan, Z. (2004). Voluntary running induces fiber type-specific angiogenesis in mouse skeletal muscle. Am J Physiol Cell Physiol *287*, C1342-1348.

Webb, A.E., and Brunet, A. (2014). FOXO transcription factors: key regulators of cellular quality control. Trends Biochem Sci *39*, 159-169.

Weidberg, H., Shvets, E., Shpilka, T., Shimron, F., Shinder, V., and Elazar, Z. (2010). LC3 and GATE-16/GABARAP subfamilies are both essential yet act differently in autophagosome biogenesis. Embo J *29*, 1792-1802.

Weyburne, E.S., Wilkins, O.M., Sha, Z., Williams, D.A., Pletnev, A.A., de Bruin, G., Overkleeft, H.S., Goldberg, A.L., Cole, M.D., and Kisselev, A.F. (2017). Inhibition of the Proteasome beta2 Site Sensitizes Triple-Negative Breast Cancer Cells to beta5 Inhibitors and Suppresses Nrf1 Activation. Cell Chem Biol *24*, 218-230.

White, Z., White, R.B., McMahon, C., Grounds, M.D., and Shavlakadze, T. (2016). High mTORC1 signaling is maintained, while protein degradation pathways are perturbed in old murine skeletal muscles in the fasted state. Int J Biochem Cell Biol *78*, 10-21.

Wick, M.J., Dong, L.Q., Riojas, R.A., Ramos, F.J., and Liu, F. (2000). Mechanism of phosphorylation of protein kinase B/Akt by a constitutively active 3-phosphoinositide-dependent protein kinase-1. J Biol Chem *275*, 40400-40406.

Wolfson, R.L., Chantranupong, L., Saxton, R.A., Shen, K., Scaria, S.M., Cantor, J.R., and Sabatini, D.M. (2016). Sestrin2 is a leucine sensor for the mTORC1 pathway. Science *351*, 43-48.

Xie, Y., and Varshavsky, A. (2001). RPN4 is a ligand, substrate, and transcriptional regulator of the 26S proteasome: a negative feedback circuit. Proc Natl Acad Sci U S A *98*, 3056-3061.

Xu, Z., Chen, L., Leung, L., Yen, T.S., Lee, C., and Chan, J.Y. (2005). Liver-specific inactivation of the Nrf1 gene in adult mouse leads to nonalcoholic steatohepatitis and hepatic neoplasia. Proc Natl Acad Sci U S A *102*, 4120-4125.

Yoon, M.S. (2017). mTOR as a Key Regulator in Maintaining Skeletal Muscle Mass. Front Physiol *8*, 788.

Zhang, Y., Lucocq, J.M., Yamamoto, M., and Hayes, J.D. (2007). The NHB1 (N-terminal homology box 1) sequence in transcription factor Nrf1 is required to anchor it to the endoplasmic reticulum and also to enable its asparagine-glycosylation. Biochem J *408*, 161-172.

Zhang, Y., Nicholatos, J., Dreier, J.R., Ricoult, S.J., Widenmaier, S.B., Hotamisligil, G.S., Kwiatkowski, D.J., and Manning, B.D. (2014). Coordinated regulation of protein synthesis and degradation by mTORC1. Nature *513*, 440-443.

Zhang, Y., and Xiang, Y. (2016). Molecular and cellular basis for the unique functioning of Nrf1, an indispensable transcription factor for maintaining cell homoeostasis and organ integrity. Biochem J *473*, 961-1000.

Zhao, J., Brault, J.J., Schild, A., Cao, P., Sandri, M., Schiaffino, S., Lecker, S.H., and Goldberg, A.L. (2007). FoxO3 coordinately activates protein degradation by the autophagic/lysosomal and proteasomal pathways in atrophying muscle cells. Cell Metab *6*, 472-483.

Zheng, H.Z., Fu, J.Q., Xue, P., Zhao, R., Dong, J., Liu, D.X., Yamamoto, M., Tong, Q.C., Teng, W.P., Qu, W.D., *et al.* (2015). CNC-bZIP Protein Nrf1-Dependent Regulation of Glucose-Stimulated Insulin Secretion. Antioxid Redox Signal *22*, 819-831.

Zoncu, R., Bar-Peled, L., Efeyan, A., Wang, S., Sancak, Y., and Sabatini, D.M. (2011). mTORC1 senses lysosomal amino acids through an inside-out mechanism that requires the vacuolar H(+)-ATPase. Science *334*, 678-683.